OFFICE OF CIVILIAN RADIOACTIVE WASTE MANAGEMENT

CALCULATION COVER SHEET

1. QA: QA
Page: 1 Of: 82

2. Calculation Title

EQ6 Calculation for Chemical Degradation of Pu-Ceramic Waste Packages: Effects of Updated Materials Composition and Rates

3. Document Identifier (Including Revision Number)

CAL-EDC-MD-000003 REV 00

MOL.19990928.0235

4. Total Attachments	5. Attachment Numbers – Number of pages in each
2	I-8; II-7

	Print Name	Signature	Date
6. Originator	Peng-Chu Zhang and Harlan W. Stockman	Harlan W. Stockman	9/29/1999
7. Checker	Susan LeStrange	Susan L. LeStrange	9/29/1999
8. Lead	Peter Gottlieb	Peter Gottlieb	9/29/1999

9. Remarks

Revision History

10. Revision No.	11. Description of Revision
00	Revision 00

CONTENTS

FIGURES

Page

TABLES

Page

1. PURPOSE

The Monitored Geologic Repository (MGR) Waste Package Operations (WPO) of the Civilian Radioactive Waste Management System Management and Operating Contractor (CRWMS M&O) performed calculations to provide input for disposal of Pu-ceramic waste forms. The Pu-ceramic (Refs. 1 and 2) is designed to immobilize excess plutonium from weapons production, and has been considered for disposal at the potential Yucca Mountain site. Because of the high content of fissile material in the ceramic, the waste package (WP) design requires special consideration of the amount and placement of neutron absorbers, and the possible loss of absorbers and fissile materials over geologic time. For some WPs, the corrosion-allowance material (CAM) and the corrosion-resistant material (CRM) may breach (Ref. 3, Section 10.5.1.2), allowing the influx of water. Water in the WP will moderate neutrons, increasing the likelihood of a criticality within the WP; and the water may, in time, gradually leach the fissile components and neutron absorbers out of the WP, further affecting the neutronics of the system.

This study presents calculations of the long-term geochemical behavior of WPs containing Pu-ceramic disks arranged according to the "can-in-canister" concept. The cans containing Pu-ceramic disks are embedded in canisters filled with high-level waste (HLW) glass (Ref. 1). The objectives of this calculation were to determine:

- The extent to which criticality control material, suggested for this WP design, will remain in the WP after corrosion/dissolution of the initial WP configuration (such that it can be effective in preventing criticality).

- The extent to which fissile plutonium and uranium will be carried out of the degraded WP by infiltrating water (such that internal criticality is no longer possible, but the possibility of external criticality may be enhanced).

- The nominal chemical composition for the criticality evaluations of the WP design, and to suggest the range of parametric variations for additional evaluations.

The chemical compositions (and subsequent criticality evaluations) for some of the simulations are calculated for time periods to ~$6 \cdot 10^5$ years. The longer time is based on the analysis in Reference 4 (Figure C-13), which suggests that 5% of the WPs may remain flooded for longer than $2 \cdot 10^5$ years. However, it is important to note that after 10^5 years of flooding, most of the materials of interest (fissile and absorber materials) will have either been removed from the WP, reached a steady state, or been transmuted.

The calculation included elements with high neutron absorption cross sections, notably gadolinium (Gd), as well as the fissile materials. The results of this calculation will be used to ensure that the type and amount of criticality control material used in the WP design will prevent criticality.

A previous calculation of the degradation of Pu-ceramic WPs found maximum losses of ~15% of

the original Gd content of the Pu-ceramic WP (Ref. 5, Table 5.3-1). However, the water and HLW glass compositions, and the ceramic degradation rates, used in that prior study, have been superceded by new information. In addition, the development of a faster and more flexible version of the reaction-path code has made it possible to calculate degradation of the WPs under a wider range of rate combinations. Consequently, the current study provides a greater understanding of the effects of composition and rate uncertainty on the potential losses of Gd and fissile materials.

This calculation was prepared under procedure AP-3.12Q, Revision 0, ICN 0.

2. METHOD

The method used for this calculation involves the following steps:

- Use of the qualified and modified version of the EQ3/6 reaction-path code (software package, Section 4.1) for tracing the degradation of the WP. The software estimates the concentrations remaining in the aqueous solution and the composition of the precipitated solids. (EQ3 is used to determine a starting fluid composition for EQ6 calculations; it does not simulate reaction progress.)

- Evaluation of available data for degradation rates of package materials, to be used as EQ6 reaction rates (rk1 in the EQ6 "6i" files).

- Use of "solid-centered flow-through" mode (SCFT) in EQ6; in this mode, an increment of aqueous "feed" solution is added continuously to the WP system, and a like volume of the existing solution is removed, simulating a continuously-stirred tank reactor. This mode is discussed in Section 4.

- Determination of fissile material concentrations in solution as a function of time (from the output of EQ6 simulated reaction times up to $6 \cdot 10^5$ years).

- Calculation of the amount of fissile material released from the WP as a function of time (fissile material loss reduces the chance of criticality within the WP).

- Determination of concentrations of neutron absorbers, such as Gd and B, in solution as a function of time (from the output of EQ6 over times up to $6 \cdot 10^5$ years).

- Calculation of the amount of neutron absorbers retained within the WP as a function of time.

- Determination of composition and amounts of solids (precipitated minerals or corrosion products, and unreacted package materials).

Detailed description of each step is available in Section 5 of this calculation.

3. ASSUMPTIONS

All assumptions are for preliminary design; these assumptions will require verification before this calculation can be used to support procurement, fabrication, or construction activities. All assumptions are used throughout Section 5 and Section 6.

3.1 It is assumed that an aqueous solution fills all voids within WPs, and that the solutions that drip into the WP will have a composition approximating that of the J-13 well water (as given in Ref. 6, Tables 4.1 and 4.2; this composition is given in Table 5-4 of the current document) for ~10^6 years. (The J-13-like compositions are hereafter referred to as "incoming water", rather than "J-13 well water", to distinguish the idealized compositions from actual well water samples.) The basis for the first part of this assumption is that it provides the maximum degradation rate with the potential for the fastest flushing of the neutron absorber from the WP, and is thereby conservative. The basis for the second part of the assumption is that the groundwater composition is controlled largely by transport through the host rock, over pathways of hundreds of meters, and the host rock composition is not expected to change substantially over 10^6 years. For a few thousand years after waste emplacement, the composition may differ because of perturbations resulting from reactions with engineered materials and from the thermal pulse. These are not taken into account in this calculation because the corrosion allowance barrier and CRM are not expected to breach until after that perturbed period. Therefore, the early perturbation is not relevant to the calculations reported in this document. See Assumption 3.3.

3.2 It is assumed that the density of the incoming water is 1.0 g/cm^3. The basis for this assumption is that for dilute solutions, the density is extremely close to that for pure water, and that any differences are insignificant in respect to other uncertainties in the data and calculations. Moreover, this value is used only initially in EQ3/6 to convert concentrations of dissolved substances from parts per million to molalities.

3.3 The assumption that the water entering the WP can be approximated by the J-13 well water implicitly assumes: (1) that the incoming water will have only a minimal contact, if any at all, with undegraded metal in the corrosion allowance barrier, and (2) that any effects of contact with the drift liner will be minimal after a few thousand years. The basis for the first part of this assumption is that the water will move sufficiently rapidly through openings in the WP barriers such that its residence time in the corroded barrier will be too short for significant reaction to occur, and the corrosion products lining the cracks should consist primarily of inert Fe oxides. The second part of this assumption is justified by the following: (A) the drift liner at the top of the drift is expected to collapse with the roof support well before 1000 years; and (B) the water flowing through the concrete liner, dominantly along fractures, will be in contact with the degradation products of the liner, which will have come close to equilibrium with the water moving through the rock above the repository (most recent drift designs do not contain significant amounts of concrete); and (C) recent evaluations of codisposal WPs show that

degradation of the WP materials (specifically, HLW glass and steel) overwhelms the native chemistry of the incoming water (Figures 5-2 through 5-20 of Ref. 7 show pH variations of 3 to 10 in WP). Thus, even though the chemistry of the infiltrating water may vary substantially, the effects of the variations will likely be insignificant in a WP that undergoes significant alteration. An evaluation of the effects of varying incoming water chemistry is given in Section 5.3.2 of the current document.

3.4 It is assumed that water may circulate sufficiently freely in the partially degraded WP that all degraded solid products may react with each other through the aqueous solution medium. The basis for this assumption is that this provides one bound for the extent of chemical interactions within the WP.

3.5 It is assumed that 25 °C thermodynamic data can be used for the calculations. The bases of this assumption are two-fold. First, the initial breach and filling of a WP is unlikely to occur before 10^4 years (Ref. 4, Figure C-12), when the WP contents have cooled to < 50 °C (Ref. 8, Figures 3-22 and 3-24). Second, the assumption is conservative, with respect to loss of the Gd, the criticality control material. Gd carbonates and phosphates are likely to be the solubility-limiting solids for the Gd. Since the solubilities of solid carbonates and $GdPO_4 \cdot H_2O$ are temperature-independent or retrograde (Ref. 9, Tables IV and V), use of the lower-temperature database is likely to be conservative.

3.6 In most calculations, it is assumed that chromium and molybdenum will oxidize fully to chromate (or dichromate) and molybdate, respectively. The first basis of the assumption is the body of available thermodynamic data (the data0 file in the accompanying electronic media, Ref. 10), which indicates that in the presence of air the chromium and molybdenum would both oxidize to the VI valence state. Laboratory observation of the corrosion of Cr- and Mo-containing steels and alloys, however, indicates that any such oxidation would be extremely slow. In fact, oxidation to the VI state may not occur at a significant rate with respect to the time frame of interest, or there may exist stable Cr(III) or Cr(VI) solids (not present in the EQ3/6 thermodynamic database) that substantially lower aqueous Cr concentration. For the present analyses, the assumption is made that over the times of concern the oxidation will occur. The second basis of the assumption is that it is conservative with respect to solubility of $GdOHCO_3$ (the expected solubility-controlling phase for Gd); extreme acidification of the water will enhance solubility (Ref. 5, Section 5.3) and transport of Gd out of the WP, thereby separating it preferentially from fissile material.

3.7 It is assumed that the CRM (the inner barrier) of the WP will react so slowly with the infiltrating water (and the water already in the WP) as to have negligible effect on the chemistry. The bases for this assumption consist of the facts that the CRM is fabricated from Alloy 22 (see nomenclature in Section 5.1.1), which corrodes very slowly compared (1) to other reactants in the WP and (2) to the rate at which soluble corrosion products will likely be flushed out of the WP.

3.8 In most calculations, is assumed that gases in the solution in the WP will remain in equilibrium with the ambient atmosphere outside the WP. In other words, it is assumed that there is sufficient contact with the gas phase in the repository to maintain equilibrium with the CO_2 and O_2 present, whether or not this be the normal atmosphere in open air or rock gas that seeps out of the adjacent tuff. Under these conditions, the partial pressure of CO_2 exerts important controls on the pH and carbonate concentration in the solution and hence on the solubility of uranium, gadolinium and other elements. The basis of this assumption is that it is consistent with the approach taken in the viability assessment (VA) (Ref. 11, Figure 4-27), is simple, and generally causes higher losses of gadolinium at high pH, and is thus conservative. A sensitivity study on the effects of fCO_2 is given in Section 5.3.2, and calculations with variations in oxygen fugacity are presented in Sections 6.1 and 6.2.

3.9 It is assumed that precipitated solids that are deposited remain in place, and are not mechanically eroded or entrained as colloids in the advected water. The basis for this assumption is that it conservatively maximizes the size of potential deposits of fissile material inside the WP.

3.10 It is assumed that the corrosion rates used in this calculation encompass rates for microbially assisted degradation, and that the degradation rates will not be controlled principally by bacteria. The bases for this assumption are (1) steel corrosion rates measured under environmental conditions inherently include exposure to bacteria, and (2) the lack of organic nutrients available for bacterial corrosion will limit the involvement of bacteria. It is assumed that bacteria act as catalysts, particularly for processes such as the reduction of sulfate, but this catalytic effect is not expected to change significantly the types of solids formed in the WP.

3.11 It is assumed that sufficient decay heat is retained within the WP over times of interest to cause convective circulation and mixing of the water inside the WP. The basis for this assumption is the analysis in Reference 12 (Att. VI).

3.12 It is assumed that the rate of entry of water into, as well as the rate of egress from, a WP is equal to the rate at which water drips onto the WP. The basis for this assumption is that for most of the time frame of interest, i.e., long after the corrosion barriers become largely degraded, it is more reasonable to assume that all or most of the drip will enter the degraded WP than to assume that a significant portion will instead be diverted around the remains. However, the calculations include scenarios with very low drip rates, which effectively simulate diversion of the bulk of the water striking the WP.

3.13 It is assumed that the most insoluble solids for a fissile radionuclide will form, i.e., equilibrium will be reached. The basis for this assumption is conservatism; the highest chance of internal criticality occurs when the fissile solids have lowest solubility, and are thus retained in the WP.

3.14 A number of minor assumptions have been made about the geometry of the Pu-ceramic WP. The bases of these assumptions are outlined and referenced in the spreadsheet Pu-ceram.xls (Ref. 10), and are also discussed in Section 5.1. The assumptions about WP geometry are always intended to obtain the greatest accuracy in the representation, and where inadequate information is available to choose among possible WP designs, the choice that appears to lead to greatest conservatism is made.

3.15 For any WP components that were described as "304" stainless steel, without indication of the carbon grade, the alloy was assumed to be the low-carbon equivalent (see Section 5.1.1 for nomenclature). The basis of this assumption is that, in general, the carbon in the steel is totally insignificant compared to the carbon supplied by the fixed CO_2 fugacity of the EQ3/6 calculation, and to the constant influx of carbonate via the incoming water.

3.16 It is assumed that the thermodynamic behavior of hafnium (Hf) can be treated as if it were zirconium (Zr). The basis of this assumption is the extreme similarity of the chemical behaviors of the two elements (Ref. 13, p. 272). Thermodynamic data for many important Hf solids and aqueous species are lacking, thus Zr was substituted for Hf in the calculation.

3.17 It is assumed that the decay of ^{239}Pu to ^{235}U can be conservatively approximated by a simple exponential correction to the reported amounts of solids in the EQ6 runs, after completion of each run. EQ6 currently has no built-in capability to handle radioactive decay. The basis of this assumption is that it is conservative for internal criticality since Pu solids are generally less soluble than U solids. The assumption causes an overestimate of the amount of ^{235}U remaining in the WP with time. The exponential correction is not made in the tables and figures presented in this document, but is left up to the user of the calculation results. For the calculations with significant Gd loss, the loss generally occur within two half lives of ^{239}Pu, so that the correction is less than a factor of four.

4. USE OF COMPUTER SOFTWARE AND MODELS

This section describes the computer software used to carry out the calculation.

EQ3/6 Software Package–The EQ3/6 software package originated in the mid-1970s at Northwestern University (Ref. 14). Since 1978, Lawrence Livermore National Laboratory (LLNL) has been responsible for maintenance of EQ3/6. The software has most recently been maintained under the sponsorship of the Civilian Radioactive Waste Management Program of the United States Department of Energy (DOE). The major components of the EQ3/6 package include: EQ3NR, a speciation-solubility code; EQ6, a reaction-path code, which simulates water/rock interaction or fluid mixing in either a pure reaction progress mode or a time mode; EQPT, a data file preprocessor; EQLIB, a supporting software library; and various supporting thermodynamic data files. The software deals with the concepts of the thermodynamic equilibrium, thermodynamic disequilibrium, and reaction kinetics. The supporting data files contain both standard state and activity coefficient-related data. Most of the data files support the use of the Davies or B-dot equations for the activity coefficients; two others support the use of Pitzer's equations. The temperature range of the thermodynamic data on the data files varies from 25 °C only for some species to a full range of 0-300 °C for others. EQPT takes a formatted data file (a "data0" file) and writes an unformatted "data1" file, which is actually the form read by EQ3NR and EQ6. EQ3NR is useful for analyzing groundwater chemistry data, calculating solubility limits, and determining whether certain reactions are in states of partial equilibrium or disequilibrium. EQ3NR is also required to initialize an EQ6 calculation.

EQ6 simulates the consequences of interactions among an aqueous solution and a set of degrading reactants. This code operates both in a pure reaction progress frame and in a time frame. In a time frame calculation, the user specifies rate laws for the progress of the irreversible reactions. Otherwise, only relative rates are specified. EQ3NR and EQ6 use a hybrid Newton-Raphson technique to make thermodynamic calculations. This method is supported by a set of algorithms that create and optimize starting values. EQ6 uses an ordinary differential equation (ODE) integration algorithm to solve rate equations in time mode. The codes in the EQ3/6 package are written in FORTRAN 77 and have been developed to run on personal computers (PCs) running Microsoft DOS or Windows, and under the UNIX operating system. Further information on the codes of the EQ3/6 package is provided in References 14, 15, 16, and 17.

Solid-Centered Flow-through Mode–EQ6 Version 7.2b, as distributed by LLNL, does not contain an SCFT mode. To add this mode, it is necessary to change the eq6.for source code, and recompile the source. However, by using a variant of the "special reactant" type built into EQ6, it is possible to add the functionality of SCFT mode in a very simple and straightforward manner. This mode was added to EQ6 per Software Change Request (SCR) LSCR198 (Ref. 18), and the Software Qualification Report (SQR) for Media Number 30084-M04-001.

The new mode is induced with a "special-special" reactant. The EQ6 input file nomenclature for this new mode is jcode=5; in the Daveler format, it is indicated by the reactant type

DISPLACER. The jcode=5 is immediately trapped and converted to jcode=2, and a flag is set to indicate the existence of the DISPLACER reactant. Apart from the input trapping, the distinction between the DISPLACER and SPECIAL reactants is seen only in one 9-line block of the EQ6 FORTRAN source code (in the reacts subroutine), where the total moles of elements in the rock plus water system (mte array) is adjusted by adding in the DISPLACER reactant, and subtracting out a commensurate amount of the total aqueous elements (mteaq array).

4.1 SOFTWARE APPROVED FOR QUALITY ASSURANCE (QA) WORK

The addendum to EQ6 was approved for QA work by the M&O (M&O identifier CSCI: UCRL-MA-110662 V 7.2b; final approval in Ref. 18). An installation and test report (Ref. 19) was written and submitted to Software Configuration Management (SCM), and the proper installation was verified before the runs described in this calculation were made. The implementation of the SCFT mode is covered by SCR LSCR198, and the SQR for Media Number 30084-M04-001. The SCFT addendum was installed on three of the Central Processing Units (CPUs), and the installation and test reports were filed and returned to SCM before the calculations were run. All calculations were run under the Windows 95 operating system. In this study EQ3/6 was used to provide the following:

- A general overview of the expected chemical reactions.
- The degradation products from corrosion of the waste forms and canisters.
- An indication of the minerals, and their amounts, likely to precipitate within the WP.

The programs have not been used outside the range of parameters for which they have been verified. Some runs with high HLW glass degradation rates and low flush rates had temporary excursions to high ionic strength, above the range for which the B-Dot ionic strength correction has been validated. However, the excursions were temporary, and they occurred in the early part of the calculation, which principally sets up the mass balance for the completion of the run. Results from these high-ionic strength runs are included for conservatism since such runs likely overestimate Gd loss. The EQ3/6 calculations reported in this document used Version 7.2b of the code, which is appropriate for the application, and were executed on Pentium series (including "Pentium II") PCs.

The EQ3/6 package has been verified by its present custodian, LLNL. The source codes were obtained from SCM in accordance with the Office of Civilian Radioactive Waste Management AP-SI.1Q Revision 1, ICN 0 procedure. The code was installed on the Pentium and Pentium II PCs according to an M&O-approved Installation and Test procedure (Ref. 19).

4.2 SOFTWARE ROUTINES

Spreadsheet analyses were performed with the Office 97 version of Microsoft Excel, installed on a PC running Microsoft Windows 95. The specific spreadsheets, used for results reported in this document, are included in the electronic media (Ref. 10).

4.3 MODELS

None used.

5. CALCULATION

The calculations begin with selection of data for compositions, amounts, surface areas, and reaction rates of the various components of Pu-ceramic WPs. These quantities are recalculated to the form required for entry into EQ6. For example, weight percentages of elements or component oxides are converted to mole fractions of elements; degradation rates in μm/y are converted to mole/(cm^2·s), etc. Spreadsheets (Ref. 10) provide details of these calculations. The final part of the input to EQ6 consists of the composition of incoming water together with a rate of influx to the WP that corresponds to suitably chosen percolation rates into a drift and drip rate into a WP (Section 5.1.1.3). The EQ6 output provides the results of the chemical degradation calculations for the WP, or components thereof. In selected cases, the degradation of the WP is divided into phases, e.g., degradation of HLW glass before breach of the stainless steel cans, and subsequent exposure of the Pu-ceramic to water. The results include the compositions and amounts of solid products and of elements dissolved in solution. Details of the results are presented in Section 6.

In all tables from this document, the number of digits reported does not necessarily reflect the accuracy or precision of the calculation. In most tables, two to four digits after the decimal place have been retained, to prevent round-off errors in subsequent calculations.

Some "preliminary" and "prototype" drawings (Refs. 22 and 23) have been used to calculate geometric surface areas and masses of WP components, as inputs for EQ6. However, the results of the EQ6 runs should change little due to changes in package design. The surface areas are used only as part of the rate equation, such that the total rate is: (surface area)·(EQ6 rk1 parameter). The variation in rk1 is far larger than the variation in component surface areas that may results from design differences. Geometric surface areas of HLW glass, ceramic, and stainless steel are not expected to vary by more than 50% among WP designs (as judged by the comparison of areas used in this calculation, versus Ref. 5). In contrast, the rk1 are highly uncertain and are varied, as part of this calculation, over 1 to 3 orders of magnitude. Therefore, any variations in the geometric surface areas are trivial and are subsumed in the parametric rate study built into this calculation. Similar arguments can be made about the compositions and masses of HLW glass and steel; Section 5.3.3 (Table 5-9) shows that large variations in HLW glass composition have relatively small effects.

5.1 CALCULATION INPUTS

5.1.1 WP Materials and Performance Parameters

This section provides a brief overview of the physical and chemical characteristics of Pu-ceramic WPs, and describes how the WP is represented in the EQ6 inputs. The conversion of the WP physical description, into parameters suitable for the EQ6 input files, is performed by the spreadsheet Pu-ceram.xls (Ref. 10). Additional details of the description may be found in References 1, 2, 20, 21, 22, and 23, and the references cited therein.

Material nomenclature used throughout this document includes: SB-575 N06022 (hereafter referred to as Alloy 22), UNS N06625 and SA-240 S30403 (hereafter referred to as 304L), and SA-516 (hereafter referred to as A516).

5.1.1.1 Physical and Chemical Form of Pu-Ceramic WPs

It is convenient to consider the Pu-ceramic WP as several structural components, as illustrated in Figures 5-1 and 5-2 (the latter from Ref. 2); specifically:

(1) The outer shell, consisting of the CAM and the inner Alloy 22 CRM.

(2) The "outer web", a carbon steel (A516) structural basket designed to hold the HLW glass pour canisters (GPCs) in place.

(3) The 5 GPCs, which consist of 304L canisters filled with solidified HLW glass.

(4) The 28 cans that contain the Pu-ceramic disks; the 7 magazines that hold the cans; and the rack that holds the 7 magazines in place within the GPC. These are all constructed of 304L stainless steel. After the rack-and-magazine assembly is emplaced within the GPC, molten HLW glass will be poured into the GPC, encasing the internal components.

(5) The Pu-ceramic disks. Each can holds 20 ceramic disks, for a total of 560 = (20 disks)·(4cans)·(7 magazines) disks per GPC, or 2800 disks in all 5 GPCs.

The details of each component are given in spreadsheet Pu-ceram.xls (Ref. 10).

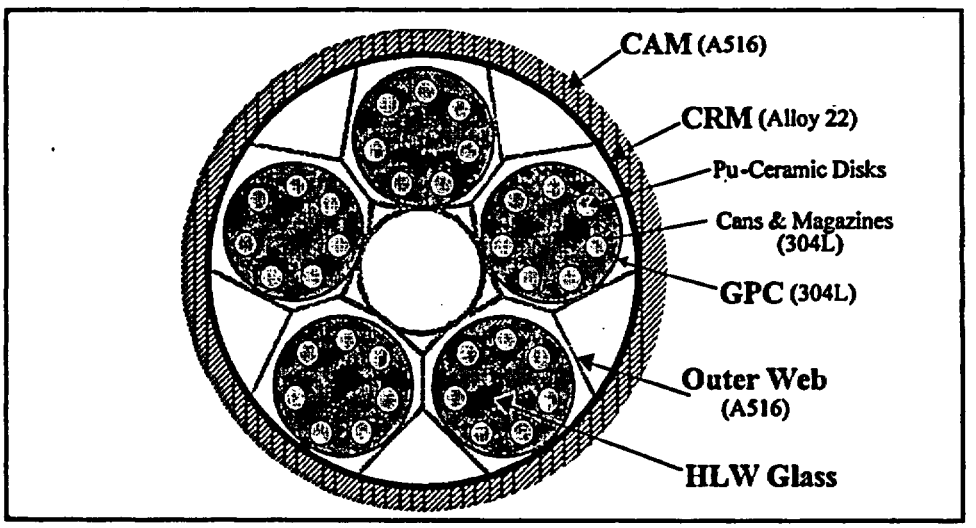

Figure 5-1. Cross-section of Pu-ceramic Waste Package

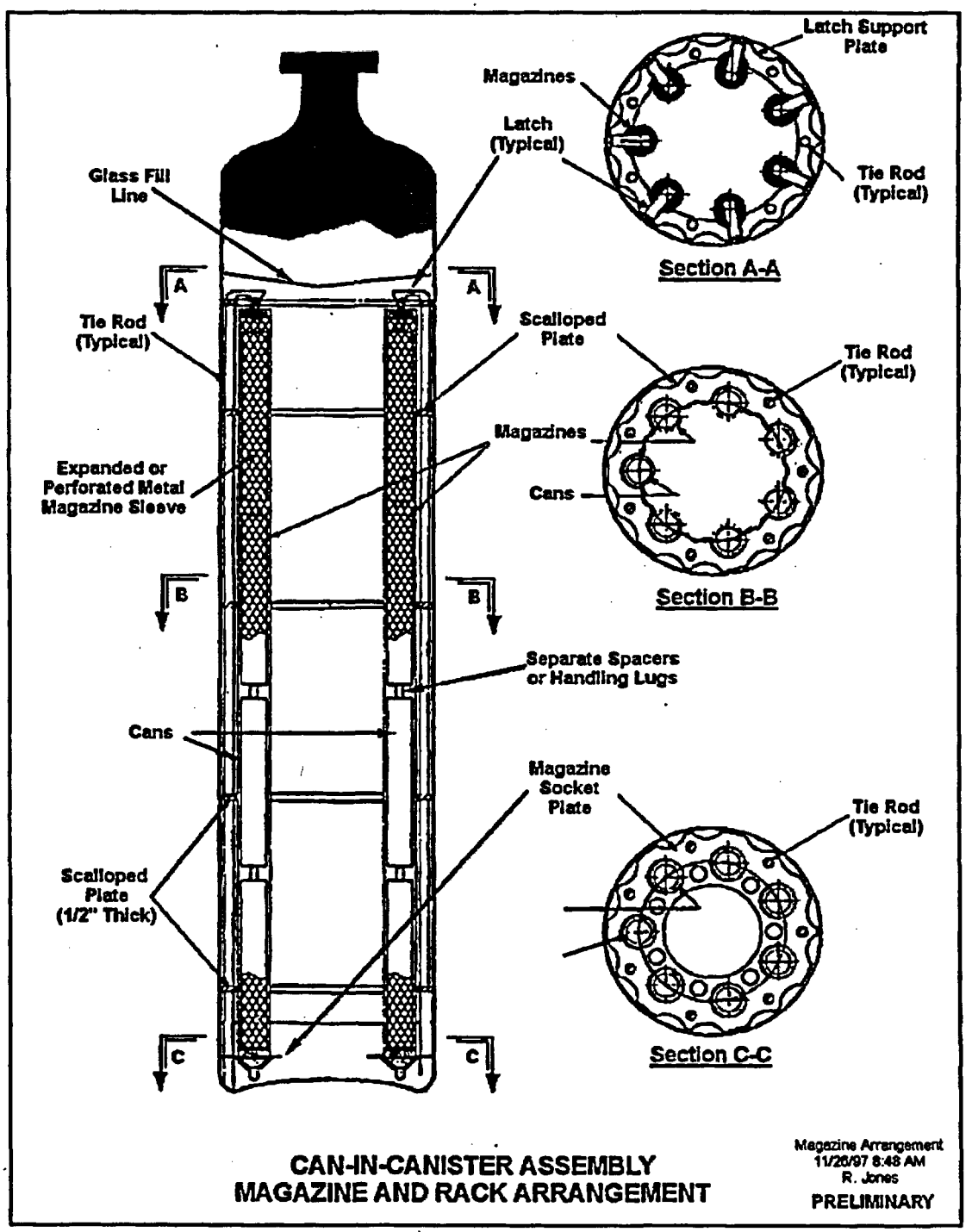

Figure 5-2. Lengthwise Section of GPC, with Magazine and Rack Assembly

Table 5-1 provides a summary of the compositions of the principal alloys used in the calculations, along with reasonable high and average degradation rates. For a comparable specific surface area, the carbon steel is expected to degrade much more rapidly than the stainless steels (304L). In addition, the stainless steels contain significant amounts of Cr and Mo, and under the assumption of complete oxidation (Assumption 3.6), should produce more acid, per unit volume, than the carbon steel.

Table 5-1. Steel Compositions[a] and Degradation Rates[b]

	A516 Carbon Steel		304L Stainless Steel	
Element	(wt%)	(mole)	(wt%)	(mole)
C	0.28	2.3312E-02	0.03	2.4977E-03
Mn	1.045	1.9021E-02	2.00	3.6405E-02
P	0.035	1.1299E-03	0.045	1.4528E-03
S	0.035	1.0915E-03	0.03	9.3557E-04
Si	0.29	1.0326E-02	0.75	2.6704E-02
Cr	0.000	0.000E+00	19.00	3.6541E-01
Ni	0.000	0.000E+00	10.00	1.7039E-01
N	0.000	0.000E+00	0.10	7.1394E-03
Fe	98.315	1.7604E+00	68.045	1.2184E+00
Total	100.00	1.8153	100.00	1.8294
Density (g/cm^3)	7.850		7.940	
Rate	(μm/y)	(mole/(cm^2·s))[c]	(μm/y)	(mole/(cm^2·s))[c]
Average	35	6.7063E-12	0.1	2.5160E-14
High	100	2.4875E-11	1	2.5160E-13

NOTES: [a]Compositions from Reference 24, pages 10 and 17 (Sections 5.2 and 5.4). Details given in Pu-ceram.xls, sheet 'Compositions'.
[b]Degradation rates from Reference 25, pages 11-13 (304L), and Reference 26, pages 5-44 to 5-55, Figures 5.4-3, 5.4-4, and 5.4-5 (carbon steel). Conversions performed in Pu-ceram.xls, sheet "Rates".
[c]For 1 mole = 100 g.

Table 5-2 gives the molar composition of the HLW glass used in the calculations (Ref. 27, Att I, p. I-7). The actual HLW glass composition used in the GPCs may vary significantly from these values since the sources of the HLW glass and melting processes are not currently fixed. For example, compositions proposed for Savannah River HLW glass vary by a factor of ~6 in U_3O_8 content, from 0.53 to 3.16 wt% (Ref. 28, Table 3.3.8). The silica and alkali contents (Na, Li, and K) of the HLW glass have perhaps the most significant bearing on EQ6 calculations. The amount of silica in the HLW glass strongly controls the amount of clay that forms in the WP, and the silica activity controls the presence of insoluble uranium phases, such as soddyite ($(UO_2)_2SiO_4 \cdot 2H_2O$). The alkali content can induce pH to rise in the early stages of the EQ6 run,

as HLW glass degrades. The Si and alkali contents in Table 5-2 are typical for proposed DOE HLW glasses (Ref. 28, Table 3.3.8). The effects of such compositional variations are examined in the sensitivity studies discussed in Section 5.3 of this document.

Rates for HLW glass degradation were taken from Reference 26 (Figure 6.2-5) and normalized in spreadsheet Pu-ceram.xls, sheet "Rates" (Ref. 10). The high rate corresponds approximately to pH 9 at 70 °C, and the low rate to pH 8 at 25 °C. In the transmuted composition of the HLW glass, the content of an element in the HLW glass is the sum of its isotopes listed in HLW glass composition in Table 5-2.

Table 5-2. HLW Glass Composition and Rates

Element[a]	Composition	
	(wt%) Not Normalized[b]	(mole) Normalized[c]
O	4.452E+01	2.808E+00
U	1.867E+00	7.915E-03
Np	9.471E-04	4.032E-06
Pu	1.480E-02	6.242E-05
Ba	1.120E-01	8.258E-04
Al	2.319E+00	8.672E-02
S	1.287E-01	4.051E-03
Ca	6.582E-01	1.657E-02
P	1.398E-02	4.555E-04
Cr	8.210E-02	1.593E-03
Ni	7.308E-01	1.257E-02
Pb	6.062E-02	2.952E-04
Si	2.177E+01	7.820E-01
Ti	5.934E-01	1.251E-02
B	3.193E+00	2.980E-01
Li	1.468E+00	2.134E-01
F	3.167E-02	1.682E-03
Cu	1.518E-01	2.410E-03
Fe	7.349E+00	1.328E-01
K	2.972E+00	7.671E-02
Mg	8.201E-01	3.405E-02
Mn	1.549E+00	2.845E-02
Na	8.580E+00	3.766E-01
Cl	1.153E-01	3.281E-03
Total	9.909E+01	4.901E+00
Rate	g/(m^2·day)[d]	mole/(cm^2·s)
Low	1.00E-04	1.157E-15
High	3.00E-02	3.472E-13

NOTES: [a] ^{238}Pu decayed to ^{234}U; ^{241}Pu decayed to ^{237}Np; Ag, Cs, Zn, and Th removed because of low quantity, chemical insignificance, and/or lack of reliable thermodynamic data.
[b] Basic Reference 27, Attachment I, page I-7.
[c] Normalized to 1 mole = 100 g. Conversions performed in spreadsheet Pu-ceram.xls, sheet "Compositions."
[d] Reference 26, page 6-5 and Figure 6.2-5; fracture factor = 30, conversions performed in Pu-ceram.xls, sheet "Rates".

Table 5-3 summarizes the composition of the "baseline" ceramic used for all the calculations reported herein. The three rates chosen for the calculations are based on Slide 32 of Reference 21; these rate data were the best available at the time the study began. Very recently, LLNL has provided updated rates that are a factor of 3 to 10 lower for the same conditions (Figure 6.1 of

Ref. 2). The new LLNL rate data are shown in Figure 5-3. However, LLNL has also determined that the specific surface areas of the Pu-ceramic samples were ~3 to 10 times higher than previously thought, due in part to the sample porosity. Since the total reaction rate for the ceramic is the product of surface area and the fundamental rate constant, the two new observations by LLNL (of lower rates and higher specific surface area) tend to cancel out. Hence this study retains the original range of rates, given in Table 5-3, spanning nearly three orders of magnitude.

Table 5-3. Composition[a] and Degradation Rates[b] of Pu-ceramic

Oxide	Composition	
	(wt%)	(moles metal)
CaO	10.0	1.78E-01
HfO_2 [c]	10.6	5.04E-02
UO_2	23.7	8.78E-02
PuO_2	11.9	4.35E-02
NpO_2	0.0	3.91E-04
Gd_2O_3	7.9	4.36E-02
TiO_2	35.9	4.49E-01
Al_2O_3	0.0	0.00E+00
Total	100.0	8.53E-01

Rate	(g/(m²·day))	(mole/(cm²·s))[d]	Conditions
Low	5.00E-05	5.78704E-16	25 °C, pH=6, crystalline
Average	1.00E-03	1.15741E-14	75 °C, pH=2 to 4, crystalline
High	3.00E-02	3.47222E-13	75 °C, pH=2 to 4, radiation-damaged (average rate times factor 30 multiplier; Ref. 1, Section 6)

NOTES: [a]Reference 1, Table 3.1.
[b]Reference 21, slide 32.
[c]Replaced by Zr in EQ6 runs, then converted back to Hf for mass calculations.
[d]For 1 mole special reactant = 100 g.

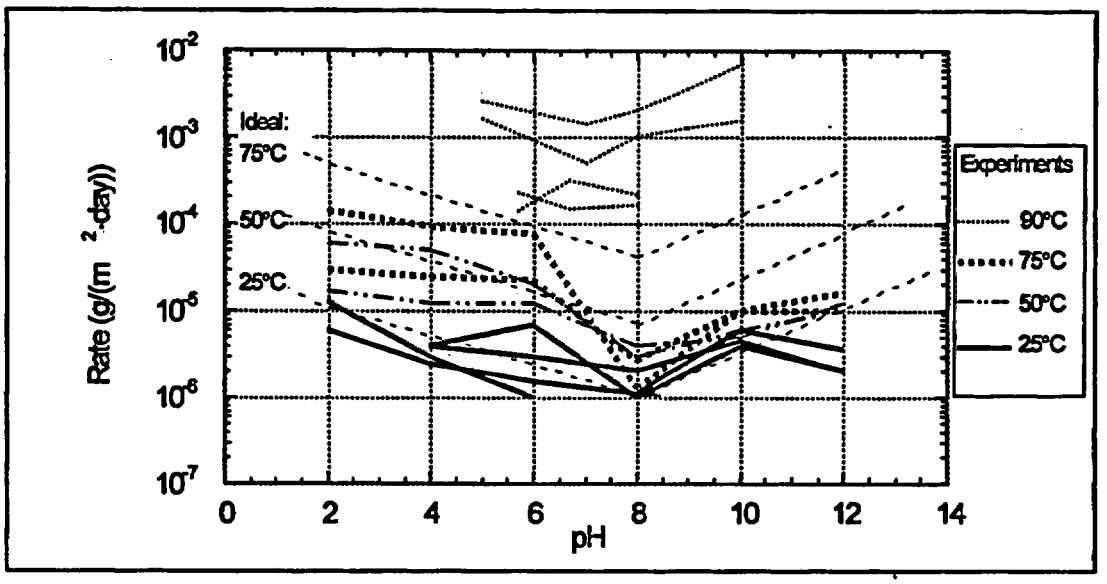

NOTE: Data for all tests of pyrochlore-based composite ceramics, and single-phase zirconolite and pyrochlore (Ref. 2, Figure 6.1). The thin, dashed "Ideal" lines (for 25, 50, and 75 °C) give LLNL model.

Figure 5-3. Normalized Rates for Single-pass Flow Test

5.1.1.2 Chemical Composition of Incoming Water

It was assumed that the incoming water would have a composition approximating that of the J-13 well water (Assumptions 3.1 and 3.3). Table 5-4 contains the EQ3NR constraints for the incoming water (based on EQ3NR input file j13noc30.3i), and the EQ6 elemental molal composition used for this calculation. The basic composition is taken from Harrar et al. (Ref. 6, Tables 4.1 and 4.2) and represents the best estimates of a committee assembled specifically to review the composition of J-13 well water. For those elements listed as "trace" constituents in Table 5-4, an arbitrary small molality (10^{-16}) was added to assure numerical stability. Section 5.3.2 of the current document contains a discussion on the effect of varying the incoming water compositions.

Table 5-4. EQ3NR and EQ6 Compositions of Incoming Water

EQ3NR Input File Constraints for Incoming Water Composition					EQ6 Input File Elemental Composition for Incoming Water	
Component/ Species	Basis Switch	Concentration	Units		Element	(moles)
redox		-0.7	log fO_2		O	5.552E+01
Na^+		4.580E+01	mg/l		Al	2.553E-08
$SiO_2(aq^a)$		6.097E+01	mg/l		B	1.239E-05
Ca^{++}		1.300E+01	mg/l		Ba	1.000E-16
K^+		5.040E+00	mg/l		Ca	3.244E-04
Mg^{++}		2.010E+00	mg/l		Cl	2.014E-04
Li^+		4.800E-02	mg/l		Cr	1.000E-16
H^+		8.1	pH		Cu	1.000E-16
HCO_3^-	$CO_2(g)$	-3	log fCO_2		F	1.147E-04
$O_2(aq^a)$		5.600E+00	mg/l		Fe	3.600E-12
F^-		2.180E+00	mg/l		Gd	1.000E-16
Cl^-		7.140E+00	mg/l		H	1.110E+02
NO_3^-	$NH_3(aq^a)$	8.780E+00	mg/l		C	2.094E-03
SO_4^{--}		1.840E+01	mg/l		P	1.261E-06
$B(OH)_3(aq^a)$		7.660E-01	mg/l		K	1.289E-04
Al^{+++}	Diaspore	0	Mineral		Li	6.915E-06
Mn^{++}	Pyrolusite	0	Mineral		Mg	8.270E-05
Fe^{++}	Goethite	0	Mineral		Mn	3.054E-16
HPO_4^{--}		1.210E-01	mg/l		Mo	1.000E-16
Ba^{++}	Trace	1.000E-16	Molality		N	1.416E-04
CrO_4^{--}	Trace	1.000E-16	Molality		Na	1.992E-03
Cu^{++}	Trace	1.000E-16	Molality		Ni	1.000E-16
Gd^{+++}	Trace	1.000E-16	Molality		Np	1.000E-16
MoO_4^{--}	Trace	1.000E-16	Molality		Pb	1.000E-16
Ni^{++}	Trace	1.000E-16	Molality		Pu	1.000E-16
Np^{++++}	Trace	1.000E-16	Molality		S	1.915E-04
Pb^{++}	Trace	1.000E-16	Molality		Si	1.015E-03
Pu^{++++}	Trace	1.000E-16	Molality		Tc	1.000E-16
TcO_4^-	Trace	1.000E-16	Molality		Ti	1.000E-16
$Ti(OH)_4(aq^a)$	Trace	1.000E-16	Molality		U	1.000E-16
UO_2^{++}	Trace	1.000E-16	Molality		Zr	1.000E-16
$Zr(OH)_2^{++}$	Trace	1.000E-16	Molality			

NOTE: [a]Aqueous

5.1.1.3 Drip Rate of Incoming Water

It is assumed (Assumption 3.12) that the drip rate onto a WP is the same as the rate at which water flows through the WP. Four drip rates were used: 0.0015, 0.015, 0.15, and 0.5 m^3/year per WP. The justification for these rates is given in Section 5.1.1.3 of Reference 7.

5.1.1.4 Densities and Molecular Weights of Solids

The current SCFT version of EQ6 (Section 4.2 of this document) automatically calculates total mineral volumes, using the molar volume values (`VOPrTr`) embedded in the EQ3/6 data0.nuc.R8d file (included in the electronic media, Ref. 10). Molar volumes are not available for many solids that are in the EQ6 database; such solids are flagged in the database with fictitious molar volumes of "500.000." However, the data0 file contains valid molar volume entries for the solids that comprise the vast bulk of the volume in the current study. The new SCFT version of EQ6 automatically calculates the total volume of solids, and outputs the volumes in the *.elem_min.txt and *.elem_tot.txt files (where the asterisk denotes the root file name in Table 6-1); the placeholder "500.000" entries are ignored.

5.1.1.5 Atomic Weights

Atomic weights were taken from References 29 and 30, and are listed in spreadsheet Pu-ceram.xls, sheet "AtomWts" (Ref. 10).

5.2 DATA CONVERSION

The data presented in Section 5.1 are transformed into EQ3/6 format by converting mass fractions into mole fractions; normalizing surface areas, volumes, and moles to 1 liter reactive water in the system; and converting rates to mole/(cm^2·s). Most of these conversions are straightforward and are performed in the spreadsheets, which are included in the electronic media for this document (Ref. 10). Spreadsheet Pu-ceram.xls (1) calculates volumes and areas of WP components (sheets "Magazine,Rack,Can,Disk" and "GPC & Outer Web"); (2) converts raw percent compositions to normalized molar compositions (sheet "Compositions"); (3) converts experimental reaction rates (in units such as μm/y) to EQ6 units (mole/(cm^2·s)), and converts drip rates in m^3/y to normalized mole/(cm^2·s) for the EQ6 system (sheet "Rates"); and (4) calculates the system void volume, normalizes the WP component volumes and areas to the EQ6 system containing 1 liter void space, and calculates the EQ6 moles of each component from the normalized volumes, densities, and molecular weights (sheet "Void&Norm").

In Section 6, the "moles" in plots are for the sub-sampled (1 liter fluid) EQ6 system; all EQ6 solid special reactants (i.e., WP steels, HLW glass, and ceramic) are converted to 100 g/mole. To obtain the actual kg mass of a reactant in the WP, multiply *plotted* moles by 459.3965 = (0.1 kg/mole "special reactant")·(4593.965 liters void space in initial system). To obtain the actual mass of a mineral in the WP, multiply *plotted* moles by (mineral molecular weight)·(0.001 kg/g)·(4593.965 liters void space in initial system). The mineral molecular weights are given in

the EQ3/6 database (data0.nuc.R8d), which is included in the electronic file distribution for this document (Ref. 10). (Some of the older calculations used the data0.nuc.R8a (included in the Ref. 10) and dat0.nuc.R8p databases. The "R8a" version is identical to R8d, except the latter contains a molar volume for rhabdophane; since the latter phase is a trivial fraction of the total solids volume, this difference is insignificant. The "R8p" is identical to R8a, except is contains data for a hypothetical Pu-phosphate, exactly as described in Reference 7 (p. 51). Since the hypothetical Pu-phosphate solid never precipitated in these runs, there was no functional difference among the three databases.) Note that 4593.965 liters is from the variable VVOIDS in sheet "Void&Norm" of spreadsheet Pu-ceram.xls (VVOIDS is given in cm^3, and must be divided by 1000 cm^3/l to obtain 4593.965).

5.3 PREPARATORY STUDIES: UPDATED COMPOSITIONS AND THERMOCHEMICAL DATA

Since the issue of the original study of Pu-ceramic degradation geochemistry (Ref. 5), new information became available on three topics: (1) the thermochemistry of the Gd carbonate system; (2) the projected long-term chemistry of the repository waters; and (3) the chemistry of the HLW glass produced by Savannah River Site (SRS). Before the matrix of calculations described in Section 5.4 was designed, three sensitivity studies had been performed to determine how the new data might change results of EQ6 calculations. These sensitivity studies used the input files for Runs 4 and 6 from Reference 5 (Table 5.3-1); Run 4 produced the highest Gd loss in that prior study. All input and spreadsheet files referred to in this section can be found on the electronic media accompanying this calculation (Ref. 10).

5.3.1 Effects of Gd Carbonate Thermochemistry

The previous Pu-ceramic calculations (Ref. 5) used a custom version of the Swedish Nuclear Fuel and Waste Management Co. (SKB) thermodynamic database (Ref. 31), prepared by LLNL. The Pu-ceramic waste forms contain Gd, but little or no phosphate; the encasing HLW glass contains some phosphate, but not enough to precipitate all the Gd in the ceramic. Thus, when these waste forms degrade in water, Gd phosphate may not be the solubility-limiting phase. When the SKB database was used in the previous study, the calculations indicated that $GdOHCO_3$ would be the solubility-limiting phase for Gd (Ref. 5, Figures 5.3.4-2 and 5.3.4-5). However, the thermodynamic data for this phase were originally estimated from the data for $NdOHCO_3$, and there was substantial uncertainty in the SKB data for the hydroxyl and carbonate aqueous complexes of Gd.

Recently, Weger et al. (Ref. 32) performed experiments to determine the solubility of three solid Gd carbonates and one hydroxide, and estimated the formation constants for several dissolved Gd carbonate and hydroxyl complexes. A version of the SKB database was customized to include the new Weger et al. data; this new database is hereafter referred to as the Weger database. Runs 4 and 6 reported in Reference 5 (Table 5.3-1) were repeated using this new database. In brief, the new Weger et al. data appear to have no significant impact and produce approximately the same calculated Gd losses, as were obtained with the original SKB database.

5.3.1.1 Entry and Testing of the New Data

When thermodynamic data are added to the EQ3/6 databases, it is important to achieve the highest possible consistency. Large errors can occur if the logarithms of stability constants (*log K*) are derived from reaction free energies (ΔG^{rxn}) reported in the literature, without correcting for the differences in standard state free energies G_f^0. In most experiments, the measured quantities are actually closer to the *log K*s. While $G_f^0/(RT)$ values are used in the formal statement of the statistical sum f(χ) (e.g., Equation 8 in Ref. 32), quantities of the form:

$$-\ln K = (G_f^0/RT)_{NaGd(CO_3)_2\cdot 6H_2O} - (G_f^0/RT)_{Na^+} - (G_f^0/RT)_{Gd^{3+}} - 2\cdot(G_f^0/RT)_{CO_3^{2-}} - 6\cdot(G_f^0/RT)_{H_2O} \quad \text{(Eq. 1)}$$

are actually determined in the minimization of f(χ).

For the current calculations, the $G_f^0/(RT)$ values reported in Table 2 of Reference 32 were used to calculate *log K*'s in terms of the basis species used in EQ3/6 (H^+, H_2O, HCO_3^-, Na^+, and Gd^{3+}).

The spreadsheet GdCO3_Weger_Rai_2_EQ6.xls was used to perform thermochemical conversions. As a cross-check, the *log K*'s for formation of $Gd(OH)_3^0$ (aq), $Gd_2(CO_3)_3$, and $NaGd(CO_3)_2\cdot 6H_2O$ were calculated in terms of the basis species used in Reference 32, and compared with the values in Table 4 of Reference 32. The results agree to the number of significant digits reported by Weger et al. Table 5-5, derived from GdCO3_Weger_Rai_2_EQ6.xls, details the conversion of the Weger et al. data into EQ3/6 format. The value of the gas constant, 1.987216 cal/(mole·K), was taken from Reference 30 (p. 57). The Weger et al. speciation does not use all the hydroxyl and carbonate complexes included in the SKB database; these additional SKB complexes were removed from the Weger database for the purposes of testing.

Table 5-5. Conversion of Weger et al. Data to EQ3/6 Basis

Species	G_f^o/(RT) (Ref. 32, Table 2)	G_f^o, kcal 25 °C, (Ref. 32)	G_f^o, kcal 25 °C, EQ3/6	NOTES	$-\ln K$	$\log_{10} K$	Equation, EQ6 Format
H_2O	-95.663	-56.6792	-56.688	basis			
Na^+	-105.651	-62.597	-62.591	basis			
OH^-	-63.435	-37.5845	-37.595	basis			
CO_3^{2-}	-212.944	-126.167	-126.191	basis (Ref. 32)			
HCO_3^-	-236.751	-140.272	-140.282	basis, EQ6			
Gd^{3+}	-266.65	-157.987	-158.6	basis			
$Gd(OH)_2^+$	-418.603				-39.373	17.09948	$Gd(OH)_2^+ + 2H^+ = Gd^{3+} + 2H_2O$
$Gd(OH)_3$ (aq[a])	-491			≥ -491 (Ref. 32)	-62.639	27.20377	$Gd(OH)_3$ (aq) + $3H^+ = Gd^{3+} + 3H_2O$
$Gd(OH)_5^{2-}$	-626.5				-118.465	51.4487	$Gd(OH)_5^{2-} + 5H^+ = Gd^{3+} + 5H_2O$
$Gd(CO_3)^+$	-497.015				-6.386	2.773405	$Gd(CO_3)^+ + H^+ = Gd^{3+} + HCO_3^-$
$Gd(CO_3)_2^-$	-720.837				-19.315	8.388398	$Gd(CO_3)_2^- + 2H^+ = Gd^{3+} + 2HCO_3^-$
$Gd(CO_3)_3^{3-}$	-940.412				-36.491	15.84784	$Gd(CO_3)_3^{3-} + 3H^+ = Gd^{3+} + 3HCO_3^-$
$Gd(OH)_3$ (c)	-519.19				-34.449	14.96101	$Gd(OH)_3$ (c) + $3H^+ = Gd^{3+} + 3H_2O$
$NaGd(CO_3)_2{:}6H_2O$	-1419.77				-0.011	0.004777	$NaGd(CO_3)_2{:}6H_2O + 2H^+ = Na^+ + Gd^{3+} + 2HCO_3^- + 6H_2O$
$Na_3Gd(CO)_3$	-1275.54			Ignore H_2O	-18.316	7.954538	$Na_3Gd(CO_3)_3$ (c) + $3H^+ = 3Na^+ + Gd^{3+} + 3HCO_3^-$
$Gd_2(CO_3)_3$	-1255.81			Ignore H_2O	12.257	-5.32315	$Gd_2(CO_3)_3 + 3H^+ = 2Gd^{3+} + 3HCO_3^-$

NOTES: [a]Aqueous

To test the Weger database, EQ6 runs were used to simulate the solubility experiments for $Gd_2(CO_3)_3$ (Ref. 32, Figure 3 and Table A.3). The EQ3NR and EQ6 input files are included in the electronic attachment (Ref. 10), as files weger.3i, weger2s.6i, and weger3s.6i. Figure 5-4 shows the results of the comparison (calculated via weg_fig3.xls). The discrete symbols represent the experimental data (Ref. 32, Table A.3). The agreement between the EQ6 calculation and the experiments is good, given the spread in experimental results and the inherent uncertainty in the EQ6 "B-Dot" ionic strength corrections. The B-Dot method is normally considered accurate only for ionic strength < 1, and the Weger et al. experiments reached ionic strengths > 3.

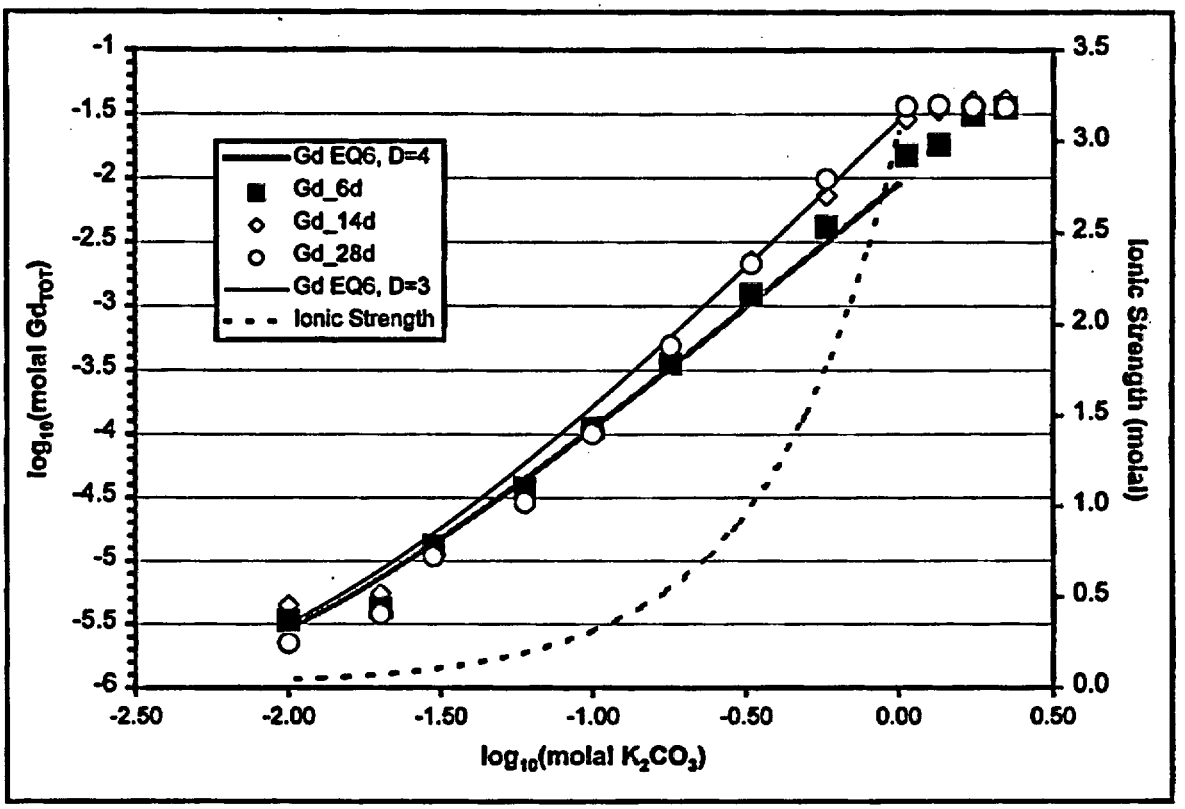

NOTES: EQ6 calculations are given by lines; Weger et al. (Ref. 32) 6-day, 14-day, and 28-day experiments are given by discrete symbols. The top unbroken line is calculated assuming a B-Dot hard-core diameter (D) of 3.0 Å for $Gd(CO_3)_3^{3-}$, and the bottom, thicker unbroken line uses the default hard-core diameter of 4.0 Å. The dashed line shows the ionic strength calculated by EQ6.

Figure 5-4. Comparison of EQ6 Calculations with Weger et al. Experiments

5.3.1.2 Comparison of Pu-Ceramic Runs with and without New Data

To test the consequences of using the Weger database, versus the SKB database, run numbers 4 and 6 from Reference 5 (Table 5.3-1) were repeated with both datasets. To ensure a uniform basis for comparison, both calculations were performed with the new addendum to EQ3/6 (described in Section 4.2 of this calculation).

Table 5-6 summarizes the net Gd losses for the two runs, using both databases. Figures 5-5 and 5-6 plot results for runs 4 and 6, respectively (the "moles" on the right are for the normalized EQ6 system, as discussed in Reference 5 (p. 24).

Table 5-6. Percent Loss of Gadolinium for Entire WP

Database	Run 4	Run 6
SKB	14.8625	12.9599
Weger	14.4983	12.9537

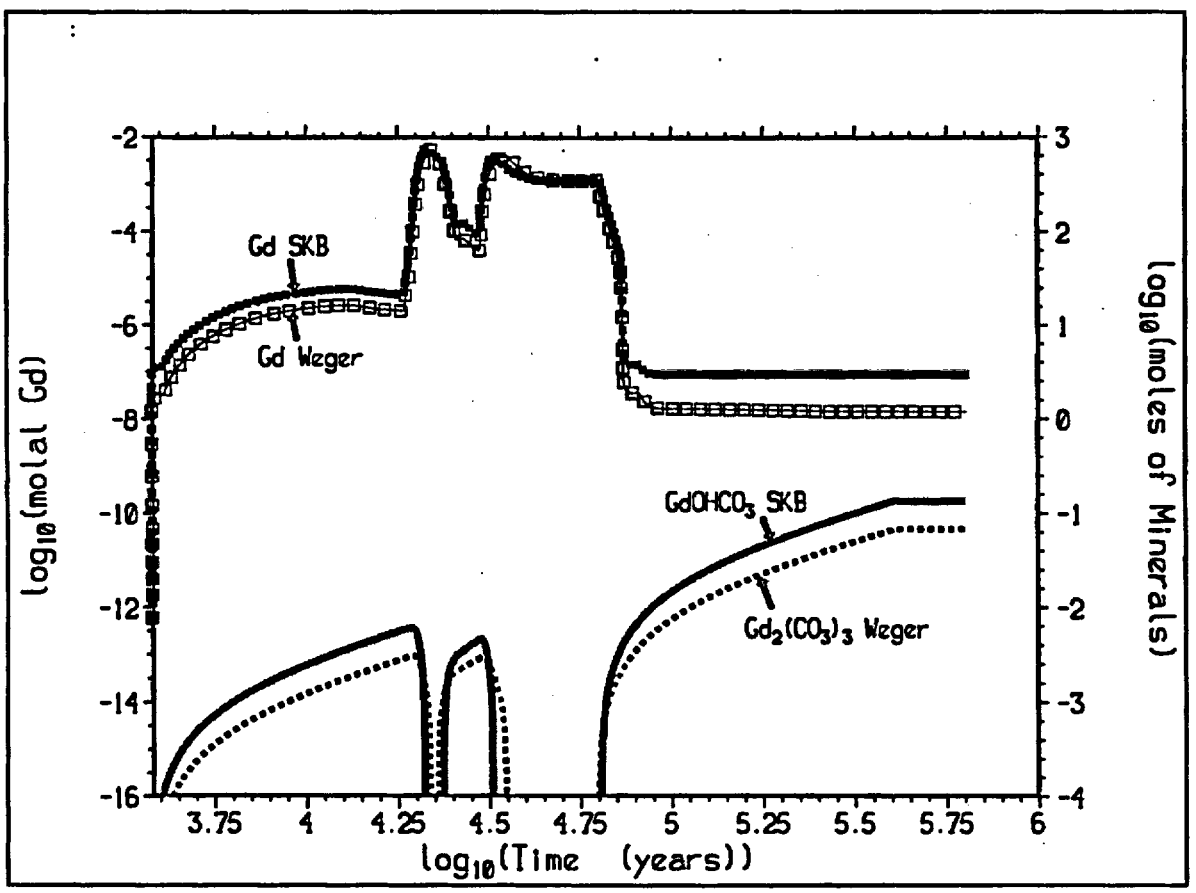

NOTE: Runs described in Reference 5, Table 5.3-1.

Figure 5-5. Run 4: Aqueous Gd and Gd Minerals Formed, SKB versus Weger et al.

For old run 4 (Figure 5-5), the CO_2 fugacity is buffered to ~$10^{-2.5}$ bar, and the pH stays moderate (< 8); consequently, $Gd_2(CO_3)_3$ is stabilized relative to $GdOHCO_3$ for the calculation with the Weger database. For run 6 (Figure 5-6), the CO_2 pressure is lower (~$10^{-3.5}$ bar), the average pH is higher; consequently, both databases yield $GdOHCO_3$ as the solubility determining solid.

5.3.1.3 Summary of Results for Thermodynamic Data Sensitivity Study

It is apparent from Table 5-6 and Figures 5-5 and 5-6 that the Weger et al. data do not significantly alter the calculation results, and use of the SKB database is slightly conservative for systems where the solid Gd phases are carbonates.

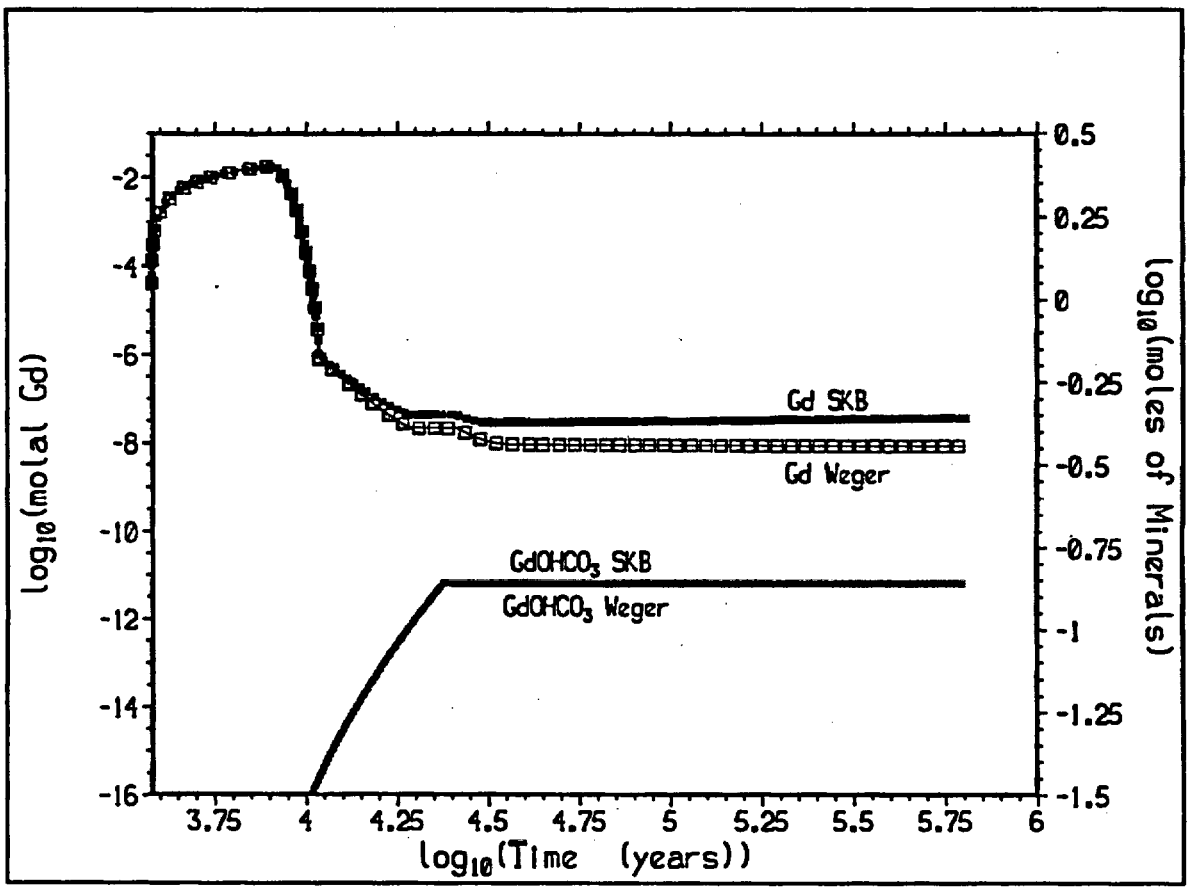

NOTE: Runs described in Reference 5, Table 5.3-1.

Figure 5-6. Run 6: Aqueous Gd and Gd Minerals Formed, SKB versus Weger et al.

5.3.2 Chemistry of Incoming Water

There were several motivations for this study. First, the incoming water composition used in previous WPO studies (Ref. 5, Assumptions 3.8 and 3.12) was derived by a somewhat involved process, and resulted in log_{10} O_2 and CO_2 fugacities of –0.6778 and –2.5390, respectively. These specific and high-precision values made comparison against other studies somewhat difficult (in the literature and the VA, it is more common to use "round" values like –0.7 and

–3). Second, the previously assumed CO_2 fugacity is not consistent with the value log_{10} fCO_2 = –3.0 assumed in the VA calculations (Ref. 11, Figure 4-27). The source of this discrepancy is subtle: the author of Reference 33 (Assumption 3.8) attempted to obtain the highest consistency between log_{10} fCO_2 and reported analyses for J-13 well water (Ref. 6, Tables 4.1 and 4.2). However, the J-13 well water is drawn from below the water table, under a substantial head; thus true J-13 well water is probably in equilibrium with a higher CO_2 fugacity than the fracture and pore waters at the repository level. Since the solubility of actinides and gadolinium can depend very strongly on the effective CO_2 pressure, it is appropriate to use the VA value as the recommended mean. Third, to make the reported J-13 well water analyses consistent, the analysis used in Reference 33 (Assumption 3.8) required adjustments to the reported Na^+ to maintain charge balance; these adjustments are difficult to justify since Na is generally analyzed to high accuracy. Fourth, a slight error was discovered in the original data reduction for the J-13 well water analyses, used for Reference 33; the concentration of Fe in J-13 water was accidentally assigned to the concentration of F. This very minor error has a small effect on pH, but for the sake of consistency, it was desirable to recalculate the water compositions. Fifth, it is desirable to have standard water compositions with trace elements added in sufficient quantity to prevent numerical instabilities. It was recently discovered that some species (e.g., MoO_4^-) require minimal concentrations, ~10^{-16} molal, compared to ~10^{-22} molal used previously.

The sensitivity analysis for incoming water composition consisted of several steps:

(1) Six initial EQ3NR input files were created (j13noc25.3i, j13noc30.3i, j13noc35.3i, j13cal25.3i, j13cal30.3i, and j13cal35.3i). The files either held Ca concentrations at saturation with calcite (those files have "cal", for calcite, as the 4th, 5th, and 6th letters), or allowed Ca^{++} to be fixed at the average value reported in Table 4.2 of Reference 6 (those files have "noc" for "no calcite" as the middle letters). The log_{10} fCO_2 values were set at –2.5, –3.0, or –3.5 (corresponding to 25, 30, and 35, as the last two digits of the file names), to encompass the VA mean value, the approximate value suggested in Reference 33, and the normal ambient value (Ref. 34, p. F-210). The concentrations of Fe^{2+}, Al^{3+}, and Mn^{2+} were set to equilibrium with goethite, diaspore, and pyrolusite, respectively.

(2) Six EQ6 files, analogous to Cerd2N0_5I.6i in run 4 of Reference 5 (p. 23, Table 5.3-1), were created by substituting in the water compositions from the 3p pickup files created in step (1) above; these files were named r4noc25.6i, r4noc30.6i, r4noc35.6i, r4cal25.6i, r4cal30.6i, and r4cal35.6i. These files cover "stage I" of the run, in which a high drip rate of 0.5 m^3/day is assumed to enter the WP, reacting with the steels and HLW glass, but not the ceramic. The runs terminate after ~3800 years, when the pH has stabilized and all the HLW glass (but not all the steel) is degraded. These files were formatted to use the new EQ6 SCFT mode described in Section 4.2. A seventh file, r4base.6i, was created by reformatting Cerd2N0_5I.6i to be compatible with the new SCFT mode, and was used for base-case comparisons. The new SCFT method dynamically adjusts step size, and produces results slightly different from the allpost/nxtinput method described in Reference 5, pp. 11-14.

(3) Six EQ6 files, analogous to Cerd2W0_0015I.6i in run 4 of Reference 5 (p. 23, Table 5.3-1), were created by picking up the results of the runs described in step (2), adjusting the ending time, adding in the Pu-ceramic as a reactant, and adjusting the drip rate to 0.0015 m^3/y. These runs constitute the second stage of the calculation, out to ~$6 \cdot 10^5$ years. The file names are r4noc25_.6i, r4noc30_.6i, r4noc35_.6i, r4cal25_.6i, r4cal30_.6i, and r4cal35_.6i, with the obvious correspondence to the files described in step (2). A seventh file, r4base_.6i, was made from Cerd2W0_0015I.6i, formatted for consistency with the new SCFT method, to act as a base case (unchanged J-13 well water composition).

(4) The Gd, Pu, and U % loss were calculated from the elem_tot.txt files generated by step (3).

Table 5-7 shows the comparison of Gd, Pu, and U losses for the 7 runs. Overall, the differences are small. It is notable that the highest Gd losses occur in the samples with the lowest overall CO_2 fugacity, and that these runs have the highest average pH. However, the runs with log_{10} $fCO_2 = -3.5$ have lower dissolved H_2CO_3 and HCO_3^-, and are less able to buffer the system pH during the degradation of metals.

Table 5-7. Gd, Pu, and U % Losses for Run 4, Using Varied Incoming Water Compositions

Case	Gd	Pu	U	log_{10} fCO_2	Calcite Saturation
r4base_ (base case)	13.933	0.000	0.031	-2.539	No
r4cal25_	13.192	0.000	0.031	-2.500	Yes
r4cal30_	14.147	0.000	0.019	-3.000	Yes
r4cal35_	14.712	0.000	0.012	-3.500	Yes
r4noc25_	13.663	0.000	0.031	-2.500	No
r4noc30_	14.178	0.000	0.019	-3.000	No
r4noc35_	14.574	0.000	0.012	-3.500	No

5.3.3 Effects of HLW Glass Composition Variations

A sensitivity study, investigating effects of HLW glass composition variations, was undertaken for two reasons. First, the previous study of Pu-ceramic degradation used a single composition to represent "typical" HLW glasses produced at the SRS (Ref. 5, Table 5.1.1.1-2, p. 16). A very similar, standardized HLW glass composition was recently developed in Reference 27 (Att. I, p. I-7). Ultimately, these two compositions trace to a 1987 report, issued before SRS had finalized its HLW glass production process. In addition, other reports suggested large composition ranges for SRS HLW glass (Ref. 28, Table 3.3.8). Second, in the previous calculation, all phosphorus was eliminated from the idealized HLW glass composition. The phosphorus was removed from the previous calculation, to prevent EQ6 from precipitating low-solubility Gd phosphates; the removal was conservative since there was uncertainty about the accuracy of HLW glass phosphorus analyses, and elimination of phosphorus would lead to greater Gd losses from the WP.

There is a mechanism to obtain current HLW glass compositions, and these current compositions show phosphorous is a real and predictable component of the SRS HLW glasses. The "Waste Acceptance Product Specifications for Vitrified High-Level Waste Forms", or WAPS, specifies (Ref. 35, p. 7) that the producer shall project the composition in the WQR (Waste Qualification Report). Reference 36 (Tables 1 through 3) is such a report, and gives seven extreme compositions expected for SRS HLW glass. The most widely varying compositions from that report are given in Table 5-8 (converted into moles), along with the "base" composition used for HLW glass in previous Pu-ceramic calculations (Ref. 5, Table 5.1.1.1-2).

Table 5-8. Elements (in moles) in HLW Glass, Normalized to 100 g/mole

	HLW Glass Types					
Element	Base	Blend	Batch1	Batch3	HM	Purex
Al	8.595E-02	7.857E-02	9.596E-02	6.439E-02	1.408E-01	5.671E-02
B	2.954E-01	2.313E-01	2.220E-01	2.235E-01	2.021E-01	2.933E-01
Ba	6.001E-04	1.167E-03	9.508E-04	1.129E-03	7.841E-04	1.247E-03
Ca	1.642E-02	1.849E-02	2.224E-02	1.811E-02	1.849E-02	1.978E-02
Cr	1.579E-03	1.593E-03	1.327E-03	1.733E-03	1.137E-03	1.849E-03
Cu	2.389E-03	5.581E-03	5.072E-03	5.095E-03	3.195E-03	5.300E-03
Fe	1.316E-01	1.310E-01	1.575E-01	1.411E-01	9.371E-02	1.595E-01
K	7.601E-02	8.247E-02	7.431E-02	7.443E-02	4.598E-02	7.609E-02
Li	2.115E-01	2.958E-01	2.970E-01	2.984E-01	3.137E-01	2.083E-01
Mg	3.374E-02	3.379E-02	3.403E-02	3.394E-02	3.658E-02	3.313E-02
Mn	2.820E-02	2.873E-02	2.915E-02	2.585E-02	2.967E-02	2.802E-02
Na	3.732E-01	2.897E-01	2.880E-01	2.842E-01	2.729E-01	3.996E-01
Ni	1.245E-02	1.189E-02	9.993E-03	1.438E-02	5.445E-03	1.626E-02
Si	7.751E-01	8.398E-01	8.328E-01	8.399E-01	9.181E-01	7.416E-01
Ti	0.000E+00	1.124E-02	8.208E-03	8.244E-03	7.000E-03	8.043E-03
U	7.837E-03	7.656E-03	1.905E-03	1.133E-02	3.658E-03	1.030E-02
Pb	2.927E-04	4.433E-04	5.319E-04	4.643E-04	2.765E-04	5.518E-04
Np	3.168E-06	4.686E-06	2.863E-06	3.268E-06	1.167E-05	1.075E-06
Pu	5.163E-05	7.445E-05	9.303E-06	2.392E-05	2.175E-04	8.148E-07
Tc	1.092E-04	1.002E-04	7.089E-05	6.424E-05	2.252E-04	2.531E-05
Zr	2.896E-04	1.214E-03	7.417E-04	8.466E-04	3.024E-03	2.785E-04
O	2.755E+00	2.829E+00	2.840E+00	2.808E+00	2.939E+00	2.748E+00
F	1.667E-03	1.490E-03	1.706E-03	1.568E-03	1.598E-03	1.530E-03
Cl	3.251E-03	3.280E-03	5.350E-03	3.814E-03	1.600E-03	4.466E-03
S	4.017E-03	2.764E-03	3.054E-03	2.833E-03	2.033E-03	3.312E-03
P	0.000E+00	4.964E-04	4.052E-04	5.706E-04	3.604E-04	6.294E-04

NOTES: References for HLW glass: Spreadsheet: glass2sensitivity.xls; Base from Reference 5, Table 5.1.1.1-2, and associated spreadsheets; all others from Reference 36, Tables 1 to 3.

The recent glass analysis given by Bibler et al. (Ref. 37, Table 1) is akin to batch1 in Table 5-8 above. However, the analyses in Reference 37 are for tank 51, which is the oldest tank at SRS; this tank was filled with residue from an early process, and may not be typical of the overall SRS production.

To test the effects of the variability in HLW glass composition, Run 4 from Reference 5 (Table 5.3-1) was redone with each of the HLW glass compositions in Table 5-8. This run had produced the highest Gd loss in the previous study. The stage1 calculation involved exposure of just the steel components and HLW glass at a high drip rate (0.5 m^3/year), and the stage2 part of the calculation added the Pu-ceramic as a reactant and dropped the drip rate (water entry into the

WP) to 0.0015 m^3/year. The new SCFT mode (Section 4.2) was used. (Note: when the new mode is used on a second-stage input file generated by the older mode described in Reference 5, pages 11-13, the new mode calculates the same Gd loss [~14.8%], as found in Table 5.3-1 of Reference 5.) However, for the results in Table 5-9 of this document, it was necessary to redo the first-stage of the calculation as well, which yields a slightly lower overall loss for the Base case (~13.9%). The first stage calculation involves very rapid and dramatic changes in chemical composition, and the newer method provides a slightly more accurate solution to the differential equations in such circumstances.

From Table 5-9, it is apparent that the new HLW glass compositions from Reference 36 ("Blend" through "Purex") generate slightly lower Gd losses than does the Base case. The principal reason for the lower loss appears to be the small phosphate content for the newer compositions. The phosphate converts some of the Gd into insoluble $GdPO_4 \cdot H_2O$, which lowers overall Gd loss in the system. Overall, the wide variations in the new HLW glass compositions appear to have little effect on the total calculated Gd loss. Other elements (particularly Pb) compete with Gd for the phosphate, so there is no simple correlation between phosphate content and Gd loss.

Table 5-9. Gadolinium Losses for Run 4, Using Different HLW Glass Compositions

Glass	%Gd loss
Base	13.93
Blend	10.59
Batch1	9.58
Batch3	10.13
HM	9.30
Purex	9.46

NOTE: References for glass: Spreadsheets case4_tot.xls, glass2sensitivity.xls; Reference 36, Tables 1-3. Reference for Run 4: Reference 5, Table 5.3-1.

5.4 EQ6 CALCULATIONS

5.4.1 Scenarios Considered

The rationale for selection of EQ6 simulation scenarios is to provide conservative assessments of solubility and transport of criticality control materials (Gd and Hf, the neutron absorbers) and fissile materials (i.e., U and Pu compounds) in the WP. The proposed criticality control materials are incorporated into the ceramic. Upon degradation of the ceramic, the Hf is expected to form insoluble Hf oxides, which will remain in the WP. Degradation of the ceramic is also expected to yield varied amounts of (1) aqueous (dissolved) Gd; (2) a solid Gd carbonate (most likely $GdOHCO_3$); and (3) possibly $GdPO_4 \cdot H_2O$ (Ref. 5, Section 5.3; and Ref. 7, Section 5.3.1). Gadolinium phosphate is sparingly soluble in neutral solutions, though the solubility does increase at low and high pH (Ref. 7, Section 5.3.1). Formation of $GdPO_4 \cdot H_2O$ will be limited by

the availability of phosphate from degrading HLW glass. Dissolution of solid Gd carbonates and phosphates, at high pH, is also enhanced by dissolved carbonate. Uranium and plutonium are also quite soluble in the alkaline, carbonate-rich solutions produced when HLW glass degrades. Thus the matrix of EQ6 calculations should include scenarios that may yield high pH, particularly high pH with high dissolved carbonate.

However, solid $GdOHCO_3$ also dissolves readily under acid conditions (Ref. 5, Section 5.3). Low-pH conditions might occur if steel degrades separately from the HLW glass. To obtain sustained, low-pH conditions, it is generally necessary to break the degradation process into two stages. The first stage involves an early breach of the 304L stainless steel canisters holding the HLW glass, followed by fast degradation of the HLW glass and removal of the alkaline components during a period of relatively high drip rate. In the second stage, the 304L cans holding the ceramic are allowed to breach, exposing some portion of the Pu-U-Gd-Hf-ceramic to acid conditions. To keep the pH low, the drip rate must be reduced for the second stage. One difficulty with these two-stage runs is that they require very high HLW glass degradation rates, to ensure the HLW glass is degraded and leached before exposure of the ceramic. The two-stage runs are somewhat unrealistic, in that the 304L cans are thin, and unlikely to last for long periods after breach of the HLW glass canisters. A few two-stage runs are included in the matrix, just to test the sensitivity of the system to sustained, low-pH conditions capable of dissolving $GdOHCO_3$.

Thus, the reaction scenarios can be divided into two general categories. The first category comprises single-stage cases, in which all reactants (steels, HLW glass, and fissile materials) are *exposed* simultaneously to the water in the WP. Because the reaction rates of the materials in the WP may vary greatly, all materials do not necessarily *degrade* simultaneously. The second category comprises two-stage runs. In the first stage, the A516 outer web (basket) and the GPCs (HLW glass and 304L steel) are first exposed to water, until the HLW glass is completely degraded and its alkalinity largely flushed out of the system. The first stage is actually run twice; once up to approximately three times as long as is required to degrade the HLW glass, in order to locate the true pH minimum; and it is run a second time, just to the commencement of the low-pH plateau, to create an EQ6 pickup file for the second stage. This repetitive process ensures that the maximum acidity will be achieved in the second stage. In the second stage, the 304L cans, magazines, rack, and Pu-ceramic disks are added as reactants. The aim of the two-stage runs is to force a "conservative" condition of high acidity, by degrading the HLW glass rapidly, before all the acid-producing steel is degraded. The early HLW glass degradation and flushing requires very high HLW glass degradation rates; the total effective rate of the HLW glass is further increased by considering cracks as part of the total surface area. These high HLW glass degradation rates, if used with a slow flush rate, can produce unreasonably high ionic strengths (> 1); such high ionic strengths are beyond the applicability of EQ3/6's "B-Dot" corrections.

The primary cases for this study included 20 single-stage and 5 two-stage runs, with varied combinations of steel, HLW glass, and ceramic degradation rates and different water fluxes. These 25 cases used ambient gas fugacities of 0.2 bar for O_2, and 10^{-3} bar for CO_2. The CO_2 pressure used is consistent with the long-term ambient assumed for the VA (Ref. 11, Figure 4-

27). Tables 5-10 and 5-11 present a summary of EQ6 runs and corresponding degradation configurations for the ambient gas fugacities.

Table 5-10. Summary of Single-stage EQ6 Cases for Pu-ceramic WP

Case Number	Rates of Degradation for:			Water Drip Rates (m^3/y)	Case ID
	Steel	Glass	Pu-ceramic		
1	Average	Low	Low	0.0015	p00_1111
2	Average	Low	Low	0.15	p00_1113
3	Average	Low	High	0.0015	p00_1131
4	Average	Low	High	0.15	p00_1133
5	Average	Low	Average	0.015	p00_1122
6	Average	High	Low	0.0015	p00_1211
7	Average	High	Low	0.15	p00_1213
8	Average	High	High	0.0015	p00_1231
9	Average	High	High	0.15	p00_1233
10	Average	High	Average	0.015	p00_1222
11	High	Low	Low	0.0015	p00_2111
12	High	Low	Low	0.15	p00_2113
13	High	Low	High	0.0015	p00_2131
14	High	Low	High	0.15	p00_2133
15	High	Low	Average	0.015	p00_2122
16	High	High	Low	0.0015	p00_2211
17	High	High	Low	0.15	p00_2213
18	High	High	High	0.0015	p00_2231
19	High	High	High	0.15	p00_2233
20	High	High	Average	0.015	p00_2222

Table 5-11. Summary of Multiple-stage EQ6 Cases for Pu-ceramic WP

Case Number	Rates of Degradation for:			Water Drip Rates (m^3/y)	Case ID	Fe Oxide
	Steel	Glass	Pu-ceramic			
21(a)	High	High	No Ceramic	0.5	p01h2204	Hematite
21(b)	High	No Glass Present	Average	0.015	p02h2022	Hematite
22(a)	High	High	No ceramic	0.5	p01g2204	Goethite
22(b)	High	No Glass Present	Average	0.015	p02g2022	Goethite
23(a)	High	High	No Ceramic	0.15	p01g2203	Goethite
23(b)	High	No Glass Present	Average	0.0015	p02g2021	Goethite
24(a)	Average	High	No Ceramic	0.15	p01g1203	Goethite
24(b)	Average	No Glass Present	Average	0.0015	p02g1021	Goethite
25(a)	High	High	No Ceramic	0.15	p01g2203	Goethite
25(b)	High	No Glass Present	High	0.0015	p02g2031	Goethite

In addition to the 25 cases reacted under the ambient gas-phase conditions, a number of cases were done under low-oxygen fugacity constraints to test sensitivity of reaction-paths to fO_2 (oxygen fugacity, or idealized partial pressure of oxygen). Table 5-12 summarizes the configurations for the sensitivity tests. Cases were selected on the basis of whether Gd loss was larger than 1% at the end of the reaction-path. In the test, the $\log_{10}(f(O_2))$ is changed from –0.7 to –10 (Cases 26 through 30) and –15 bar (Cases 31 through 35). As will be shown later, the range of fO_2 used here is reasonable.

Table 5-12. Summary of Sensitivity Tests for Selected EQ6 Cases for Pu-ceramic WP

Case Number	Steel Rate	Glass Rate	Pu-ceramic Rate	Water Drip Rates (m^3/yr)	Log[f(O_2)] changed from -0.7 to	Case ID
26	Average	Low	High	0.0015	-10.0	ps0_1131
27	Average	Low	Average	0.015	-10.0	ps0_1122
28	Average	High	Average	0.015	-10.0	ps0_1222
29	High	Low	High	0.0015	-10.0	ps0_2131
30	High	Low	High	0.15	-10.0	ps0_2133
31	Average	Low	High	0.0015	-15.0	ps2_1131
32	Average	Low	Average	0.015	-15.0	ps2_1122
33	Average	High	Average	0.015	-15.0	ps2_1222
34	High	Low	High	0.0015	-15.0	ps2_2131
35	High	Low	High	0.15	-15.0	ps2_2133
36	High	Low	High	0.0015	Not Changed; High Ceramic Rate Lowered	pr0_2131

An additional test case (Case 36 in Table 5-12) was conducted to determine the effect of reducing the highest Pu-ceramic rate by a factor of 3. This test (pr0_2131, where the "r" stands for "rate") is a slight modification of p00_2131, the case with the highest total Gd loss (78%). The motivation for this case was LLNL's discovery that their previously reported rates had been overestimated by a factor of at least 3, due to an underestimate of the experimental surface area (Ref. 2, Table 6.2). Substitution of this lower rate roughly halved the Gd loss.

5.4.2 EQ6 Run Conditions and Nomenclature

Cases 1 through 20 in Table 5-10 were single-stage runs. Cases 21 through 25 of Table 5-11 were multiple-stage runs.

Tables 5-10 through 5-12, under "Case ID" column, give the root-file names used to describe the runs. The EQ6 input files corresponding to these runs end with the extension ".6i" (e.g., p00_1111.6i is the EQ6 input file name for Case 1); these input files are included in the electronic media accompanying this calculation (Ref. 10). Each EQ6 run has associated tab-delimited text files, also included in the electronic media (e.g., p00_1111.elem_aqu.txt for Case 1). Most of the important run conditions could be inferred from the root-file name. For most cases, the Case ID is evaluated from left to right, as follows:

- The first letter "p" indicates Pu-ceramic.
- The second and third characters (first and second digits after "p") indicate sensitivity studies and revisions of the input file, with the third digit ranging from 0 to 9 (for the current document, the third digit never exceeded 2).
- The fourth character indicates the form of Fe oxide in the reaction products in multiple-

stage runs (e.g., "h" for hematite and "g" for goethite, respectively). In single-stage runs, the default third character is an underscore ("_"), and hematite is always allowed to form. Hematite and goethite are the primary Fe(III) iron oxide minerals observed to form in rust. Hematite is thermodynamically more stable, and its stability increases with temperature.

- The fifth digit is 1 or 2, indicating the average or high rate of steel corrosion in Table 5-1.
- The sixth digit in this block is 1, 2, or 0, with 1 and 2 indicating the low and high HLW glass corrosion rates listed in Table 5-2, respectively, and 0 indicating that no undegraded HLW glass is present in that stage of the EQ6 run.
- The seventh digit in the block is 1, 2, 3, or 0, with 1, 2, and 3 indicating the rates of Pu ceramic dissolution of low, average, and high, respsctively, as defined in Table 5-3, and 0 indicating no Pu-ceramic is corroding in that stage of the EQ6 run.
- The last digit in the block indicates the choice of water flush rate, with 1, 2, 3, and 4 indicating 0.0015 m^3/y, 0.015 m^3/y, 0.15 m^3/y, and 0.5 m^3/y, respectively.

An example is Case 21 in Table 5-11, which lists root file names p01h2204/p02h2022 for the two input files. The first root name, p01h2204, covers the time period before the breach of the 304L cans and exposure of the 304L magazines and rack, and represents stage number one, 01 (second and third characters) of a multiple-stage run. The fourth character, h, indicates that hematite is allowed to form (is not suppressed) in this case. The fifth character, 2, indicates the selection of the faster degradation rates for the A516 and 304L steels in the WP (Table 5-1). The sixth character, 2, indicates the faster HLW glass degradation rate in Table 5-2. The seventh character, 0, indicates the absence of Pu-ceramic in the EQ6 system (since the run is pre-breach, the ceramic is not yet exposed to chemical corrosion). The last character is 4, indicating the highest water flush rate of 0.5 m^3/year. The second root-file name, p02h2022, covers the time after breach of the cans and magazines containing Pu-ceramic, and is Case 21, stage two (second and third characters). As always, the last block of characters, 2022, gives the rates. The fifth character again indicates the faster steel corrosion rates. The sixth character is 0 since no HLW glass remains in the EQ6 system (though the HLW glass corrosion products are carried through the calculation). The seventh character indicates the Pu-ceramic corrosion has the "average" rate in Table 5-3, and the last character corresponds to a water drip rate of 0.015 m^3/year. In general, the first stage of a multistage run is comparatively short (~10^3 to ~10^4 years), and the second stage of the run is carried out to at least 10^5 years, and up to $6 \cdot 10^5$ years. While the first stage is important in setting up the chemical conditions, the second stage is generally of greater interest for neutronics calculations since the corrosion product compositions can vary widely in the first stage, but achieve a quasi-steady state at longer times.

The case IDs in Table 5-12 are for the sensitivity test cases. The second character indicates the type of test: "s" for fO_2 sensitivity, or "r" for ceramic rate sensitivity. For the fO_2 sensitivity cases, the third character is 0 or 2, representing $fO_2 = 10^{-10}$ bar or 10^{-15} bar, respectively.

6. RESULTS

6.1 SUMMARY OF RESULTS

Table 6-1 summarizes the total percentage Gd, Pu, and U lost at the end of the EQ6 runs. The complete output tables (aqueous, mineral, and total moles) for all the cases are included in the electronic media, as tab-delimited text files. A summary of the files included in the electronic media is given in Attachment II.

Table 6-1. Summary of Gd, Pu, and U Losses for all EQ6 Cases

Case ID	Root Name	Years/10^6	%Gd Loss	%Pu Loss	%U Loss
1	p00_1111	6.3	0.02	0.17	47.52
2	p00_1113	0.45	0.00	0.02	0.01
3	p00_1131	6.3	20.45	0.00	100.00
4	p00_1133	0.46	0.69	0.00	0.01
5	p00_1122	4.2	8.33	0.41	33.44
6	p00_1211	6.3	0.01	0.91	33.19
7	p00_1213	0.46	0.01	0.08	34.48
8	p00_1231	6.3	0.02	29.94	89.16
9	p00_1233	0.45	0.36	0.07	59.68
10	p00_1222	4.4	17.06	1.80	38.41
11	p00_2111	6.3	0.14	0.62	47.42
12	p00_2113	0.43	0.03	0.05	0.07
13	p00_2131 / p!0_2131	6.3	77.92	0.01	100.00
14	p00_2133	0.43	49.01	0.20	0.22
15	p00_2122	4.2	0.34	1.42	37.27
16	p00_2211	6.3	0.01	0.59	39.88
17	p00_2213	0.44	0.02	0.04	34.55
18	p00_2231	6.3	0.02	13.99	72.95
19	p00_2233	0.46	0.09	0.03	56.13
20	p00_2222	4.0	0.07	1.62	36.43
21	p01h2204/p02h2022	4.9	0.07	0.00	0.33
22	p01g2204/p02g2022	5.3	0.07	0.26	0.49
23	p01g2203/p02g2021	6.3	0.01	0.00	0.07
24	p01g1203/p02g1021	6.3	2.28	0.00	0.04
25	p01g2203/p02g2031	6.3	13.89	0.00	0.04
26	ps0_1131	6.3	1.30	0.00	100.0
27	ps0_1122	4.2	10.60	0.00	34.90
28	ps0_1222	4.5	15.80	0.00	38.40
29	ps0_2131	6.3	1.40	0.00	100.00
30	ps0_2133	0.44	37.50	0.00	0.20
31	ps2_1131	6.3	0.00	0.00	100.00
32	ps2_1122	4.4	0.10	0.00	28.20
33	ps2_1222	4.8	0.10	0.00	38.40
34	ps2_2131	6.3	0.00	0.00	100.00
35	ps2_2133	0.44	0.10	0.00	0.00
36	pr0_2131	6.3	32.68	0.07	100.00

In the following sections, Cases 3, 8, 13, 14, 18, 22, 25, and 26 will be discussed in more detail. Cases 3, 8, 13, 14, and 18 were selected for detailed discussion because they represent the runs with the highest net Gd, Pu, or U loss. Case 3 is discussed with Case 26 (its lower fO_2 analogue), to illustrate the indirect effect of fO_2 on Gd loss. Cases 22 and 25 were selected as representative of the two-stage scenarios; Case 25 is closest to the cases that produced highest Gd loss in the prior study of Pu-ceramic degradation (Ref. 5, Table 5.3-1).

Table 6-2 summarizes several aspects of the selected cases, focussing on conditions tied to Gd loss.

Table 6-2. Gd Loss Characteristics and pH of Selected Cases

Case	Number of Stages	Corrosion Rates[a]	Water Drip Rate (m^3/y)	Years/10^6	pH min / max	Peak Gd Conc.[b] (molal)	Width Gd Peak[b] (y)	%Gd Loss
3	1	HLW: Low Steel: Average Ceramic: High	0.0015	6.3	5.8 / 9.4	7.2E-3; 1.4E-3	3.6E3; 3.3E4	20.45
8	1	HLW: High Steel: Average Ceramic: High	0.0015	6.3	7.3 / 10.1	4.9E-6; 5E-7	4.6E3; 1E4	0.02
13	1	HLW: Low Steel: High Ceramic: High	0.0015	6.3	5.3 / 9.3	5E-2	5.4E3	77.92
14	1	HLW: Low Steel: High Ceramic: High	0.15	0.43	5.8 / 8.2	9.7E-4; 3.9E-4	1.1E3; 1.4E3	49.01
18	1	HLW: High Steel: High Ceramic: High	0.0015	6.3	7.9 / 10.0	3.9E-6; 2.6E-7; 7.3E-8	2.2E3; 1.6E5; 3.3E5	0.02
22	2	HLW: High Steel: High Ceramic: Medium	0.5 / 0.015	0.031 / 5.3	5.2 / 8.6	6E-8	4.7E5	0.07
25	2	HLW: High Steel: High Ceramic: High	0.15 / 0.0015	0.035 / 6.3	5.0 / 8.1	4.4E-2	1.2E3	13.89
26[c]	1	HLW: Low Steel: Average Ceramic: High	0.0015	6.3	6.3 / 9.3	8.3E-5	5.7E4	1.30

NOTES: [a]See Tables 5-1 through 5-3 for rates.
[b]Most cases have multiple "peaks." Peaks and widths approximated from plots in Gd_peaks_Pu-ceram_083099.doc, included in the electronic media for this document (Ref. 10).
[c]Analogous to Case 3, except $\log_{10}(fO_2) = -10$ (versus –0.7).

6.2 CASES 3 AND 26 (p00_1131 and ps0_1131)

The results of Case 3 (p00_1131) and its corresponding sensitivity test, Case 26 (ps0_1131), are plotted in Figures 6-1 through 6-7 to demonstrate the general consequences of WP component degradation. The consequences include: changes in pH; variations in the dissolved Gd, Pu, and U content of the water flushed from the WP; and the formation of solubility-controlling and space-filling minerals and solid solutions. Figures 6-1 through 6-7 also demonstrate the indirect effects of oxygen fugacity on pH and Gd loss.

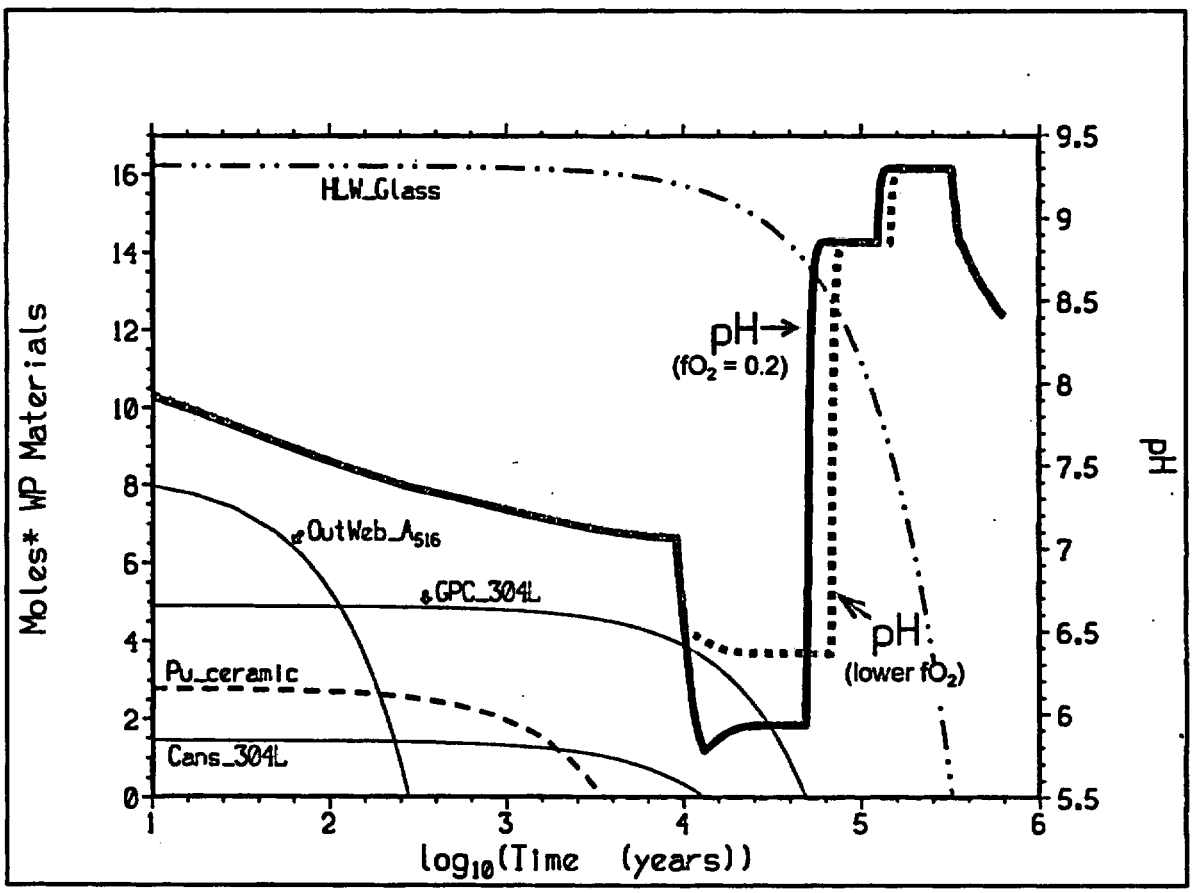

NOTES: Case 3: fO_2 = 0.2 bar (solid pH line); Case 26: $fO_2=10^{-10}$ bar (dashed pH Line). *Moles in the EQ6 normalized (1 liter fluid) system. See Section 5.2 for conversion of moles into mass in total WP.

Figure 6-1. Effect of fO_2 on pH: Cases 3 (p00_1131) and 26 (ps00_1131)

Figure 6-1 illustrates the tie between materials degradation and pH. The pH in the WP decreases with steel degradation (especially with 304L steels) until the steels are exhausted. Since this example uses a low HLW glass degradation rate, the alkalinity from HLW glass is insufficient to neutralize the pH until all the steel is consumed. The Mg and Ca carbonate minerals formed from

HLW glass dissolution do not fully neutralize the acid produced from steel degradation. The Cr contained in the steels is oxidized when it is released into water, and lowers the pH:

$$Cr + H_2O + 1.5O_2 = CrO_4^{=} + 2H^{+} \quad \text{(Eq. 2)}$$

After the steel is consumed and its associated acidity is flushed from the system, the pH climbs (at ~50,000 years) due to HLW glass dissolution. Once the HLW glass is consumed, the pH gradually drops to the ambient for the incoming water at $fCO_2 = 10^{-3}$ bar. However, in the sensitivity test, the lower oxygen fugacity ($fO_2 = 10^{-10}$) in the WP prevents the pH from increasing until ~$10^{4.81}$ years, which is ~10^4 years later than that in the case with 0.2 bar fO_2; the rapid pH increase occurs when the Pu_ceramic and "Out Web_A516" (the carbon steel support structure) have been exhausted and while the GPC_304L and Cans_304L continue to degrade. The lower oxygen fugacity in the system limits chromate oxidation, and thus lowers the production of acid via Equation 2.

The concentrations of aqueous Gd, U, and Pu as functions of time are shown in Figure 6-2 and 6-3. The solubility-limiting phase for Gd is $GdOHCO_3$; like most carbonates, this phase is more soluble under acid conditions, thus the times of highest aqueous Gd correspond to times of low pH. Thus, the case with lower fO_2 (Case 26) also yields lower Gd loss (1.3%, versus 20.45% for Case 3; Table 6-1).

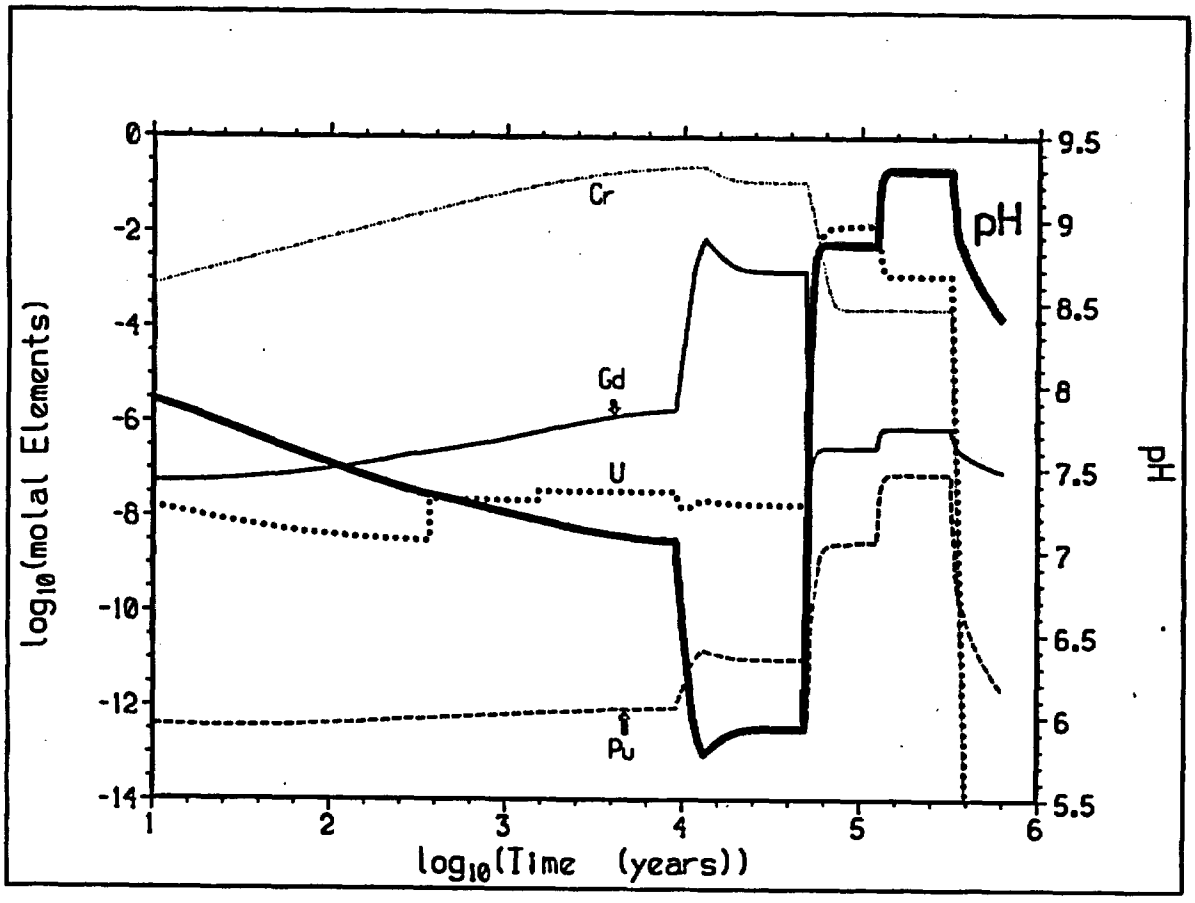

Figure 6-2. Case 3 (fO_2 = 0.2 bar): pH and Total Aqueous Cr, Gd, U, and Pu

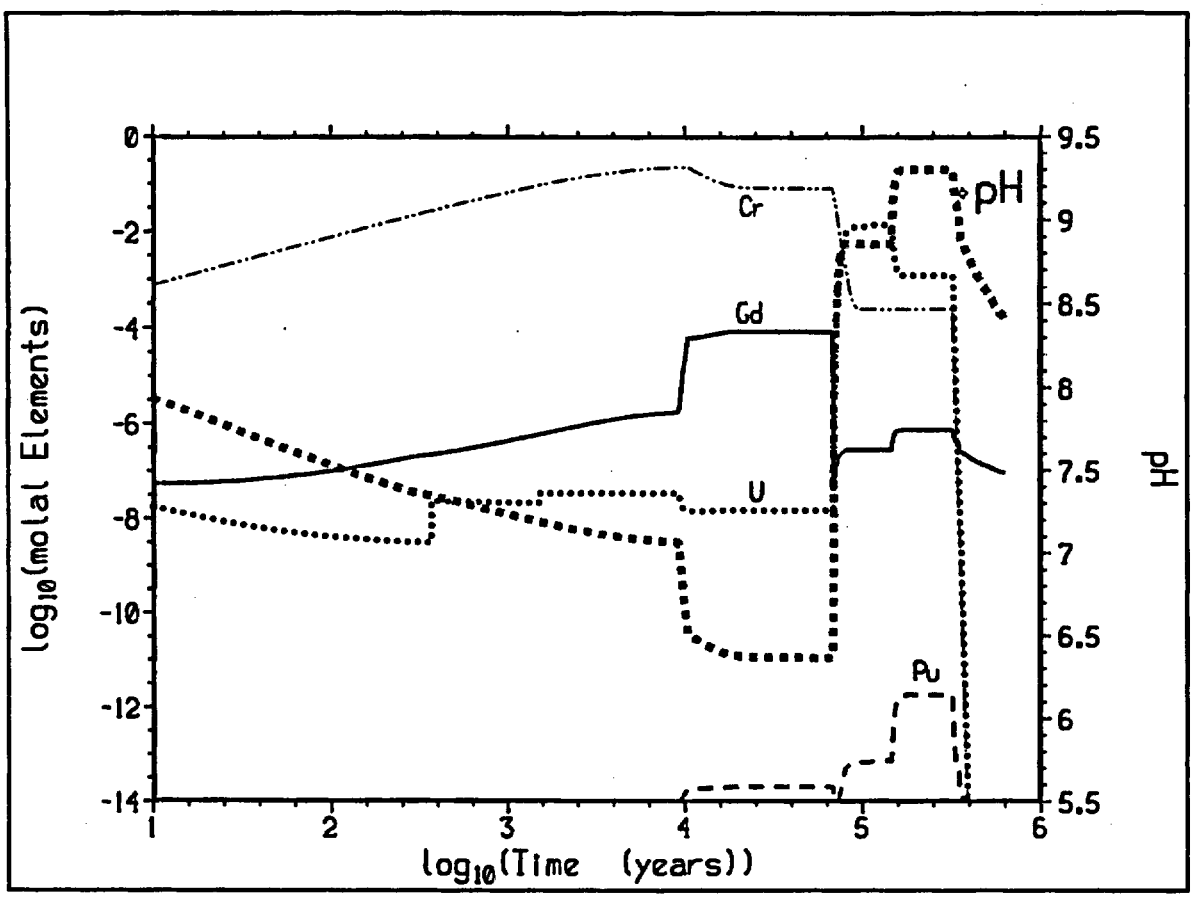

NOTES: Compare with Figure 6-2. The lower fO_2 results in slightly lower dissolved Cr and a less extreme pH minimum. Dissolved Pu is lower than that for Case 26 because aqueous Pu(VI) carbonate complexes are insignificant at this lower fO_2.

Figure 6-3. Case 26 ($fO_2 = 10^{-10}$ bar): pH and Total Aqueous Cr, Gd, Pu, and U

In Figures 6-4 and 6-5, selected minerals that control the solubility of chromium are plotted together with pH as a function of time for $fO_2 = 0.2$ and 10^{-10} bar, respectively. At the higher fO_2, the only Cr solids predicted to form are $BaCrO_4$ and crocoite ($PbCrO_4$), and there is insufficient Ba and Pb in the system to precipitate all the chromate produced by steel oxidation. The formation of solid, mixed-valence state CrO_2, in Case 26 ($fO_2 = 10^{-10}$) results in a less dramatic drop in pH; compare Figure 6-5 to Figure 6-4 (Case 3; $fO_2 = 0.2$). In summary, the formation of Cr-bearing solids affects the pH in the system and, consequently, the losses of Gd, Pu, and U from the WP. Reducing the uncertainty in the stability of Cr(III) and Cr(IV)-containing solids in the EQ3/6 thermodynamic database in EQ3/6 would significantly reduce uncertainty in simulating the degradation of Pu-ceramic.

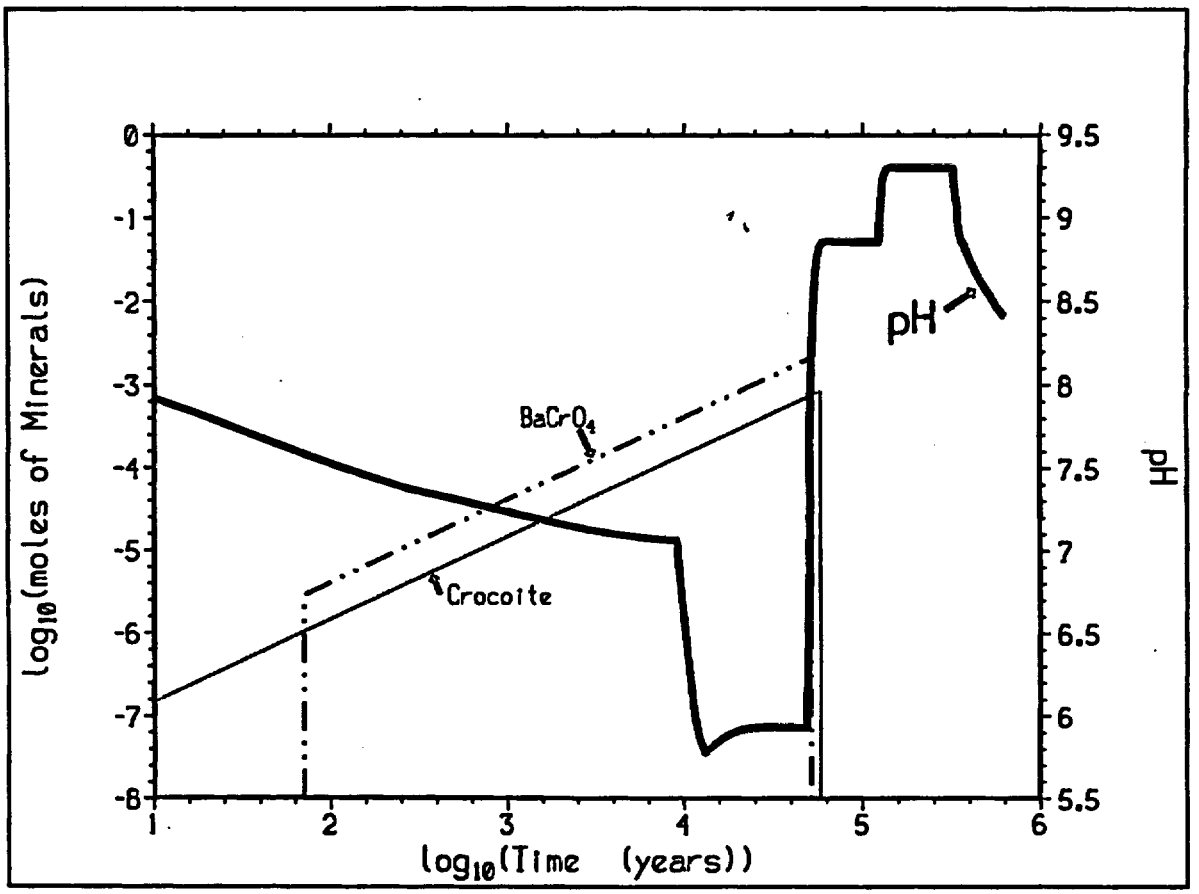

Figure 6-4. Case 3 (fO_2 = 0.2 bar): pH and Minerals Controlling Cr Solubility

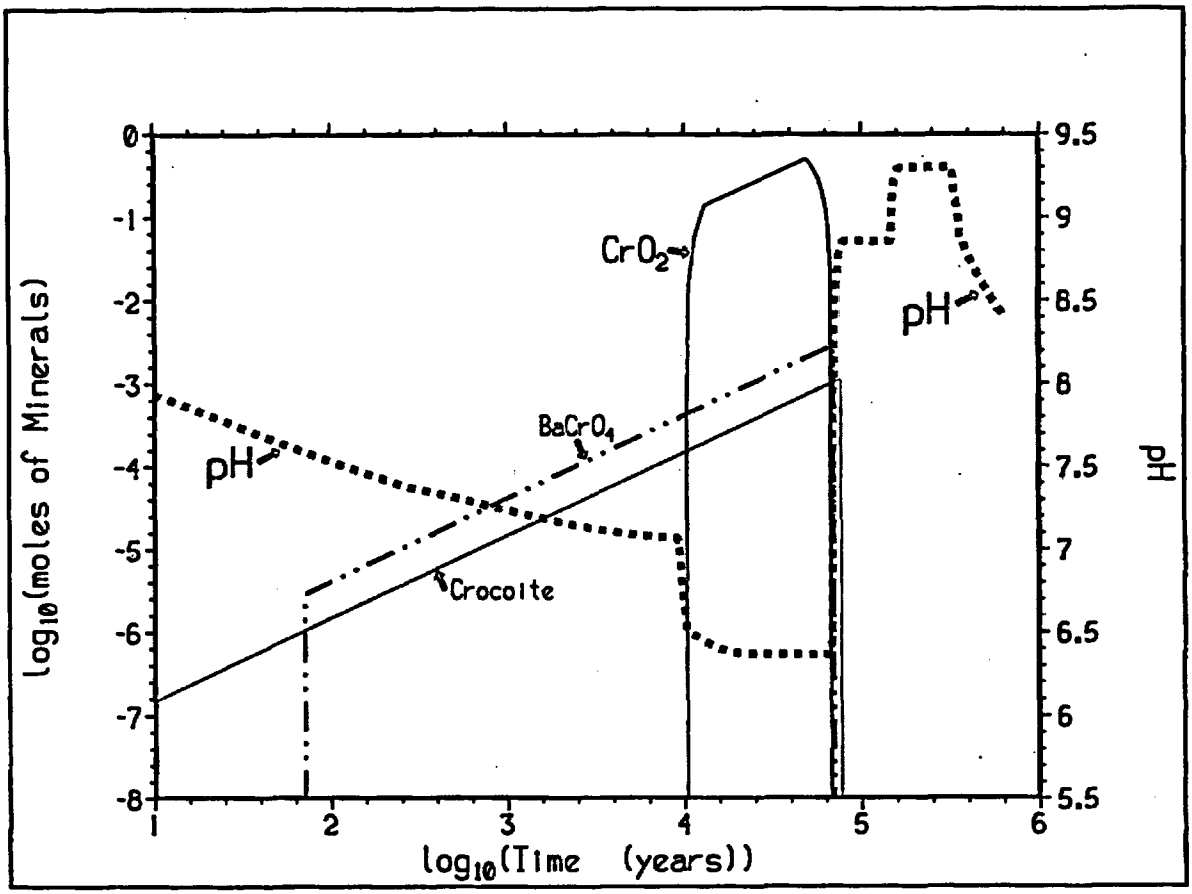

NOTE: Formation of mixed valence state CrO_2 causes a lesser drop in pH, compared to Figure 6-4.

Figure 6-5. Case 26 ($fO_2 = 10^{-10}$ bar): pH and Minerals Controlling Cr Solubility

The above results demonstrate the significant effect of oxygen fugacity on calculated pH and losses in Pu, Gd, and U from the WP. The fO_2 used in most Cases (0.2 bar) is probably higher than the average fO_2 experienced in a corroding WP. A lower fO_2 of 10^{-10} bar dramatically reduces losses of Gd, Pu, and U. This lower fO_2 value is not unreasonable. The common observation of coexisting magnetite and hematite/FeOOH in rust on cars implies local, low fO_2 during corrosion of steels.

The fO_2 of the magnetite/goethite and magnetite/hematite buffers are easily calculated from the $\log_{10}K$ values for the magnetite, hematite, and Fe^{3+} decomposition reactions, as given in the EQ3/6 data0.nuc.R8d thermodynamic constants file. Equations 3 through 6 below give the data0 reactions necessary to carry out the calculations.

$FeOOH + 3H^+ = Fe^{+++} + 2H_2O$ $\log_{10}K = 0.5345$ at 25 °C (Eq. 3)

$Fe_3O_4 + 8H^+ = Fe^{++} + 2Fe^{+++} + 4H_2O$ $\log_{10}K = 10.4724$ at 25 °C (Eq. 4)

$Fe_2O_3 + 6H^+ = 2Fe^{+++} + 3H_2O$ $\log_{10}K = 0.1086$ at 25 °C (Eq. 5)

$Fe^{+++} + 0.5 \cdot H_2O = 0.25 \cdot O_{2\,(g)} + H^+ + Fe^{++}$ $\log_{10}K = -7.7654$ at 25 °C (Eq. 6)

Combining equations algebraically [(Eq. 4) – (Eq. 6) – 3·(Eq. 3)] yields:

$Fe_3O_4 + 0.25 \cdot O_{2\,(g)} + 1.5 \cdot H_2O = 3FeOOH$ $\log_{10}K = 16.6343$ (Eq. 7)

At equilibrium:

$$\log_{10}K = 3 \cdot \log_{10}[Fe_3O_4] - 1.5 \cdot \log_{10}[H_2O] - 0.25 \cdot \log_{10}(fO_2) - \log_{10}[Fe_3O_4] \quad \text{(Eq. 8)}$$

Where the [] notation here indicates activity (~concentration). The activity of solid Fe_3O_4 in Fe_3O_4 is 1, the activity of water relative to a standard state of pure water is ~1, and the activity of solid FeOOH in FeOOH is 1, so Equation 8 reduces to:

$$\log_{10}(fO_2) = -4 \cdot \log_{10}K = -66.5372 \quad \text{(Eq. 9)}$$

Similarly, equations (Eq. 4) – (Eq. 6) – 1.5·(Eq. 4) can be combined to yield:

$Fe_3O_4 + 0.25 \cdot O_{2\,(g)} = 1.5 \cdot Fe_2O_3$ $\log_{10}(fO_2) = -72.2996$ (Eq. 10)

Thus the formal fO_2 is $\sim 10^{-67}$ to 10^{-72} bar for these commonly observed rust assemblages. These low values do not imply that only a tiny fraction of a molecule of O_2 can coexist with magnetite/Fe(III)-oxide rusts; rather, they imply that corrosion can produce locally reduced assemblages, even in the presence or air. Other redox-active couples in natural waters imply more moderate fO_2. For example, commonly observed nitrogen redox couples (e.g., nitrate-nitrite in pore waters of Chihuahuan deserts) imply $fO_2 < 10^{-10}$ bar (Ref. 38, pp. 632-634).

Figures 6-6 and 6-7 show some of the principal solubility-controlling solids predicted by the EQ6 runs for Cases 3 and 26. The hematite abundance plateaus rapidly, and results principally from degradation of the A516 outer web support structure. Because of the low HLW glass degradation rate, smectite clays form slowly. However, a "mole" of smectite clay ($((Ca,Mg)_{0.165},(K,Na)_{0.33})Fe_2Al_{0.33}Si_{3.67}H_2O_{12}$) has a much larger molar volume than a "mole" of hematite (424.293 versus 30.274 cm^3, respectively; from the V0PrTr entries in data0.nuc.R8d). $GdOHCO_3$ is the principal solubility-controlling phase for Gd, though some $GdPO_4 \cdot H_2O$ forms with the phosphate present in HLW glass and steels.

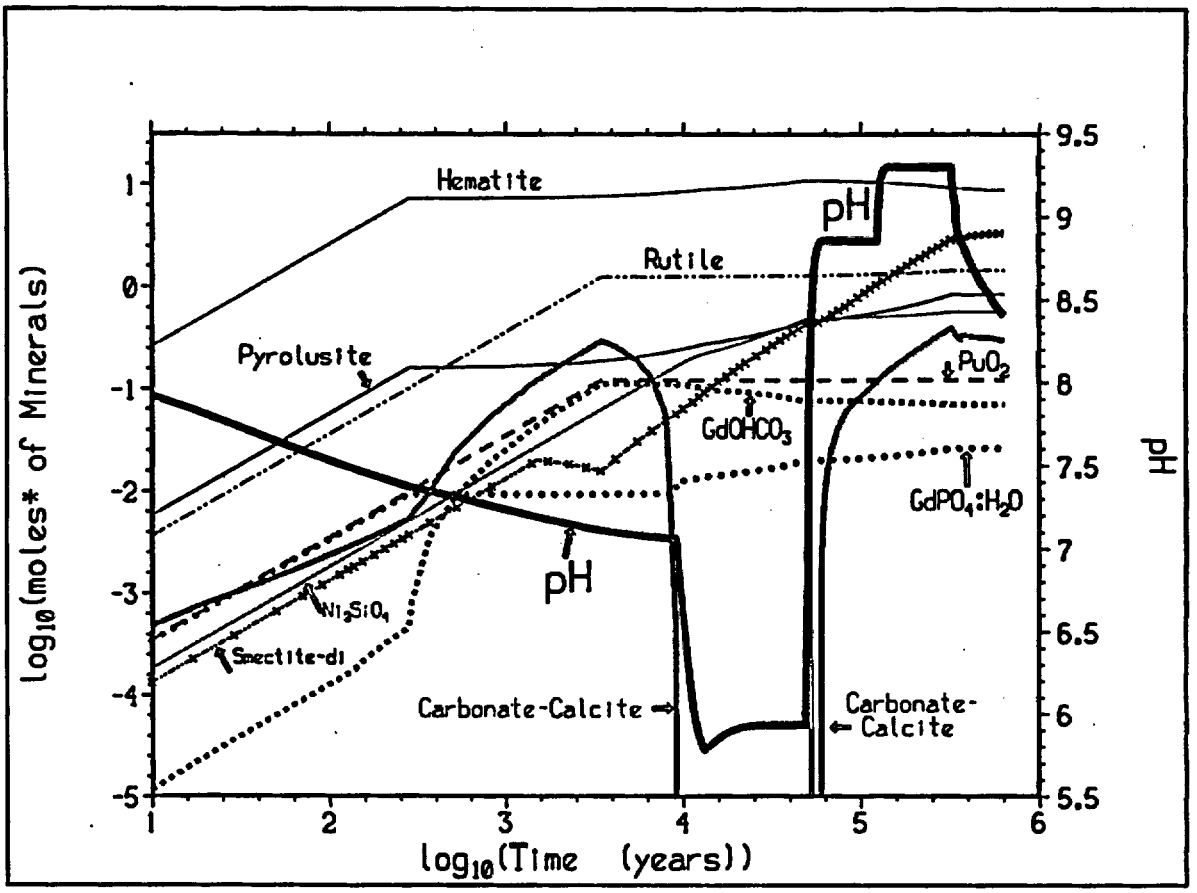

NOTE: The phosphate to form $GdPO_4:H_2O$ originates as a trace constituent of steels and waste glass; phosphate content of incoming water (≤ 1 ppm) is comparatively insignificant. Compare to Figure 6-7.

Figure 6-6. Case 3 (fO_2=0.2 bar): pH and Some Solubility-Controlling Minerals

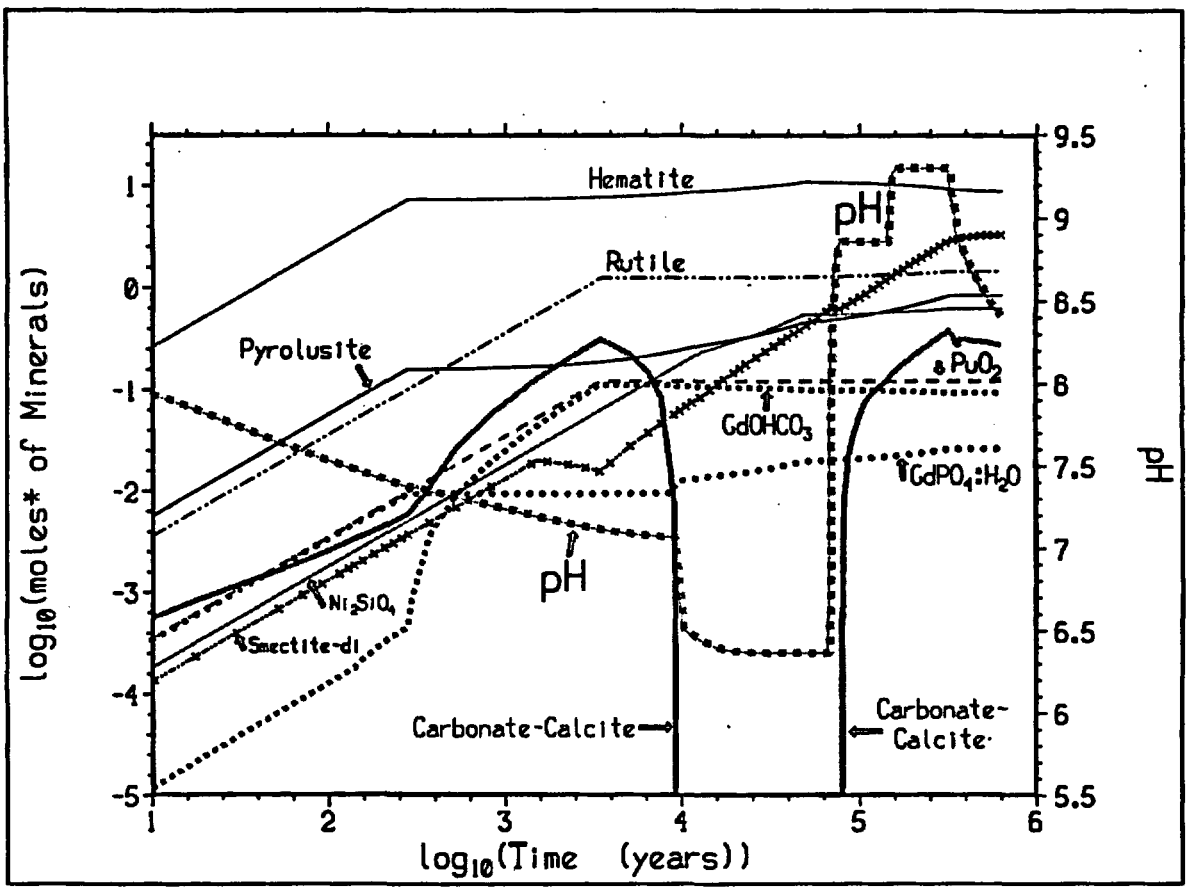

Figure 6-7. Case 26 ($fO_2=10^{-10}$ bar): pH and Some Solubility-Controlling Minerals

Tables 6-3 and 6-4 give the elemental composition for the water in the WP (aqueous phase) and for the degradation products (in mole%) for Case 3 (p00_1131) at selected reaction times.

Table 6-3. Solution Composition in Molality in Selected Years for Case 3 (p00_1131)

Years	9189	13169	30794	124270	633860
pH / Element	7.05	5.78	5.93	8.86	8.41
O	5.64E+01	5.64E+01	5.60E+01	5.58E+01	5.55E+01
Al	3.98E-09	9.62E-07	6.62E-07	8.95E-08	5.30E-08
B	4.39E-02	4.54E-02	4.59E-02	4.59E-02	1.24E-05
Ba	2.05E-08	1.22E-07	8.71E-08	4.52E-10	1.39E-09
Ca	1.54E-01	4.23E-02	2.52E-03	2.98E-05	6.88E-05
Cl	6.85E-04	7.01E-04	7.07E-04	7.07E-04	2.01E-04
Cr	2.25E-01	2.33E-01	1.13E-01	2.45E-04	1.00E-16
Cu	2.23E-06	5.11E-04	2.02E-04	9.09E-07	3.38E-07
F	9.48E-05	6.02E-04	2.81E-04	3.74E-04	1.15E-04
Fe	1.45E-12	7.28E-12	5.13E-12	1.40E-12	1.22E-12
Gd	1.93E-06	7.35E-03	1.47E-03	2.78E-07	8.97E-08
H	1.11E+02	1.11E+02	1.11E+02	1.11E+02	1.11E+02
C	4.00E-04	5.24E-05	5.50E-05	5.79E-02	4.38E-03
P	9.25E-11	2.75E-12	2.33E-12	4.87E-08	2.63E-09
K	1.04E-02	9.66E-03	8.72E-03	4.16E-03	2.58E-03
Li	3.14E-02	3.25E-02	3.29E-02	3.37E-02	6.92E-06
Mg	5.71E-03	4.43E-03	3.60E-03	4.08E-05	1.03E-04
Mn	8.30E-14	2.60E-11	1.03E-11	4.26E-16	2.08E-16
Mo	1.00E-16	1.00E-16	1.00E-16	1.00E-16	1.00E-16
N	4.53E-03	4.68E-03	2.34E-03	1.42E-04	1.42E-04
Na	5.69E-02	5.80E-02	5.80E-02	5.49E-02	2.33E-03
Ni	8.58E-05	2.32E-02	9.12E-03	1.57E-08	5.27E-08
Np	1.09E-05	1.96E-04	1.29E-04	6.21E-07	1.00E-16
Pb	3.73E-11	2.17E-10	1.51E-10	2.80E-10	8.48E-10
Pu	9.10E-13	1.53E-11	9.71E-12	2.90E-09	2.18E-12
S	1.78E-03	1.51E-03	1.10E-03	8.16E-04	1.92E-04
Si	3.84E-05	5.13E-05	5.15E-05	4.07E-05	3.62E-05
Tc	1.00E-16	1.00E-16	1.00E-16	1.00E-16	1.00E-16
Tl	2.23E-10	2.23E-10	2.24E-10	2.25E-10	2.26E-10
U	3.16E-08	2.24E-08	1.78E-08	1.39E-02	1.00E-16
Hf (Zr)[a]	6.67E-10	6.70E-10	6.72E-10	6.74E-10	6.78E-10

NOTES: [a]Hf was converted to Zr for EQ6 Calculations (Assumption 3.16).

Table 6-4. Composition of Corrosion Products (mole%) and Density in Selected Years for Case 3 (p00_1131)

Element \ Years	9189	13169	30794	124270	633860
O	6.05E+01	6.04E+01	6.03E+01	6.01E+01	5.98E+01
Al	7.58E-02	1.02E-01	2.03E-01	6.09E-01	1.09E+00
B	3.13E-14	0.00E+00	2.10E-13	0.00E+00	1.01E-14
Ba	7.22E-04	9.68E-04	1.94E-03	5.80E-03	1.04E-02
Ca	1.16E-02	1.24E-02	1.24E-02	9.28E-02	2.31E-01
Cl	2.81E-16	0.00E+00	0.00E+00	1.86E-14	0.00E+00
Cr	9.80E-04	1.31E-03	2.63E-03	3.73E-15	0.00E+00
Cu	2.09E-03	1.54E-03	2.76E-03	1.36E-02	2.77E-02
F	1.72E-03	9.83E-04	1.65E-03	5.59E-15	0.00E+00
Fe	3.21E+01	3.19E+01	3.07E+01	2.60E+01	1.90E+01
Gd	2.30E-01	1.98E-01	1.58E-01	1.09E-01	7.51E-02
H	1.45E+00	1.48E+00	1.82E+00	2.63E+00	5.61E+00
C	2.07E-01	1.74E-01	1.32E-01	2.23E-01	3.01E-01
P	2.34E-02	2.42E-02	2.52E-02	2.41E-02	2.03E-02
K	5.26E-03	1.05E-02	3.81E-02	2.78E-01	4.14E-01
Li	1.81E-15	0.00E+00	0.00E+00	8.11E-02	0.00E+00
Mg	3.06E-03	5.80E-03	2.07E-02	1.72E-01	3.88E-01
Mn	4.55E-01	4.90E-01	5.55E-01	6.37E-01	6.59E-01
Mo	6.99E-32	0.00E+00	2.05E-31	3.05E-31	0.00E+00
N	2.83E-14	0.00E+00	0.00E+00	3.28E-17	0.00E+00
Na	2.91E-03	6.30E-03	2.47E-02	2.01E-01	3.51E-02
Ni	6.33E-01	7.91E-01	1.07E+00	1.16E+00	8.94E-01
Np	2.00E-03	1.33E-03	0.00E+00	0.00E+00	0.00E+00
Pb	2.58E-04	3.46E-04	6.93E-04	2.07E-03	3.71E-03
Pu	2.30E-01	2.15E-01	1.84E-01	1.37E-01	9.50E-02
S	8.34E-14	0.00E+00	0.00E+00	1.18E-12	0.00E+00
Si	9.50E-01	1.21E+00	2.16E+00	5.83E+00	1.02E+01
Tc	3.73E-31	3.49E-31	0.00E+00	0.00E+00	1.43E-31
Ti	2.39E+00	2.24E+00	1.93E+00	1.50E+00	1.13E+00
U	4.71E-01	4.43E-01	3.90E-01	0.00E+00	3.28E-24
Hf (Zr)[a]	2.66E-01	2.49E-01	2.13E-01	1.58E-01	1.09E-01
Total (%)	100	100	100	100	100
Total[b] (g)	1.70E+03	1.81E+03	2.07E+03	2.56E+03	3.33E+03
Density (g/cm^3)	5.30	5.26	5.14	4.62	4.08

NOTES: [a]Hf was converted to Zr for EQ6, then converted back to Hf for mass and density calculations.
[b]For EQ6 system (1 liter aqueous fluid). To obtain total grams in WP, multiply by total system volume of 4593.965 liters.

6.3 CASE 8 (p00_1231)

In Case 8, the high HLW glass and high ceramic degradation rates raise the system pH over 10 in less than $5 \cdot 10^3$ years (Figure 6-8), in the process elevating the solubilities of U and Pu (Figure 6-9). In the higher pH periods, the dissolved U and Pu are almost entirely as $UO_2(CO_3)_3^{4-}$ and $PuO_2(CO_3)_3^{4-}$. Consequently, there are significant losses of U (89.2%) and Pu (29.9%). Because there is no protracted period of low pH, only 0.02% of Gd is lost (Table 6-2). The combination of fast ceramic degradation, high pH, and fixed fCO_2 leads to formation of calcite (with Ca principally from ceramic and HLW glass) and $GdOHCO_3$, the latter as the solubility-controlling phase for Gd (Figure 6-10). These solid carbonates also serve as buffers against rapid drops in pH.

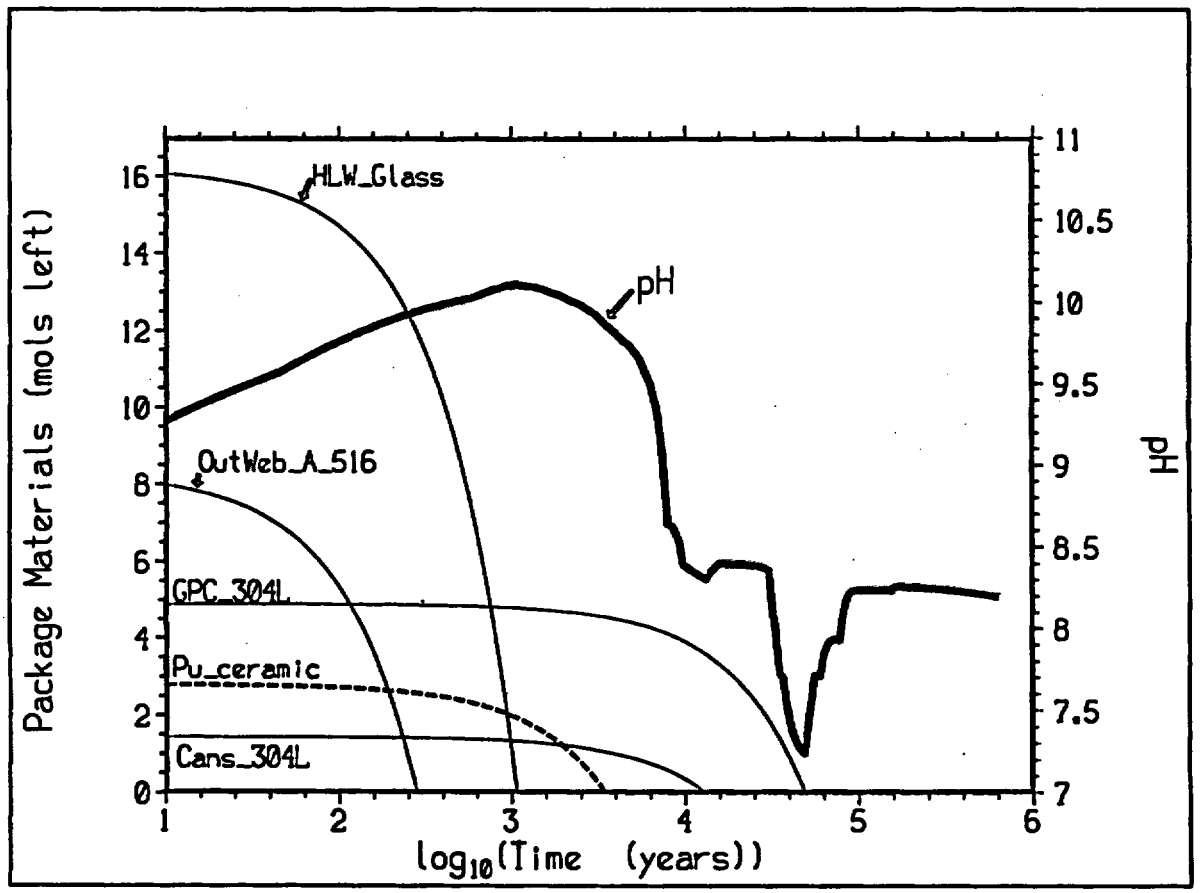

NOTE: Rapid ceramic and HLW glass degradation drives up the pH until both materials are consumed.

Figure 6-8. Case 8 (p00_1231): pH and Consumption of Package Materials

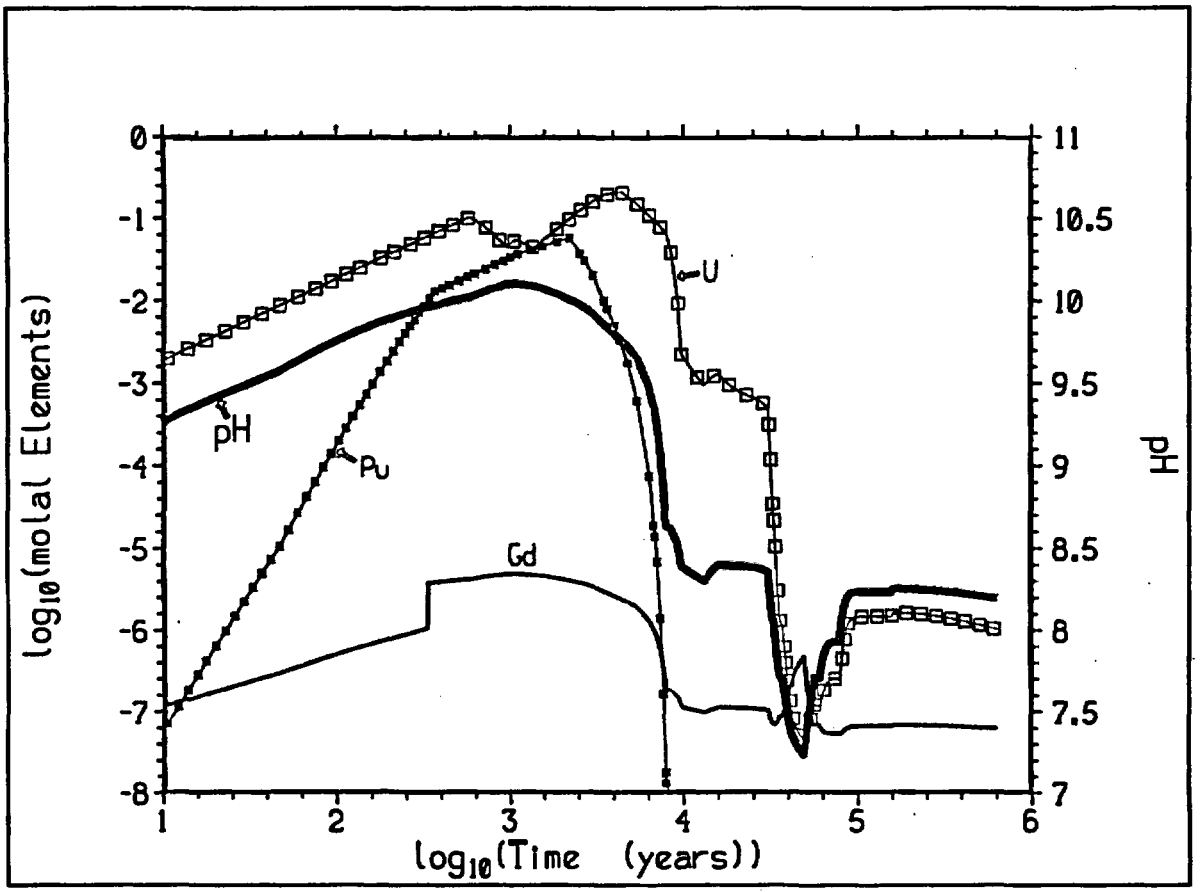

NOTE: The peaks in aqueous (dissolved) U and Pu are due to $UO_2(CO_3)_3^{4-}$ and $PuO_2(CO_3)_3^{4-}$ complexes.

Figure 6-9. Case 8: pH and Total Aqueous Gd, Pu, and U

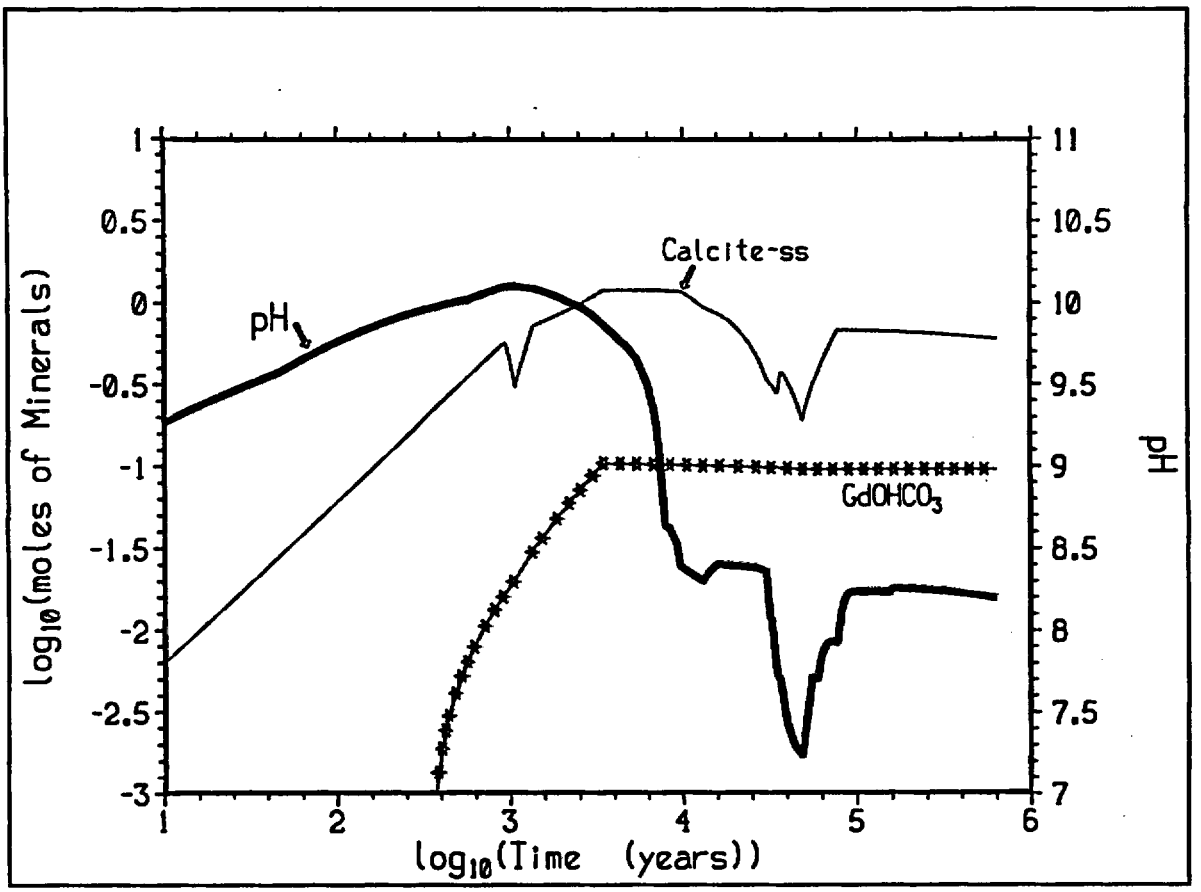

NOTE: $GdOHCO_3$ controls Gd solubility after ~400 years.

Figure 6-10. Case 8: pH and Carbonate Minerals

Tables 6-5 and 6-6 give the aqueous phase composition and the composition of the solid corrosion products in the WP for Case 8.

Table 6-5. Solution Composition In Molality in Selected Years for Case 8 (p00_1231)

Years	4360	9767	30506	126670	633860
pH / Element	9.77	8.39	8.36	8.24	8.20
O	5.67E+01	5.66E+01	5.73E+01	5.55E+01	5.55E+01
Al	1.77E-09	1.45E-08	3.65E-08	3.57E-08	3.26E-08
B	1.69E-01	1.98E-01	2.08E-01	1.24E-05	1.24E-05
Ba	2.75E-11	5.90E-09	5.65E-09	2.99E-09	3.47E-09
Ca	4.84E-06	3.43E-04	4.30E-04	1.48E-04	1.84E-04
Cl	1.53E-02	2.67E-03	2.03E-04	2.01E-04	2.01E-04
Cr	1.87E-01	2.25E-01	1.13E-01	1.94E-04	1.00E-16
Cu	1.40E-04	4.36E-07	4.01E-07	3.25E-07	3.24E-07
F	7.88E-03	1.38E-03	1.16E-04	1.15E-04	1.15E-04
Fe	2.92E-12	1.21E-12	1.24E-12	1.20E-12	1.20E-12
Gd	2.48E-06	1.17E-07	1.08E-07	6.71E-08	6.34E-08
H	1.03E+02	1.11E+02	1.13E+02	1.11E+02	1.11E+02
C	1.21E+00	1.37E-02	7.53E-03	2.94E-03	2.68E-03
P	2.06E-05	1.25E-08	8.75E-09	1.27E-09	1.07E-09
K	1.62E-01	3.02E-02	1.33E-02	1.77E-03	7.70E-04
Li	9.51E-01	2.15E-01	5.69E-04	6.92E-06	6.92E-06
Mg	3.89E-06	4.85E-04	3.17E-04	2.02E-04	1.99E-04
Mn	4.14E-15	3.70E-16	3.53E-16	2.32E-16	2.44E-16
Mo	1.00E-16	1.00E-16	1.00E-16	1.00E-16	1.00E-16
N	3.65E-03	4.56E-03	2.34E-03	1.42E-04	1.42E-04
Na	1.25E+00	2.76E-01	2.59E-01	1.69E-03	1.98E-03
Ni	2.60E-10	1.92E-07	1.97E-07	1.13E-07	1.30E-07
Np	5.10E-04	8.33E-05	6.19E-08	1.00E-16	1.00E-16
Pb	6.32E-12	3.00E-11	3.69E-11	1.83E-09	2.13E-09
Pu	3.41E-03	4.76E-10	1.08E-10	8.41E-13	7.05E-13
S	2.16E-02	4.19E-03	4.82E-04	1.92E-04	1.92E-04
Si	9.11E-04	4.20E-05	3.97E-05	3.69E-05	3.76E-05
Tc	1.00E-16	1.00E-16	1.00E-16	1.00E-16	1.00E-16
Ti	1.79E-10	2.17E-10	2.25E-10	2.26E-10	2.26E-10
U	2.15E-01	2.27E-03	5.22E-04	1.49E-06	1.03E-06
Hf (Zr)[a]	5.38E-10	6.52E-10	6.74E-10	6.78E-10	6.78E-10

NOTES: [a]Hf was converted to Zr for EQ6 Calculations (Assumption 3.16).

Table 6-6. Composition of Corrosion Products (mole%) and Density in Selected Years for Case 8 (p00_1231)

Element \ Years	4360	9767	30506	126670	633860
O	5.39E+01	5.44E+01	5.81E+01	5.98E+01	5.99E+01
Al	8.81E-01	8.76E-01	1.02E+00	1.08E+00	1.08E+00
B	2.74E+00	2.53E+00	1.94E+00	6.43E-16	2.70E-16
Ba	8.39E-03	8.34E-03	9.68E-03	1.03E-02	1.03E-02
Ca	4.81E-01	4.78E-01	5.55E-01	4.57E-01	4.78E-01
Cl	0.00E+00	2.16E-18	0.00E+00	0.00E+00	0.00E+00
Cr	0.00E+00	2.98E-03	3.46E-03	1.38E-03	0.00E+00
Cu	2.41E-02	2.39E-02	2.78E-02	2.95E-02	2.94E-02
F	0.00E+00	5.40E-19	0.00E+00	0.00E+00	0.00E+00
Fe	1.12E+01	1.20E+01	1.60E+01	1.88E+01	1.87E+01
Gd	7.63E-02	7.58E-02	8.80E-02	9.35E-02	9.33E-02
H	1.76E+01	1.66E+01	8.69E+00	5.55E+00	5.60E+00
C	8.25E-01	8.03E-01	3.29E-01	6.03E-01	5.47E-01
P	1.12E-02	1.22E-02	1.68E-02	1.99E-02	2.00E-02
K	4.44E-01	4.39E-01	4.49E-01	2.59E-01	1.32E-01
Li	1.92E-01	1.19E-01	0.00E+00	0.00E+00	0.00E+00
Mg	3.46E-01	3.44E-01	3.97E-01	3.44E-01	3.30E-01
Mn	4.09E-01	4.32E-01	5.66E-01	6.52E-01	6.52E-01
Mo	0.00E+00	0.00E+00	2.14E-31	0.00E+00	0.00E+00
N	0.00E+00	0.00E+00	0.00E+00	0.00E+00	0.00E+00
Na	1.61E+00	1.54E+00	4.57E-01	2.33E-02	3.20E-02
Ni	2.25E-01	3.45E-01	7.02E-01	9.87E-01	9.86E-01
Np	0.00E+00	0.00E+00	8.67E-17	0.00E+00	0.00E+00
Pb	3.00E-03	2.98E-03	3.46E-03	3.67E-03	3.67E-03
Pu	5.21E-02	5.34E-02	6.20E-02	6.59E-02	6.58E-02
S	0.00E+00	2.43E-16	0.00E+00	0.00E+00	0.00E+00
Si	8.01E+00	7.98E+00	9.32E+00	9.96E+00	1.01E+01
Tc	0.00E+00	1.23E-31	0.00E+00	1.51E-31	1.42E-31
Ti	9.14E-01	9.08E-01	1.05E+00	1.12E+00	1.12E+00
U	0.00E+00	2.81E-02	2.91E-02	3.12E-02	3.10E-02
Hf (Zr)[a]	8.82E-02	8.76E-02	1.02E-01	1.08E-01	1.08E-01
Total (%)	100	100	100	100	100
Total[b] (g)	3.19E+03	3.31E+03	3.31E+03	3.35E+03	3.35E+03
Density (g/cm^3)	3.28	3.37	3.84	4.09	4.10

NOTES: [a]Hf was converted to Zr for EQ6, then converted back to Hf for mass and density calculations.
[b]For EQ6 system (1 liter aqueous fluid). To obtain total grams in WP, multiply by total system volume of 4593.965 liters.

6.4 CASE 13 (p00_2131)

Case 13 combines fast steel and ceramic degradation with slow HLW glass degradation and a very low drip rate. These conditions allow early degradation of the ceramic, and exposure of the Gd solids to sustained, low pH. Consequently, this case experienced the highest Gd loss, ~79%. Figure 6-11 shows the relationship of WP materials degradation to pH, and Figure 6-12 shows the total dissolved Gd (Gd [aq]), and the total Gd in solids, per liter of void space. It is apparent that for a substantial period, the dissolved Gd is more significant than the Gd present in solids. The dissolved Gd is largely lost from the system by the flushing action. Because of the low flush rate, the pH eventually reaches high values (due to HLW glass dissolution); consequently, this system loses much of the U to aqueous carbonate complexes.

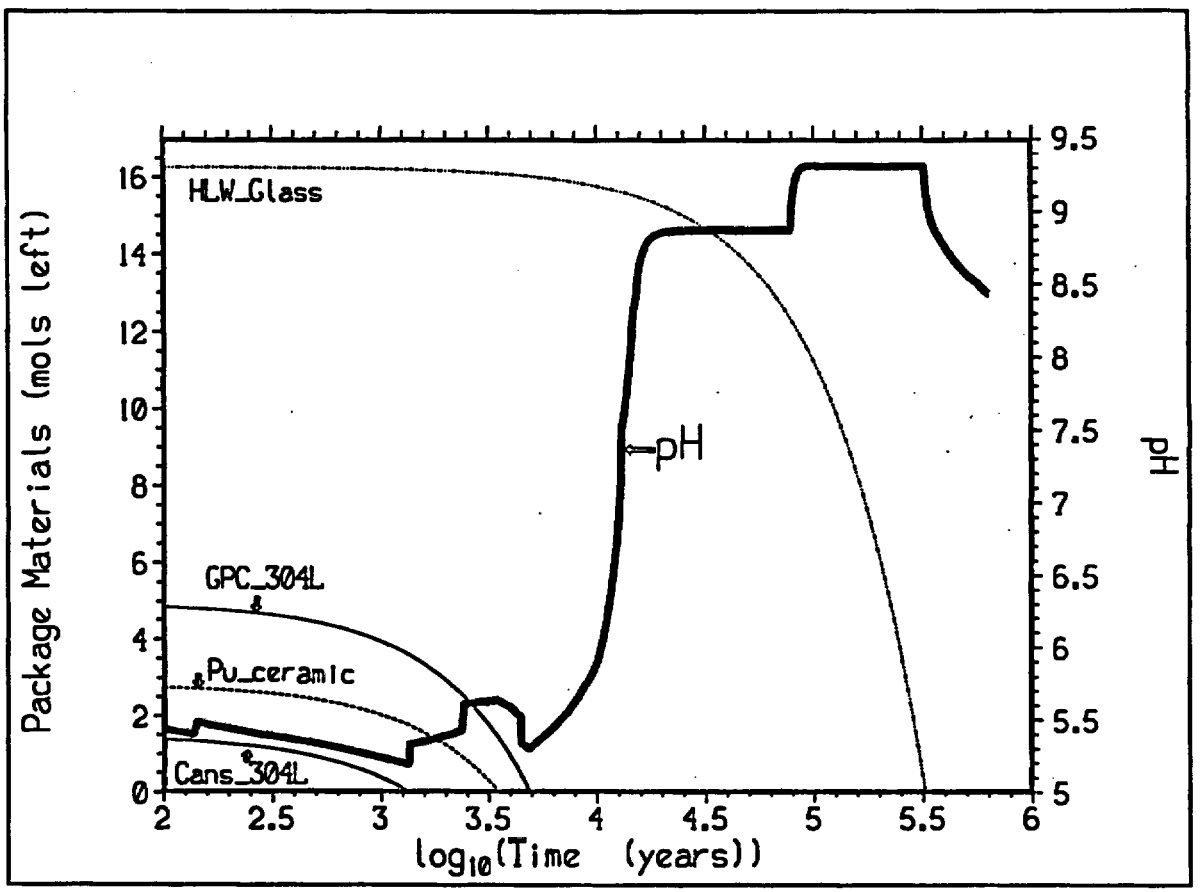

Figure 6-11. Case 13 (p00_2131): pH and Package Materials Remaining

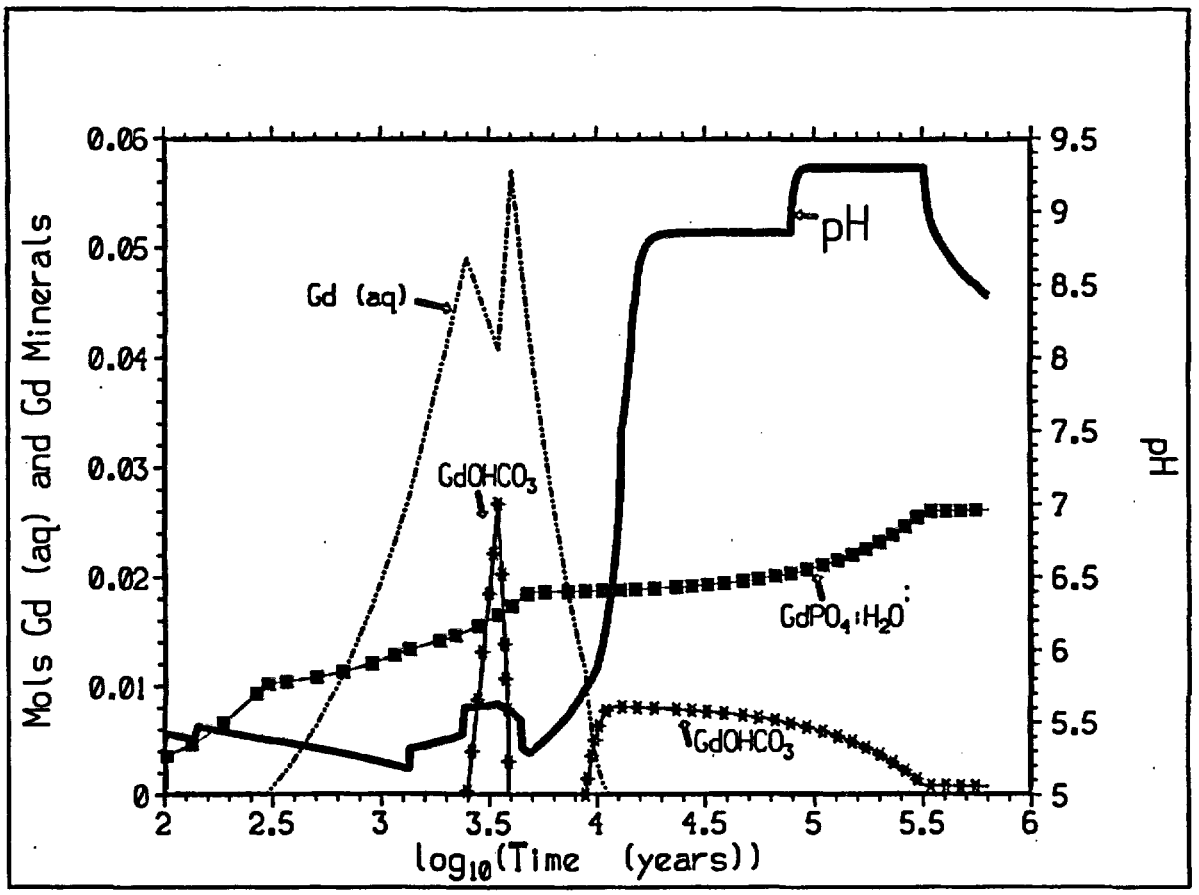

NOTES: Moles solids calculated per liter of void space.
This case had the highest Gd loss. Gd (aq) is the total dissolved (aqueous) Gd concentration.

Figure 6-12. Case 13: pH, Moles Aqueous Gd, and Moles Gd Solids

Tables 6-7 and 6-8, respectively, give the concentrations of dissolved elements in the aqueous phase, and the composition and density of the corrosion products for Case 13.

Table 6-7. Solution Composition in Molality in Selected Years for Case 13 (p00_2131 and pl0_2131)

Years	1351	13175	33377	112990
Element \ pH	5.19	7.51	8.86	9.30
O	5.84E+01	5.58E+01	5.58E+01	5.57E+01
Al	5.47E-12	8.82E-09	9.68E-08	8.07E-08
B	1.65E-02	4.54E-02	4.59E-02	4.59E-02
Ba	3.89E-07	2.41E-08	4.50E-10	6.74E-11
Ca	1.56E-01	1.35E-02	2.97E-05	8.19E-06
Cl	3.83E-04	7.01E-04	7.07E-04	7.07E-04
Cr	8.29E-01	6.49E-02	3.07E-04	2.45E-04
Cu	1.33E-04	5.41E-07	9.06E-07	4.19E-06
F	2.16E-04	2.16E-04	3.74E-04	3.74E-04
Fe	2.63E-11	1.24E-12	1.40E-12	1.84E-12
Gd	2.87E-02	1.40E-07	2.78E-07	7.34E-07
H	1.11E+02	1.11E+02	1.11E+02	1.11E+02
C	2.95E-05	7.66E-04	5.71E-02	5.18E-02
P	1.10E-11	2.14E-10	4.86E-08	3.14E-07
K	4.00E-03	9.08E-03	3.90E-03	4.03E-03
Li	1.18E-02	3.25E-02	3.19E-02	3.31E-02
Mg	1.67E-03	3.84E-03	4.07E-05	8.96E-06
Mn	4.68E-10	7.49E-15	4.25E-16	1.02E-15
Mo	1.00E-16	1.00E-16	1.00E-16	1.00E-16
N	1.63E-02	1.41E-03	1.43E-04	1.42E-04
Na	2.26E-02	5.75E-02	5.61E-02	5.49E-02
Ni	2.19E-01	7.81E-06	1.57E-08	1.76E-09
Np	3.44E-04	3.82E-06	7.12E-07	6.21E-07
Pb	7.25E-10	4.18E-11	2.78E-10	2.98E-11
Pu	8.22E-11	4.80E-13	2.84E-09	7.70E-08
S	8.43E-03	1.09E-03	8.16E-04	8.16E-04
Si	1.87E-04	3.69E-05	4.06E-05	5.51E-05
Tc	1.00E-16	1.00E-16	1.00E-16	1.00E-16
Ti	2.19E-10	2.24E-10	2.25E-10	2.25E-10
U	5.41E-08	1.27E-07	1.36E-02	1.22E-03
Hf (Zr)[a]	6.56E-10	6.72E-10	6.74E-10	6.73E-10

NOTES: [a]Hf was converted to Zr for EQ6 Calculations (Assumption 3.16).

Table 6-8. Composition of Corrosion Products (mole%) and Density at Selected Times for Case 13 (p00_2131 and p10_2131)

Element \ Years	1351	13175	33377	112990
O	6.03E+01	6.04E+01	6.04E+01	6.02E+01
Al	1.19E-02	8.46E-02	2.03E-01	5.71E-01
B	3.52E-15	1.02E-17	0.00E+00	0.00E+00
Ba	1.12E-04	8.04E-04	1.94E-03	5.44E-03
Ca	4.54E-03	7.40E-03	4.84E-02	1.26E-01
Cl	1.76E-15	0.00E+00	3.14E-14	1.65E-14
Cr	1.53E-04	1.09E-03	7.78E-15	1.29E-15
Cu	1.92E-16	9.70E-04	4.34E-03	1.47E-02
F	1.33E-13	4.29E-04	9.50E-15	4.58E-15
Fe	3.64E+01	3.30E+01	3.15E+01	2.67E+01
Gd	2.71E-02	3.97E-02	3.77E-02	3.12E-02
H	5.13E-01	1.10E+00	1.29E+00	2.53E+00
C	0.00E+00	1.20E-02	8.46E-02	2.05E-01
P	2.71E-02	2.77E-02	2.70E-02	2.45E-02
K	8.74E-04	1.01E-02	9.17E-02	3.13E-01
Li	1.48E-14	0.00E+00	3.91E-02	2.45E-02
Mg	7.21E-04	5.33E-03	5.76E-02	2.07E-01
Mn	5.29E-01	6.00E-01	6.10E-01	6.38E-01
Mo	0.00E+00	0.00E+00	5.00E-31	1.57E-31
N	9.28E-13	3.19E-19	5.48E-17	3.55E-18
Na	5.17E-04	6.22E-03	5.88E-02	2.15E-01
Ni	4.10E-01	1.00E+00	9.72E-01	8.64E-01
Np	1.01E-12	7.21E-05	0.00E+00	0.00E+00
Pb	4.06E-05	2.88E-04	6.93E-04	1.94E-03
Pu	9.51E-02	1.79E-01	1.70E-01	1.41E-01
S	4.30E-12	6.38E-19	1.95E-12	1.10E-12
Si	4.34E-01	1.15E+00	2.21E+00	5.49E+00
Tc	0.00E+00	0.00E+00	1.38E-31	2.86E-32
Ti	9.85E-01	1.86E+00	1.78E+00	1.54E+00
U	1.93E-01	3.69E-01	2.60E-01	0.00E+00
Hf (Zr)[a]	1.10E-01	2.07E-01	1.97E-01	1.63E-01
Total (%)	100	100	100	100
Total[b] (g)	1.58E+03	2.17E+03	2.24E+03	2.49E+03
Density (g/cm^3)	5.25	5.21	5.06	4.62

NOTES: [a]Hf was converted to Zr for EQ6, then converted back to Hf for mass and density calculations.
[b]For EQ6 system (1 liter aqueous fluid). To obtain total grams in WP, multiply by total system volume of 4593.965 liters.

6.5 CASE 14 (p00_2133)

In Case p00_2133, the combination of rapid steel degradation and low HLW degradation causes low pH (< 6) for ~$6 \cdot 10^3$ years (Figure 6-13). The HLW glass remains largely intact after most of the steel has corroded (Figure 6-13). Once the steel is exhausted, HLW glass dissolution raises the pH in the system. However, because the drip rate is comparatively high, the pH swings are less extreme than those in Case 13 (Figures 6-11 and 6-12). The concentration of soluble Gd (primarily Gd^{3+} or $Gd(CO_3)_2^-$) is high (~10^{-3} mole/l) for several thousand years (Figure 6-14). Because of the high drip rate, the peak Gd concentration is less extreme than that in Case 13, but the net Gd fluence (concentration × drip rate) is sufficient to remove a significant portion of Gd from the WP. This Case has the second highest Gd loss (49%). However, the lack of very high pH lessens formation of U and Pu carbonate complexes; consequently, U and Pu losses, 0.22 and 0.2%, respectively, are low (Table 6-1). In the sensitivity tests, Cases 30 and 35, Gd loss is decreased to 37.5, and 0.10%, respectively, by changing fO_2 from 0.2 to 10^{-10}, and from 0.2 to 10^{-15} bar, respectively (Table 6-1).

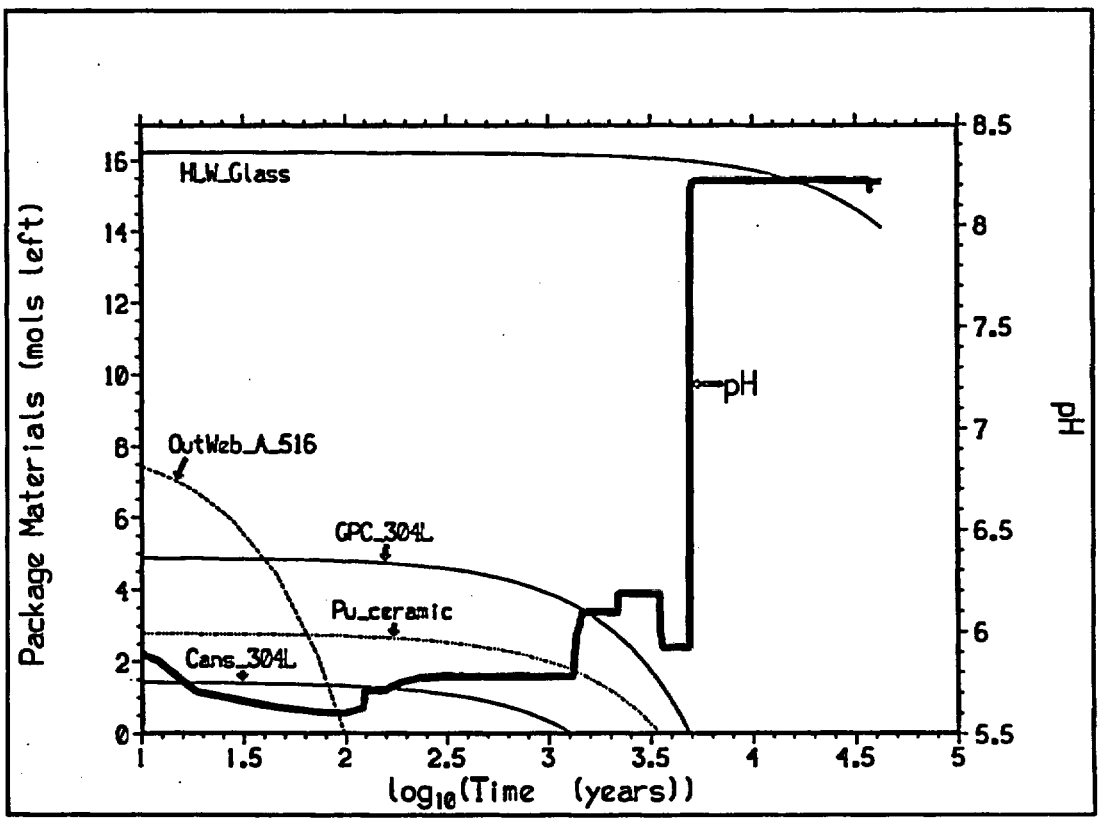

NOTES: This case shows the effects of combining high steel dissolution rates with a low HLW glass rate. Corrosion of steels decreases pH until the steels are exhausted; glass dissolution then increases pH.

Figure 6-13. Case 14 (p00_2133): pH and Package Materials Remaining

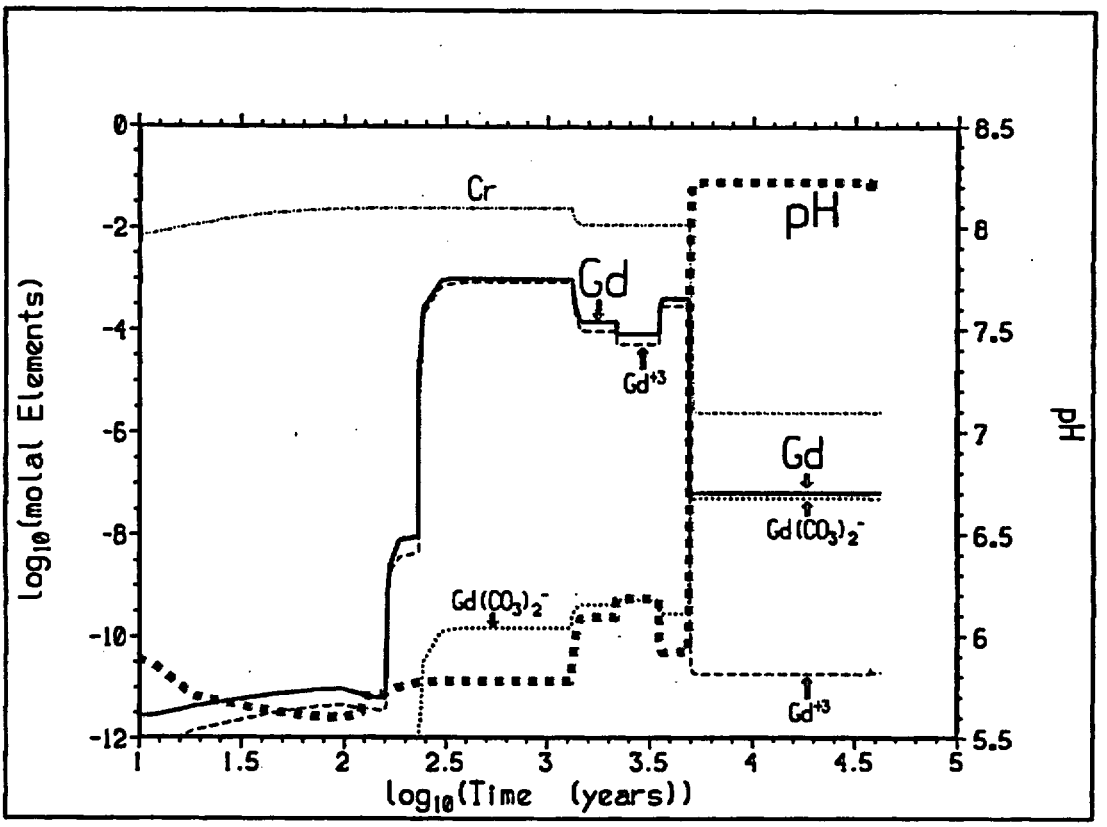

NOTES: The degradation of steel, and subsequent oxidation of Cr(0) to Cr(VI), lowers pH until the steel is exhausted. In the low pH period, Gd occurs mainly as Gd^{3+}. After exhaustion of steel (Figure 6-13), Gd solubility decreases and $Gd(CO_3)_2^-$ becomes the primary dissolved Gd species.

Figure 6-14. Case 14: pH, Gd Species, and Total Aqueous Gd and Cr

Tables 6-9 and 6-10, respectively, give the concentrations of dissolved elements in the aqueous phase, and the composition and density of the corrosion products for Case 13.

Table 6-9. Solution Composition in Molality in Selected Years for Case 14 (p00_2133)

Years	19	10017	30200	42518
pH / Element	5.71	8.22	8.22	8.21
O	5.56E+01	5.55E+01	5.55E+01	5.55E+01
Al	8.37E-14	6.76E-13	6.76E-13	6.46E-16
B	2.22E-04	4.71E-04	4.71E-04	4.71E-04
Ba	2.63E-07	3.14E-09	3.14E-09	3.25E-09
Ca	1.73E-03	1.95E-04	1.95E-04	2.21E-04
Cl	2.04E-04	2.06E-04	2.06E-04	2.06E-04
Cr	1.07E-02	2.45E-06	2.45E-06	2.45E-06
Cu	1.70E-06	3.25E-07	3.25E-07	3.25E-07
F	5.56E-12	1.17E-04	1.17E-04	1.17E-04
Fe	7.77E-12	1.20E-12	1.20E-12	1.20E-12
Gd	4.26E-12	6.54E-08	6.54E-08	6.47E-08
H	1.11E+02	1.11E+02	1.11E+02	1.11E+02
C	4.30E-05	2.83E-03	2.83E-03	2.77E-03
P	5.35E-04	1.14E-09	1.14E-09	1.08E-09
K	1.81E-04	2.39E-04	2.39E-04	2.38E-04
Li	1.57E-04	3.36E-04	3.36E-04	3.36E-04
Mg	1.00E-04	1.06E-04	1.06E-04	5.39E-05
Mn	1.77E-11	2.35E-16	2.35E-16	2.38E-16
Mo	1.00E-16	1.00E-16	1.00E-16	1.00E-16
N	3.52E-04	1.42E-04	1.42E-04	1.42E-04
Na	2.26E-03	2.56E-03	2.56E-03	2.56E-03
Ni	5.08E-03	7.14E-08	7.14E-08	5.38E-08
Np	4.38E-06	6.21E-09	6.21E-09	6.21E-09
Pb	3.53E-10	1.93E-09	1.93E-09	1.99E-09
Pu	6.85E-05	7.72E-13	7.72E-13	7.47E-13
S	1.51E-03	1.98E-04	1.98E-04	1.98E-04
Si	1.87E-04	1.01E-04	1.01E-04	1.91E-04
Tc	1.00E-16	1.00E-16	1.00E-16	1.00E-16
Ti	2.26E-10	2.26E-10	2.26E-10	2.26E-10
U	9.95E-07	7.56E-07	7.56E-07	1.01E-07
Hf (Zr)[a]	6.78E-10	6.78E-10	6.78E-10	6.78E-10

NOTES: [a]Hf was converted to Zr for EQ6 Calculations (Assumption 3.16).

Table 6-10. Composition of Corrosion Products (mole%) and Density in Selected Years for Case 14 (p00_2133)

Element \ Years	19	10017	30200	42518
O	6.02E+01	6.04E+01	6.01E+01	6.01E+01
Al	1.13E-03	6.38E-02	1.75E-01	2.34E-01
B	3.01E-18	0.00E+00	1.44E-19	0.00E+00
Ba	5.40E-06	5.73E-04	1.63E-03	2.20E-03
Ca	1.25E-02	4.48E-02	1.77E-01	2.42E-01
Cl	0.00E+00	1.58E-19	1.08E-19	2.05E-19
Cr	5.40E-06	2.47E-21	0.00E+00	1.05E-19
Cu	0.00E+00	8.24E-04	3.72E-03	5.25E-03
F	2.43E-03	0.00E+00	0.00E+00	5.13E-19
Fe	3.89E+01	3.27E+01	2.99E+01	2.85E+01
Gd	9.01E-03	9.08E-02	8.26E-02	7.84E-02
H	6.14E-02	1.41E+00	2.66E+00	3.19E+00
C	1.17E-12	6.74E-02	6.32E-02	7.35E-02
P	1.64E-02	2.52E-02	2.46E-02	2.44E-02
K	2.93E-05	3.87E-03	1.06E-02	1.56E-02
Li	0.00E+00	0.00E+00	0.00E+00	9.58E-19
Mg	1.27E-04	1.39E-02	3.83E-02	6.21E-02
Mn	4.33E-01	5.88E-01	5.74E-01	5.68E-01
Mo	4.97E-30	0.00E+00	1.97E-31	0.00E+00
N	0.00E+00	0.00E+00	0.00E+00	3.76E-19
Na	3.47E-05	3.90E-03	1.07E-02	1.58E-02
Nl	0.00E+00	6.85E-01	6.40E-01	6.18E-01
Np	0.00E+00	1.51E-21	0.00E+00	4.78E-20
Pb	3.83E-06	2.17E-04	5.94E-04	7.94E-04
Pu	7.90E-03	1.77E-01	1.61E-01	1.53E-01
S	0.00E+00	1.07E-18	3.60E-20	3.21E-17
Si	2.68E-01	1.38E+00	3.11E+00	4.01E+00
Tc	0.00E+00	0.00E+00	2.29E-31	0.00E+00
Ti	9.31E-02	1.84E+00	1.69E+00	1.62E+00
U	1.82E-02	3.64E-01	3.41E-01	3.30E-01
Hf (Zr)[a]	1.04E-02	2.05E-01	1.87E-01	1.78E-01
Total (%)	100	100	100	100
Total[b] (g)	2.29E+02	2.18E+03	2.30E+03	2.37E+03
Density (g/cm^3)	5.25	5.18	4.93	4.81

NOTES: [a]Hf was converted to Zr for EQ6, then converted back to Hf for mass and density calculations.
[b]For EQ6 system (1 liter aqueous fluid). To obtain total grams in WP, multiply by total system volume of 4593.965 liters.

6.6 CASE 18 (p00_2231)

Case 18 (p00_2231) and Case 8 (p00_1231) are similar in that the relatively high HLW glass dissolution rate, and low groundwater drip rate, keep pH above 7 (Figure 6-15). The loss of Gd in Case 18 is low (< 0.02%) and losses of Pu and U are significant, 13.99 and 72.95%, respectively (Table 6-1). The minimum pH for Case 18 (Figure 6-15) is higher than that for Case 8 because, in Case 18, the steel is consumed early when there is ample alkalinity from the ceramic and HLW glass to consume H^+ produced via Equation 2.

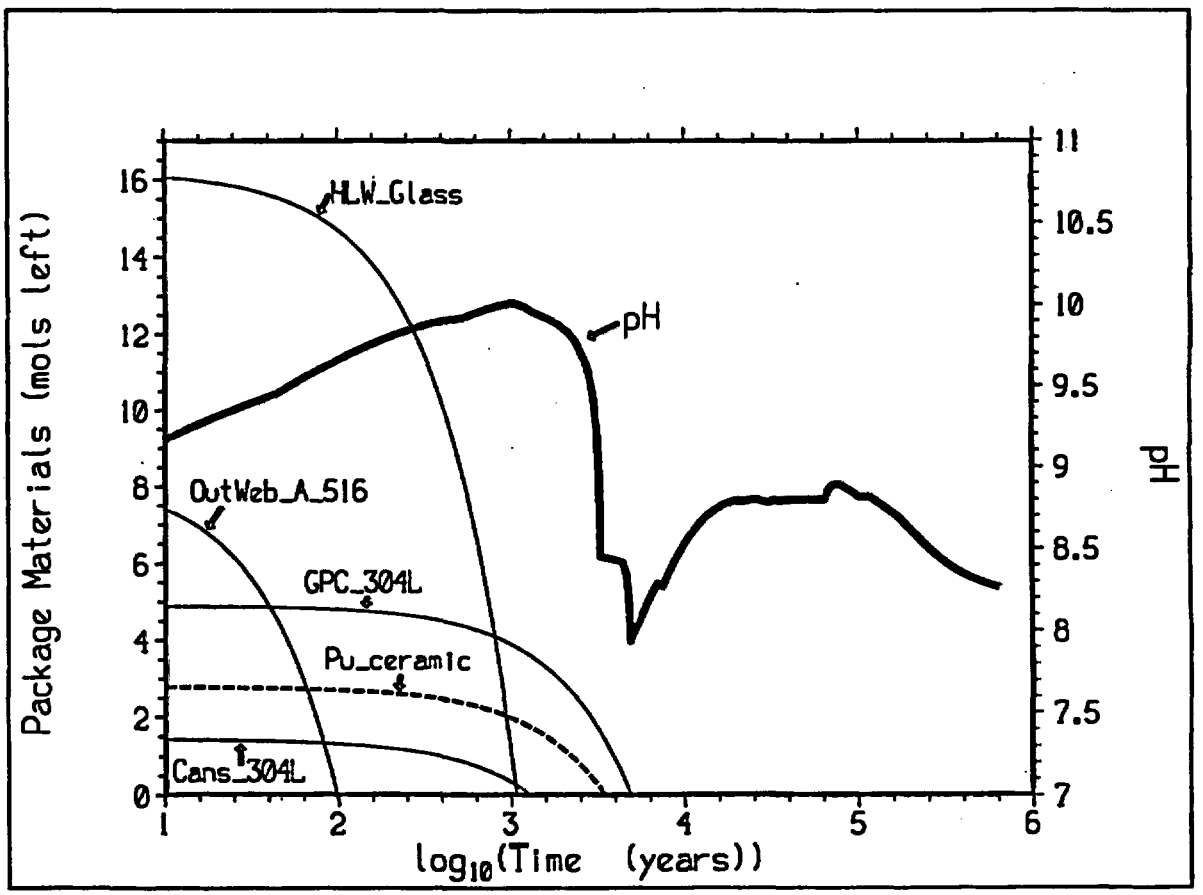

NOTE: Rapid ceramic and HLW glass degradation drives up the pH, until both materials are consumed.

Figure 6-15. Case 18 (p00_2231): pH and Package Materials Remaining

Tables 6-11 and 6-12 give the aqueous phase composition and the composition of the solid corrosion products in the WP for Case 18.

Table 6-11. Solution Composition in Molality in Selected Years for Case 18 (p00_2231)

Years	3315	13591	29400	102680	634200
pH / Element	8.45	8.69	8.78	8.81	8.26
O	5.52E+01	5.66E+01	5.65E+01	5.56E+01	5.55E+01
Al	1.08E-09	3.96E-08	9.23E-08	1.42E-07	3.78E-08
B	9.02E-02	2.23E-01	2.40E-01	1.26E-05	1.24E-05
Ba	3.16E-09	1.17E-09	5.77E-10	2.90E-10	2.62E-09
Ca	1.35E-04	1.04E-04	6.91E-05	1.74E-05	1.32E-04
Cl	2.17E-02	8.70E-04	2.04E-04	2.01E-04	2.01E-04
Cr	9.74E-01	5.52E-02	5.27E-04	1.82E-15	1.00E-16
Cu	6.06E-07	6.74E-07	7.06E-07	5.63E-07	3.26E-07
F	2.40E-03	3.90E-03	1.31E-04	1.15E-04	1.15E-04
Fe	9.67E-13	1.32E-12	1.35E-12	1.35E-12	1.20E-12
Gd	1.23E-07	2.06E-07	2.35E-07	2.21E-07	6.95E-08
H	9.93E+01	1.12E+02	1.12E+02	1.11E+02	1.11E+02
C	3.72E-01	3.95E-02	2.92E-02	1.40E-02	3.12E-03
P	5.18E-08	3.30E-08	3.57E-08	2.03E-08	1.40E-09
K	2.23E-01	1.06E-02	4.35E-03	1.80E-03	1.36E-03
Li	1.27E+00	8.19E-02	1.02E-02	6.92E-06	6.92E-06
Mg	1.64E-04	1.62E-04	1.11E-04	2.26E-05	1.71E-04
Mn	2.88E-16	3.52E-16	3.71E-16	3.43E-16	2.23E-16
Mo	1.00E-16	1.00E-16	1.00E-16	1.00E-16	1.00E-16
N	1.90E-02	1.20E-03	1.46E-04	1.42E-04	1.42E-04
Na	1.08E+00	1.43E-01	1.02E-01	1.41E-02	1.99E-03
Ni	8.89E-08	4.01E-08	2.07E-08	1.05E-08	9.81E-08
Np	6.62E-04	3.34E-05	1.45E-07	1.00E-16	1.00E-16
Pb	1.11E-11	6.82E-11	3.57E-10	1.67E-10	1.60E-09
Pu	2.37E-08	1.89E-09	1.05E-09	1.34E-10	9.26E-13
S	3.23E-02	1.25E-03	1.96E-04	1.92E-04	1.92E-04
Si	8.28E-05	4.30E-05	4.12E-05	3.72E-05	3.71E-05
Tc	1.00E-16	1.00E-16	1.00E-16	1.00E-16	1.00E-16
Ti	1.66E-10	2.23E-10	2.25E-10	2.26E-10	2.26E-10
U	1.19E-01	9.09E-03	5.12E-03	6.24E-04	1.76E-06
Hf (Zr)[a]	4.97E-10	6.68E-10	6.73E-10	6.78E-10	6.78E-10

NOTES: [a]Hf was converted to Zr for EQ6 Calculations (Assumption 3.16).

Table 6-12. Composition of Corrosion Products (mole%) and Density in Selected Years for Case 18 (p00_2231)

Element \ Years	3315	13591	29400	102680	634200
O	5.43E+01	5.51E+01	5.63E+01	5.97E+01	5.98E+01
Al	7.90E-01	8.03E-01	8.71E-01	1.06E+00	1.06E+00
B	2.55E+00	2.21E+00	1.62E+00	0.00E+00	1.10E-15
Ba	7.52E-03	7.65E-03	8.29E-03	1.01E-02	1.01E-02
Ca	4.17E-01	4.38E-01	4.76E-01	5.83E-01	6.16E-01
Cl	1.95E-18	1.49E-13	0.00E+00	4.25E-15	0.00E+00
Cr	2.69E-03	2.74E-03	0.00E+00	1.21E-25	0.00E+00
Cu	2.18E-02	2.22E-02	2.40E-02	2.92E-02	2.92E-02
F	5.03E-03	3.74E-13	0.00E+00	1.95E-15	0.00E+00
Fe	1.27E+01	1.40E+01	1.51E+01	1.84E+01	1.84E+01
Gd	6.49E-02	6.96E-02	7.54E-02	9.15E-02	9.16E-02
H	1.61E+01	1.48E+01	1.22E+01	5.40E+00	5.58E+00
C	1.01E+00	7.32E-01	7.81E-01	8.55E-01	8.19E-01
P	1.33E-02	1.48E-02	1.61E-02	1.95E-02	1.97E-02
K	3.94E-01	3.95E-01	4.14E-01	4.47E-01	2.23E-01
Li	2.09E-01	8.42E-02	0.00E+00	9.38E-17	0.00E+00
Mg	3.10E-01	3.15E-01	3.41E-01	4.14E-01	4.12E-01
Mn	4.45E-01	4.86E-01	5.26E-01	6.39E-01	6.40E-01
Mo	4.85E-32	0.00E+00	5.34E-32	0.00E+00	1.21E-31
N	1.95E-18	1.77E-15	0.00E+00	1.00E-16	0.00E+00
Na	1.87E+00	1.39E+00	1.19E+00	2.93E-01	3.06E-02
Ni	5.71E-01	7.35E-01	7.96E-01	9.66E-01	9.68E-01
Np	0.00E+00	0.00E+00	6.57E-15	0.00E+00	0.00E+00
Pb	2.69E-03	2.74E-03	2.96E-03	3.60E-03	3.60E-03
Pu	5.58E-02	6.02E-02	6.53E-02	7.92E-02	7.93E-02
S	3.90E-18	9.83E-12	0.00E+00	2.65E-13	0.00E+00
Si	7.24E+00	7.39E+00	8.02E+00	9.75E+00	9.89E+00
Tc	0.00E+00	7.74E-32	3.05E-32	0.00E+00	1.48E-31
Ti	7.84E-01	8.33E-01	9.03E-01	1.10E+00	1.10E+00
U	1.02E-01	1.44E-01	1.29E-01	8.29E-02	7.60E-02
Hf (Zr)[a]	7.50E-02	8.04E-02	8.71E-02	1.06E-01	1.06E-01
Total (%)	100	100	100	100	100
Total[b] (g)	3.74E+03	3.85E+03	3.72E+03	3.43E+03	3.42E+03
Density(g/cm^3)	3.52	3.59	3.72	4.05	4.08

NOTES: [a]Hf was converted to Zr for EQ6, then converted back to Hf for mass and density calculations.
[b]For EQ6 system (1 liter aqueous fluid). To obtain total grams in WP, multiply by total system volume of 4593.965 liters.

6.7 TWO-STAGE CASES 22 AND 25 (p01g2204/p02g2022 and p01g2203/p02g2031)

For the five two-stage tests, U contained in the HLW glass is totally lost in the first stage. At the second stage, loss of U is less than 1% in all of the cases, and losses of Pu are also not significant (Table 6-1). The high steel and HLW glass dissolution rates and high groundwater flushing rate remove most of the alkalinity from the HLW glass in the first stage. Since the Pu-ceramic is exposed only in the second stage, the potential for Gd loss occurs only in the second stage. The second stage begins with a period of low pH (Figures 6-16 and 6-17), due to corrosion and oxidation of Cr in the remaining GPC stainless steel, and in the 304L cans, magazines, and racks. Uranium solubility is not dramatic under such pH conditions (Tables 6-1 and 6-13), and U retention in the second stage is higher than in the first. Because of the lower flush rate for Case 25, the low pH persists for longer time. Of the two-stage runs, only Case 25 achieves significant Gd loss because the Gd is degraded completely in the period of low pH. However, the ceramic itself is alkaline, and its degradation counteracts acidity produced by steel degradation. Case 25 is most analogous to the cases that produced high (~15%) Gd loss in the prior study of ceramic WP degradation (Ref. 5, Table 5.3-1).

The "stair step" pH pattern, shown in Figures 6-17 and 6-18 is related to the appearance and disappearance of minerals (corrosion products). Figure 6-19 illustrates one cause of the "stair step". After all the steel has corroded, the only solid Cr phase is $BaCrO_4$. As the system is flushed with Cr-poor water, the $BaCrO_4$ transforms into $BaCO_3$, dominantly by the reaction:

$$BaCrO_4 + HCO_3^- = BaCO_3 + CrO_4^{=} + H^+. \quad \text{(Eq. 11)}$$

Thus, until the $BaCrO_4$ disappears completely, the pH drops. Once the $BaCrO_4$ is exhausted, pH returns nearly to the ambient of incoming water at 10^{-3} bars fCO_2. There is one last small stair step, related to the disappearance of crocoite ($PbCrO_4$).

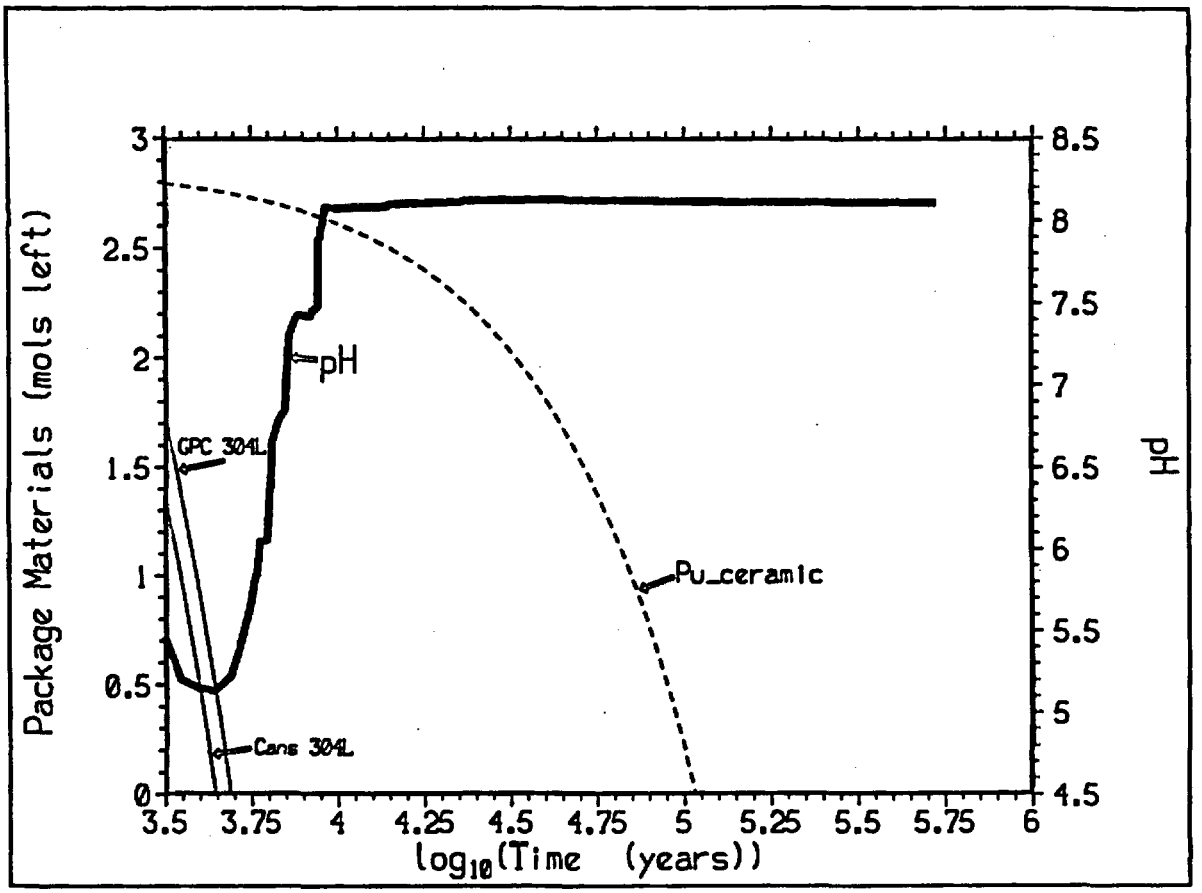

Figure 6-16. Case 22 (p02g2022, 2nd Stage): pH and Package Materials Remaining

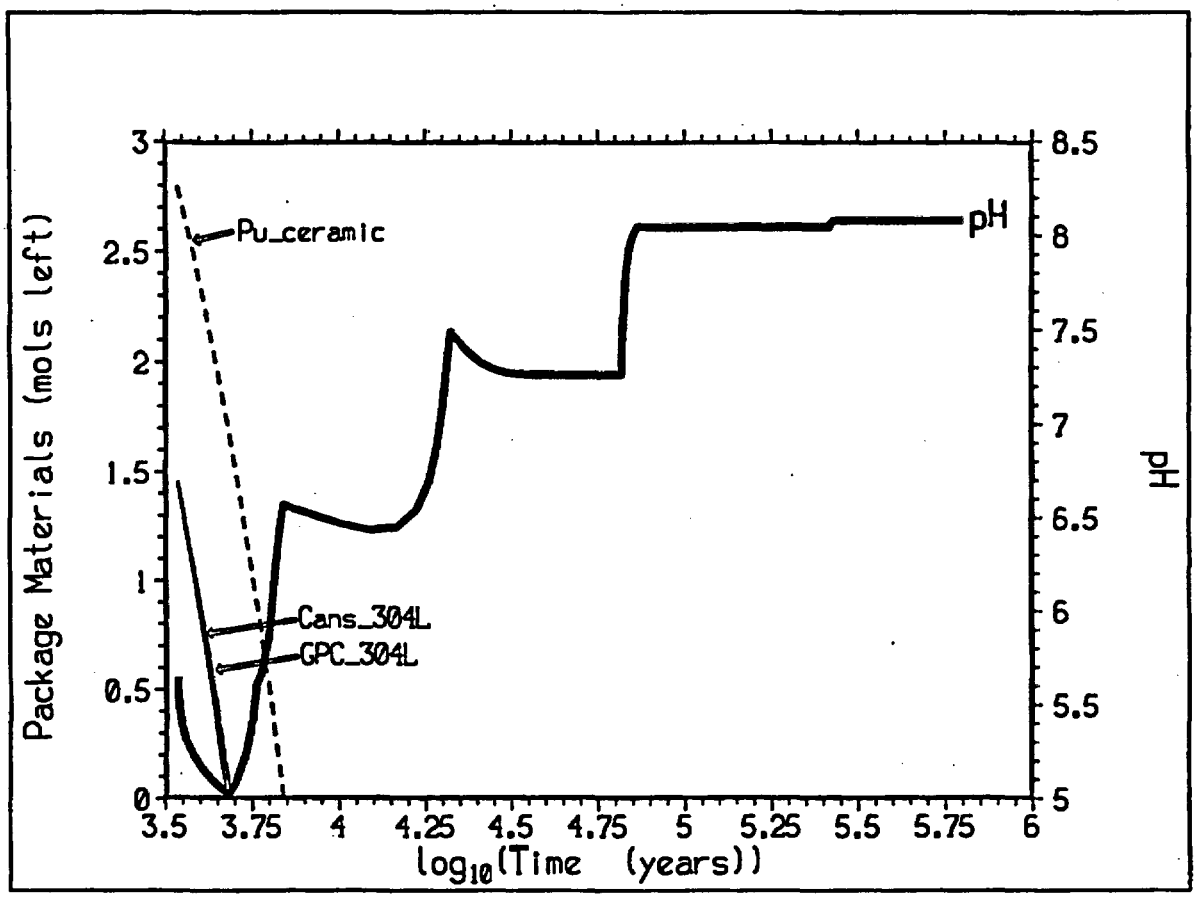

Figure 6-17. Case 25 (p02g2031, 2nd Stage): pH and Package Materials Remaining

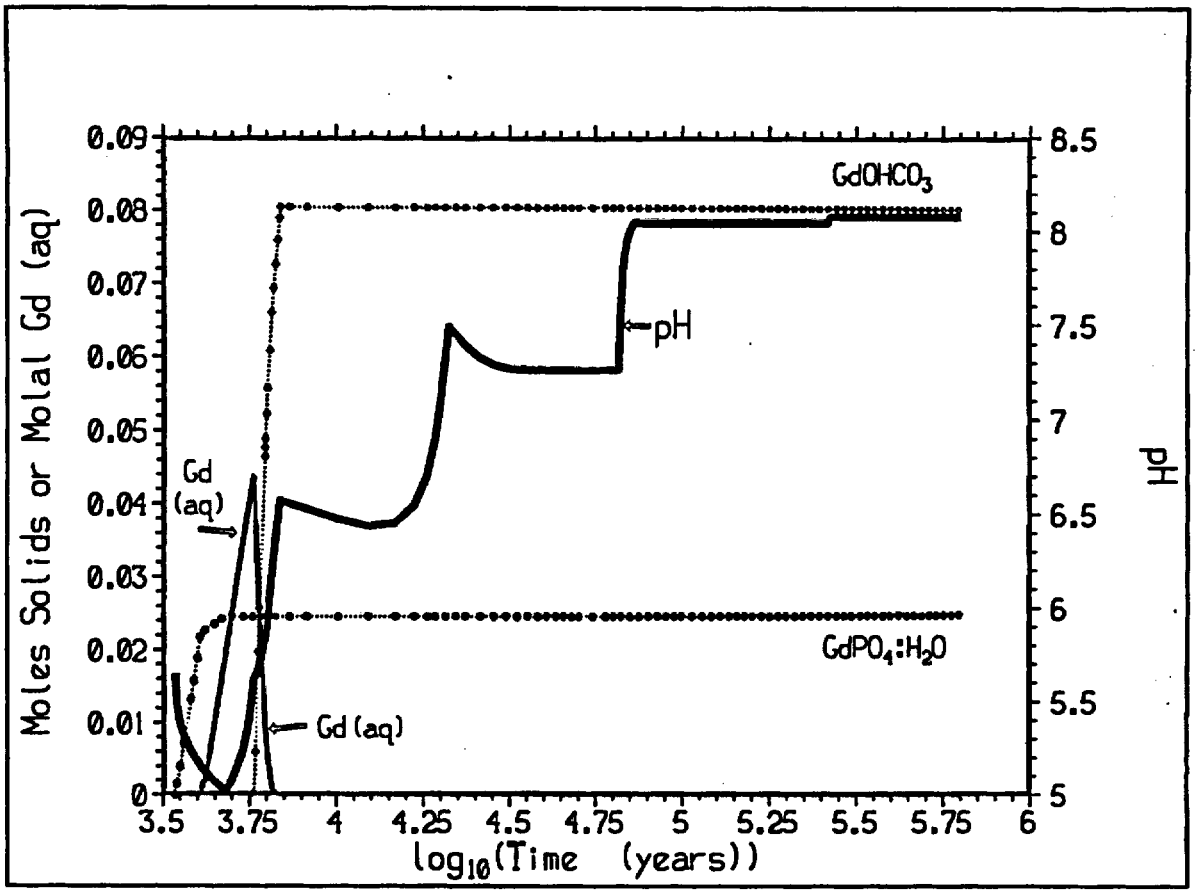

NOTES: Gd (aq) is the total dissolved (aqueous) Gd concentration. High Gd (aq) exists only as a brief, sharp peak before pH climbs and $GdOHCO_3$ precipitates.

Figure 6-18. Case 25 (2nd Stage): pH, Solid Corrosion Products, and Gd (aq)

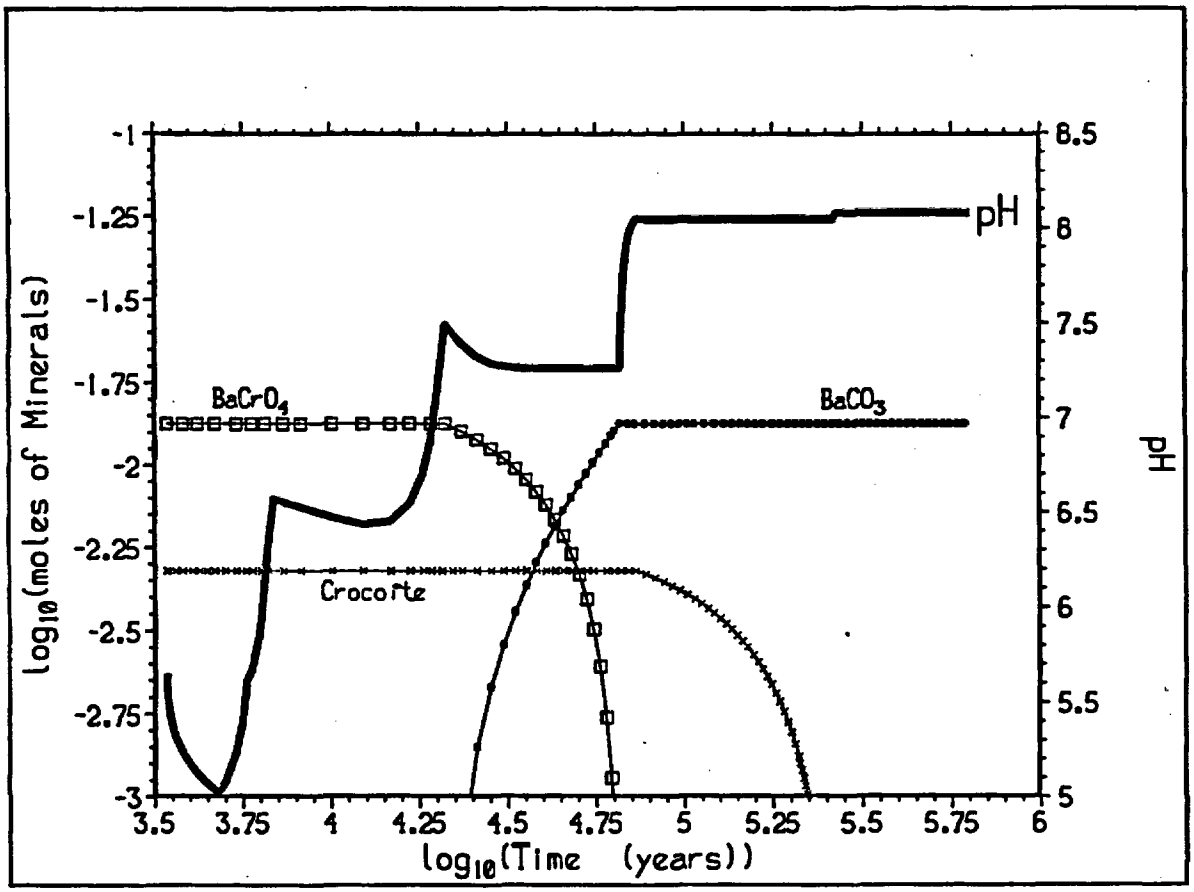

Figure 6-19. Case 25 (2nd Stage): Minerals Causing pH "Stair Step"

Tables 6-13 through 6-16 give the elemental composition of the aqueous phase and the precipitated solids (corrosion products) for Cases 22 and 25.

Table 6-13. Solution Composition in Molality in Selected Years for Case 22 (p01g2204/p02g2022)

Years	4418	10158	41581	100820	528010
pH / Element	5.13E+00	8.07E+00	8.12E+00	8.11E+00	8.11E+00
O	5.60E+01	5.55E+01	5.55E+01	5.55E+01	5.55E+01
Al	1.61E-04	2.44E-08	2.74E-08	2.68E-08	2.63E-08
B	1.24E-05	1.24E-05	1.24E-05	1.24E-05	1.24E-05
Ba	5.26E-07	6.19E-09	4.83E-09	5.06E-09	5.24E-09
Ca	1.36E-03	3.48E-04	3.01E-04	3.33E-04	3.53E-04
Cl	2.01E-04	4.23E-04	2.01E-04	2.01E-04	2.01E-04
Cr	2.33E-01	8.90E-05	1.00E-16	1.00E-16	1.00E-16
Cu	1.89E-03	3.26E-07	3.25E-07	3.25E-07	3.25E-07
F	4.30E-04	6.31E-06	1.15E-04	1.15E-04	1.15E-04
Fe	1.10E-10	3.60E-12	3.60E-12	3.60E-12	3.60E-12
Gd	5.39E-10	9.01E-09	5.81E-08	5.74E-08	5.70E-08
H	1.10E+02	1.11E+02	1.11E+02	1.11E+02	1.11E+02
C	3.32E-05	2.01E-03	2.26E-03	2.20E-03	2.16E-03
P	8.42E-04	4.02E-09	7.64E-10	7.20E-10	6.91E-10
K	7.51E-04	3.91E-04	2.49E-04	1.78E-04	1.26E-04
Li	6.92E-06	6.92E-06	6.92E-06	6.92E-06	6.92E-06
Mg	1.02E-03	2.83E-04	1.45E-04	1.02E-04	8.22E-05
Mn	5.19E-10	3.25E-16	2.83E-16	2.90E-16	2.96E-16
Mo	1.00E-16	1.00E-16	1.00E-16	1.00E-16	1.00E-16
N	4.69E-03	1.42E-04	1.42E-04	1.42E-04	1.42E-04
Na	1.83E-03	1.47E-03	1.94E-03	1.98E-03	1.99E-03
Ni	1.17E-01	4.96E-08	3.87E-08	4.05E-08	4.20E-08
Np	3.16E-06	1.67E-06	1.72E-06	1.70E-06	1.00E-16
Pb	9.32E-10	3.82E-09	2.96E-09	3.11E-09	3.22E-09
Pu	1.56E-04	4.91E-13	5.53E-13	5.37E-13	5.26E-13
S	9.28E-04	1.92E-04	1.92E-04	1.92E-04	1.92E-04
Si	3.67E-05	2.07E-05	2.09E-05	2.11E-05	2.12E-05
Ti	2.23E-10	2.26E-10	2.26E-10	2.26E-10	2.26E-10
U	1.03E-06	5.63E-07	7.82E-07	7.19E-07	6.76E-07
Hf (Zr)[a]	6.69E-10	6.78E-10	6.78E-10	6.78E-10	6.78E-10

NOTES: [a]Hf was converted to Zr for EQ6 Calculations (Assumption 3.16).

Table 6-14. Composition of Corrosion Products (mole%) and Density in Selected Years for Case 22 (p01g2204/p02g2022)

Element \ Years	4418	10158	41581	100820	528010
O	5.55E+01	5.54E+01	5.56E+01	5.58E+01	5.62E+01
Al	9.81E-01	9.62E-01	9.42E-01	9.06E-01	8.62E-01
Ba	9.35E-03	9.17E-03	8.97E-03	8.63E-03	8.39E-03
Ca	1.77E-01	1.90E-01	2.87E-01	4.59E-01	4.48E-01
Cr	1.27E-02	7.56E-04	0.00E+00	0.00E+00	0.00E+00
Cu	1.24E-02	1.05E-02	1.02E-02	9.80E-03	9.26E-03
F	1.97E-03	3.29E-03	0.00E+00	0.00E+00	2.55E-20
Fe	1.67E+01	1.68E+01	1.64E+01	1.58E+01	1.54E+01
Gd	1.07E-03	5.62E-03	3.00E-02	7.32E-02	7.64E-02
H	1.58E+01	1.59E+01	1.57E+01	1.54E+01	1.49E+01
C	0.00E+00	1.50E-02	1.39E-01	3.49E-01	2.99E-01
P	1.67E-02	1.55E-02	1.53E-02	1.48E-02	1.55E-02
K	6.19E-02	5.59E-02	4.31E-02	3.17E-02	2.50E-02
Mg	2.11E-01	2.02E-01	1.90E-01	1.78E-01	1.68E-01
Mn	5.82E-01	5.82E-01	5.70E-01	5.48E-01	5.34E-01
Na	1.51E-02	1.98E-02	3.16E-02	3.32E-02	3.71E-02
Ni	5.04E-01	4.93E-01	4.82E-01	4.64E-01	4.52E-01
Np	0.00E+00	5.56E-06	1.08E-04	2.89E-04	2.32E-31
Pb	3.34E-03	3.28E-03	3.21E-03	3.09E-03	3.00E-03
Pu	1.63E-03	6.08E-03	3.04E-02	7.35E-02	7.67E-02
Si	9.27E+00	9.11E+00	8.98E+00	8.76E+00	9.40E+00
Ti	1.53E-01	1.97E-01	4.45E-01	8.86E-01	9.16E-01
U	2.15E-03	1.13E-02	6.03E-02	1.47E-01	1.53E-01
Hf (Zr)[a]	1.24E-03	6.49E-03	3.47E-02	8.46E-02	8.83E-02
Total (%)	100	100	100	100	100
Total[b] (g)	3.17E+03	3.23E+03	3.33E+03	3.52E+03	3.62E+03
Density (g/cm^3)	3.75	3.76	3.78	3.82	3.80

NOTES: [a]Hf was converted to Zr for EQ6, then converted back to Hf for mass and density calculations.
[b]For EQ6 system (1 liter aqueous fluid). To obtain total grams in WP, multiply by total system volume of 4593.965 liters.

Table 6-15. Solution Composition in Molality in Selected Years for Case 25 (p01g2203/p02g2031)

Years	4758	5803	21187	107620	634130
pH / Element	5.03E+00	5.61E+00	7.49E+00	8.04E+00	8.08E+00
O	5.61E+01	5.61E+01	5.55E+01	5.55E+01	5.55E+01
Al	1.50E-04	1.49E-06	7.76E-09	2.29E-08	2.47E-08
B	1.21E-05	1.22E-05	1.24E-05	1.24E-05	1.24E-05
Ba	5.29E-07	1.59E-07	1.09E-07	6.94E-09	5.85E-09
Ca	1.23E-01	1.95E-01	1.91E-03	3.45E-04	2.29E-04
Cl	1.98E-04	1.99E-04	2.01E-04	2.01E-04	2.01E-04
Cr	8.33E-01	6.26E-01	2.82E-03	7.73E-05	1.00E-16
Cu	1.81E-02	1.28E-03	4.54E-07	3.27E-07	3.26E-07
F	1.19E-03	1.58E-03	3.10E-04	1.15E-04	1.15E-04
Fe	1.13E-10	3.07E-11	3.72E-12	3.60E-12	3.60E-12
Gd	1.80E-02	4.39E-02	1.02E-07	5.44E-08	5.56E-08
H	1.06E+02	1.08E+02	1.11E+02	1.11E+02	1.11E+02
C	2.62E-05	5.01E-05	5.73E-04	1.88E-03	2.03E-03
P	2.55E-11	3.45E-12	7.54E-11	5.24E-10	5.81E-10
K	1.34E-02	1.50E-02	1.46E-03	5.72E-04	3.06E-04
Li	6.78E-06	6.82E-06	6.92E-06	6.92E-06	6.92E-06
Mg	4.62E-02	5.13E-02	4.80E-04	8.76E-05	5.53E-05
Mn	9.21E-10	6.50E-11	3.92E-15	3.50E-16	3.15E-16
Mo	9.81E-17	9.86E-17	1.00E-16	1.00E-16	1.00E-16
N	1.64E-02	1.24E-02	1.97E-04	1.42E-04	1.42E-04
Na	5.19E-03	5.20E-03	8.61E-04	1.41E-03	1.97E-03
Ni	2.06E-01	1.46E-02	8.62E-07	5.56E-08	4.70E-08
Np	3.37E-04	2.85E-04	3.14E-06	1.65E-06	1.66E-06
Pb	9.87E-10	2.94E-10	1.80E-10	4.26E-09	3.60E-09
Pu	1.45E-10	2.38E-11	4.07E-13	4.59E-13	4.92E-13
S	1.68E-04	2.15E-03	2.04E-04	1.92E-04	1.92E-04
Si	2.98E-05	2.65E-05	2.20E-05	2.12E-05	2.16E-05
Tl	2.10E-10	2.15E-10	2.26E-10	2.26E-10	2.26E-10
U	3.64E-07	4.29E-08	4.22E-08	4.47E-07	5.50E-07
Hf (Zr)[a]	6.29E-10	6.44E-10	6.78E-10	6.78E-10	6.78E-10

NOTES: [a]Hf was converted to Zr for EQ6 Calculations (Assumption 3.16).

Table 6-16. Composition of Corrosion Products (mole%) and Density in Selected Years for Case 25 (p01g2203/p02g2031)

Element \ Years	4758	5803	21187	107620	634130
O	5.56E+01	5.57E+01	5.58E+01	5.58E+01	5.59E+01
Al	9.61E-01	9.45E-01	9.29E-01	9.29E-01	9.26E-01
Ba	9.15E-03	9.00E-03	8.85E-03	8.84E-03	8.81E-03
Ca	1.71E-01	1.85E-01	2.00E-01	1.97E-01	2.05E-01
Cr	1.24E-02	1.22E-02	1.20E-02	2.59E-03	2.99E-30
Cu	1.07E-02	1.94E-02	1.98E-02	1.98E-02	1.97E-02
F	3.62E-03	3.02E-03	3.50E-03	0.00E+00	2.50E-19
Fe	1.66E+01	1.64E+01	1.62E+01	1.62E+01	1.61E+01
Gd	1.76E-02	1.76E-02	6.93E-02	6.93E-02	6.90E-02
H	1.56E+01	1.53E+01	1.52E+01	1.52E+01	1.51E+01
C	0.00E+00	8.00E-05	5.31E-02	6.24E-02	6.47E-02
P	1.66E-02	1.65E-02	1.62E-02	1.62E-02	1.63E-02
K	1.26E-01	1.20E-01	1.05E-01	9.45E-02	6.46E-02
Mg	1.62E-01	1.45E-01	1.30E-01	1.29E-01	1.31E-01
Mn	5.77E-01	5.71E-01	5.62E-01	5.61E-01	5.60E-01
Mo	0.00E+00	0.00E+00	9.77E-32	5.70E-32	1.05E-31
Na	5.14E-03	4.31E-03	5.89E-03	2.19E-02	3.92E-02
Ni	6.84E-01	7.90E-01	7.85E-01	7.84E-01	7.82E-01
Np	0.00E+00	1.61E-04	4.49E-04	3.90E-04	2.01E-04
Pb	3.27E-03	3.22E-03	3.16E-03	3.16E-03	3.15E-03
Pu	3.20E-02	5.59E-02	8.09E-02	8.09E-02	8.06E-02
S	1.80E-03	4.63E-04	0.00E+00	0.00E+00	1.56E-17
Si	8.91E+00	8.77E+00	8.63E+00	8.64E+00	8.73E+00
Ti	4.62E-01	7.07E-01	9.64E-01	9.63E-01	9.60E-01
U	6.32E-02	1.12E-01	1.62E-01	1.62E-01	1.61E-01
Hf (Zr)[a]	3.63E-02	6.40E-02	9.30E-02	9.29E-02	9.26E-02
Total (%)	100	100	100	100	100
Total[b] (g)	3.30E+03	3.40E+03	3.49E+03	3.49E+03	3.50E+03
Density (g/cm^3)	3.80	3.84	3.89	3.89	3.88

NOTES: [a]Hf was converted to Zr for EQ6, then converted back to Hf for mass and density calculations.
[b]For EQ6 system (1 liter aqueous fluid). To obtain total grams in WP, multiply by total system volume of 4593.965 liters.

7. ATTACHMENTS

Attachment I. Document Input Reference Sheets (8 pages)

Attachment II. Listing of Files on Electronic Media (7 pages)

8. REFERENCES

1. LLNL 1998. *Plutonium Immobilization Project, Data for Yucca Mountain Total Systems Performance Assessment, Rev. 1.* PIP Milestone Report. Milestone 2.b.b. PIP 98-012. Livermore, California: LLNL. ACC: MOL.19980818.0349.
2. Shaw, H.F., ed. 1999. *Plutonium Immobilization Project Input for Yucca Mountain Total Systems Performance Assessment.* PIP-99-107. Livermore, California: LLNL. TIC: 245437.
3. Civilian Radioactive Waste Management System (CRWMS) Management & Operating Contractor (M&O) 1998. *Total System Performance Assessment - Viability Assessment (TSPA-VA) Analyses Technical Basis Document, Chapter 10, Disruptive Events.* B00000000-01717-4301-00010 REV 00. Las Vegas, Nevada: CRWMS M&O. ACC: MOL.19980724.0399.
4. DOE 1998. *Disposal Criticality Analysis Methodology Topical Report.* Revision 0. YMP/TR-004Q. Las Vegas, Nevada: DOE. ACC: MOL.19990210.0236.
5. CRWMS M&O 1998. *EQ6 Calculations for Chemical Degradation of Pu-Ceramic Waste Packages.* BBA000000-01717-0210-00018 REV 00. Las Vegas, Nevada: CRWMS M&O. ACC: MOL.19980918.0004.
6. Harrar, J.E.; Carley, J.F.; Isherwood, W.F.; and Raber, E. 1990. *Report of the Committee to Review the Use of J-13 Well Water in Nevada Nuclear Waste Storage Investigations.* UCID-21867. Livermore, California: LLNL. ACC: MOL.19980416.0660.
7. CRWMS M&O 1998. *EQ6 Calculations for Chemical Degradation of Fast Flux Test Facility (FFTF) Waste Packages.* BBA000000-01717-0210-00028 REV 00. Las Vegas, Nevada: CRWMS M&O. ACC: MOL.19981229.0081.
8. DOE 1998. *Viability Assessment of a Repository at Yucca Mountain, Volume 3: Total System Performance Assessment.* DOE/RW-0508. Las Vegas, Nevada: CRWMS M&O. ACC: MOL.19981007.0030.
9. Firsching, F.H. and Brune, S.N. 1991. "Solubility Products of the Trivalent Rare-Earth Phosphates." *Journal of Chemical and Engineering Data, 36,* 93-95. Washington, D.C.: American Chemical Society. TIC: 240863.
10. CRWMS M&O 1999. *Electronic Data for EQ6 Calculation for Chemical Degradation of Pu-Ceramic Waste Packages: Effects of Updated Materials Composition and Rates.* CAL-EDC-MD-000003 REV 00. Las Vegas, Nevada: CRWMS M&O. ACC: MOL.19990923.0238.
11. CRWMS M&O 1998. *Total System Performance Assessment - Viability Assessment (TSPA-VA) Analyses Technical Basis Document Chapter 4, Near-Field Geochemical Environment.* B00000000-01717-4301-00004 REV 01. Las Vegas, Nevada: CRWMS M&O. ACC: MOL.19981008.0004.

12. CRWMS M&O 1996. *Second Waste Package Probabilistic Criticality Analysis: Generation and Evaluation of Internal Criticality Configurations.* BBA000000-01717-2200-00005 REV 00. Las Vegas, Nevada: CRWMS M&O. ACC: MOL.19960924.0193.

13. Latimer, W.M. 1952. *The Oxidation States of the Elements and their Potentials in Aqueous Solutions.* pp. 8-9, 30, 215, 272-274. New York, New York: Prentice-Hall, Inc. TIC: 238748.

14. Wolery, T.J. 1992. *EQ3/6, A Software Package for Geochemical Modeling of Aqueous Systems: Package Overview and Installation Guide (Version 7.0).* UCRL-MA-110662 PT I. Livermore, California: LLNL. TIC: 205087.

15. Daveler, S.A. and Wolery, T.J. 1992. *EQPT, A Data File Preprocessor for the EQ3/6 Software Package: User's Guide and Related Documentation (Version 7.0).* UCRL-MA-110662 PT II. Livermore, California: LLNL. TIC: 205240.

16. Wolery, T.J. 1992. *EQ3NR, A Computer Program for Geochemical Aqueous Speciation-Solubility Calculations: Theoretical Manual, User's Guide, and Related Documentation (Version 7.0).* UCRL-MA-110662 PT III. Livermore, California: LLNL. TIC: 205154.

17. Wolery, T.J. and Daveler, S.A. 1992. *EQ6, A Computer Program for Reaction Path Modeling of Aqueous Geochemical Systems: Theoretical Manual, User's Guide, and Related Documentation (Version 7.0).* UCRL-MA-110662 PT IV. Livermore, California: LLNL. TIC: 205002.

18. CRWMS M&O 1999. *Software Change Request (SCR) LSCR198; Addendum To EQ6 Computer Program for Theoretical Manual, User's Guide, and Related Documentation.* UCRL-MA-110662 PT IV. Las Vegas, Nevada: CRWMS M&O. ACC: MOL.19990305.0112.

19. CRWMS M&O 1998. *EQ3/6 Software Installation and Testing Report for Pentium Based Personal Computers (PCs).* CSCI: LLYMP9602100. Las Vegas, Nevada: CRWMS M&O. ACC: MOL.19980813.0191.

20. Jones, R.H. 1998. "Weight of Can-in-Canister Assembly." Interoffice Memorandum from R.H. Jones (WSRC) to E.P. Maddux (WSRC), December 3, 1998, NMP-PLS-980153. TIC: 243808.

21. Shaw, H.; Strachan, D.; Chamberlain, D.; and Bibler, N. 1999. *4.0 Performance Testing and Qualification for Repository: Immobilization Project Review, February 24-25, 1999.* Livermore, California: LLNL. TIC: 243840.

22. Hamilton, L.; Haynes, H.; Hovis, G.; Jones, R.; Kriikku, E.; Ward, C.; and Stokes, M. 1998. *Plutonium Immobilization Canister Rack & Magazine Preliminary Design.* WSRC-TR-98-00333. Aiken, South Carolina: Westinghouse Savannah River Company. TIC: 245168.

23. Westinghouse Savannah River Company 1998. *Drawing: Rack Weldment (Cold Pour Alternate 1C) Weldment.* EES-22624-R3-028 REV A. Aiken, South Carolina: Westinghouse Savannah River Company. TIC: 245356.

24. CRWMS M&O 1999. *Waste Package Materials Properties.* BBA000000-01717-0210-00017 REV 00. Las Vegas, Nevada: CRWMS M&O. ACC: MOL.19990407.0172.

25. CRWMS M&O 1997. *Criticality Evaluation of Degraded Internal Configurations for the PWR AUCF WP Designs.* BBA000000-01717-0200-00056 REV 00. Las Vegas, Nevada: CRWMS M&O. ACC: MOL.19971231.0251.

26. CRWMS M&O 1995. *Total System Performance Assessment - 1995: An Evaluation of the Potential Yucca Mountain Repository.* B00000000-01717-2200-00136 REV 01. Las Vegas, Nevada: CRWMS M&O. ACC: MOL.19960724.0188.

27. CRWMS M&O 1999. *DOE SRS HLW Glass Chemical Composition.* BBA000000-01717-0210-00038 REV 00. Las Vegas, Nevada: CRWMS M&O. ACC: MOL.19990215.0397.

28. DOE 1992. *Characteristics of Potential Repository Wastes.* DOE/RW-0184-R1, Volume 1. Oak Ridge, Tennessee: Oak Ridge National Laboratory. ACC: HQO.19920827.0001.

29. CRWMS M&O 1996. *Material Compositions and Number Densities for Neutronics Calculations.* BBA000000-01717-0200-00002 REV 00. Las Vegas, Nevada: CRWMS M&O. ACC: MOL.19960624.0023.

30. Walker, F.W.; Parrington, J.R.; and Feiner, F. 1989. *Nuclides and Isotopes, Fourteenth Edition, Chart of the Nuclides.* San Jose, California: General Electric Co. TIC: 201637.

31. Spahiu, K. and Bruno, J. 1995. *A Selected Thermodynamic Database for REE to be Used in HLNW Performance Assessment Exercises.* SKB Technical Report 95-35. Stockholm, Sweden: Swedish Nuclear Fuel and Waste Management Co. TIC: 225493.

32. Weger, H.T.; Rai, D.; Hess, N.J.; and McGrail, B.P. 1998. *Solubility and Aqueous-Phase Reactions of Gadolinium in the K^+-Na^+-CO_3^{2-}-OH^--H_2O System.* PNNL-11864. Richland, Washington: Pacific Northwest National Laboratory. TIC: 242377.

33. CRWMS M&O 1998. *EQ6 Calculations for Chemical Degradation of PWR and MOX Spent Fuel Waste Packages.* BBA000000-01717-0210-00009 REV 00. Las Vegas, Nevada: CRWMS M&O. ACC: MOL.19980701.0483.

34. Weast, R.C., ed. 1977. *CRC Handbook of Chemistry and Physics, 58th Edition.* Cleveland, Ohio: CRC Press, Inc. TIC: 242376.

35. DQE 1996. *Waste Acceptance Product Specifications for Vitrified High-Level Waste Forms.* EM-WAPS Rev. 02. Washington, D.C.: DOE. TIC: 234751.

36. Fowler, J.R.; Edwards, R.E.; Marra, S.L.; and Plodinec, M.J. 1995. *Chemical Composition Projections for the DWPF Product.* WSRC-IM-91-116-1, Revision 1. Aiken, South Carolina: Westinghouse Savannah River Company. TIC: 232731.

37. Bibler, N.E.; Ray, J.W.; Fellinger, T.L.; Hodoh, O.B.; Beck, R.S.; and Lien, O.G. 1998. *Characterization of Radioactive Glass Currently Being Produced by the Defense Waste Processing Facility at Savannah River Site.* WSRC-MS-97-00617. Aiken, South Carolina: Westinghouse Savannah River Company. TIC: 240859.

38. Stockman, H.W. 1998. "Long-Term Modeling of Plutonium Solubility at a Desert Disposal Site, Including CO_2 Diffusion, Cellulose Decay, and Chelation." *Journal of Soil Contamination, 7(5),* 615-647. Boca Raton, Florida: Lewis Publishers. TIC: 240836.

Referenced in the Electronic Media:

Roberts, W.L.; Rapp, G.R., Jr.; and Weber, J. 1974. *Encyclopedia of Minerals*. New York, New York: van Nostrand Reinhold Company. TIC: 241917.

Attachment I. Document Input Reference Sheet

OFFICE OF CIVILIAN RADIOACTIVE WASTE MANAGEMENT

DOCUMENT INPUT REFERENCE SHEET

1. Document Identifier No./Rev.:	Change:	Title:
CAL-EDC-MD-000003 REV00		EQ6 Calculation for Chemical Degradation of Pu-Ceramic Waste Packages: Effects of Updated Materials Composition and Rates

Input Document							8. TBV Due To		
	2. Technical Product Input Source Title and Identifier(s) with Version	3. Section	4. Input Status	5. Section Used In	6. Input Description	7. TBV/TBD Priority	Unqual.	From Uncontrolled Source	Un-confirmed
2a 1	LLNL 1998. *Plutonium Immobilization Project, Data for Yucca Mountain Total Systems Performance Assessment, Rev. 1.* PIP Milestone Report. Milestone 2.b.b. PIP 98-012. Livermore, California: LLNL. ACC: MOL.19980818.0349. *INITIAL ISSUE*	Entire; Table 3.1; Section 6 (metamict factor).	TBV-3438	1, 5	Pu-ceramic description, composition, preliminary rates; and metamictization factor of 30.	3	x	N/A	N/A
2	Shaw, H.F., ed. 1999. *Plutonium Immobilization Project Input for Yucca Mountain Total Systems Performance Assessment.* PIP-99-107. Livermore, California: LLNL. TIC: 245437.	Figure 6.1; Section 6.2 (metamict factor).	N/A	1,5	N/A: Used as check that older values are consistent with newer results, but not used for input.	N/A	N/A	N/A	N/A
3	Civilian Radioactive Waste Management System (CRWMS) Management & Operating Contractor (M&O) 1998. *Total System Performance Assessment - Viability Assessment (TSPA-VA) Analyses Technical Basis Document, Chapter 10, Disruptive Events.* B00000000-01717-4301-00010 REV 00. Las Vegas, Nevada: CRWMS M&O. ACC: MOL.19980724.0399.	Section 10.5.1.2.	N/A	1	N/A: Discussion of degradation scenarios, but no numeric data used.	N/A	N/A	N/A	N/A
4	DOE 1998. *Disposal Criticality Analysis Methodology Topical Report.* Revision 0. YMP/TR-004Q. Las Vegas, Nevada: DOE. ACC: MOL.19990210.0236.	Fig. C-12 and C-13.	N/A	1,3	N/A: Flooding may last > $2 \cdot 10^5$ years; first breach of package likely to occur after 10,000 years. Used to obtain broad bounding times for calculation, but not used for numeric input.	N/A	N/A	N/A	N/A

OFFICE OF CIVILIAN RADIOACTIVE WASTE MANAGEMENT
DOCUMENT INPUT REFERENCE SHEET

1. Document Identifier No./Rev.:	Change:	Title:
CAL-EDC-MD-000003 REV00		EQ6 Calculation for Chemical Degradation of Pu-Ceramic Waste Packages: Effects of Updated Materials Composition and Rates

Input Document							8. TBV Due To		
	2. Technical Product Input Source Title and Identifier(s) with Version	3. Section	4. Input Status	5. Section Used In	6. Input Description	7. TBV/TBD Priority	Unqual.	From Uncontrolled Source	Un-confirmed
5	CRWMS M&O 1998. *EQ6 Calculations for Chemical Degradation of Pu-Ceramic Waste Packages.* BBA000000-01717-0210-00018 REV 00. Las Vegas, Nevada: CRWMS M&O. ACC: MOL.19980918.0004.	pp. 11-13 & p 24; Section 6.3;Table 6.3-1; Fig. 6.3.4-2 and 6.3.4-5	N/A	1,3,5	N/A: Discussion of mode used in EQ6 calculations for Pu-ceramic WP degradation; normalization process; expected run conditions with highest Gd loss; used as broad guidance, but not used for numeric input.	N/A	N/A	N/A	N/A
6	Harrar, J.E.; Carley, J.F.; Isherwood, W.F.; and Raber, E. 1990. *Report of the Committee to Review the Use of J-13 Well Water in Nevada Nuclear Waste Storage Investigations.* UCID-21867. Livermore, California: LLNL. ACC: MOL.19980416.0660. *INITIAL ISSUE*	Tables 4.1 & 4.2	TBV-3425	3, 5	Composition of J-13 water. AMOPE must review average composition of J-13. This composition is widely used throughout project, and was determined by peer-review panel.	3	X	N/A	N/A
7	CRWMS M&O 1998. *EQ6 Calculations for Chemical Degradation of Fast Flux Test Facility (FFTF) Waste Packages.* BBA000000-01717-0210-00028 REV 00. Las Vegas, Nevada: CRWMS M&O. ACC: MOL.19981229.0081.	p 25; Fig 5-2 through 5-0; pp 54-57; Sections 5.1.1.3 & 5.3.1	N/A	3, 5	N/A: Chemical variations expected in package, solubility conditions for Gd phosphate, used as general guidance; not used for numeric input. Justification for drip rates; range used is large, encompasses VA values, and constitutes a parametric variation.	N/A	N/A	N/A	N/A
8	DOE 1998. *Viability Assessment of a Repository at Yucca Mountain, Volume 3: Total System Performance Assessment.* DOE/RW-0508. Las Vegas, Nevada: CRWMS M&O. ACC: MOL.19981007.0030.	Fig 3-22 & 3-24, pp 3-34 to 3-37.	N/A	3	N/A: Discussion of temperature at which initial breach of waste package will occur. Used to indicate broad constraints on run conditions, and to justify use of 25C data, but not used for numeric input.	N/A	N/A	N/A	N/A
9	Firsching, F.H. and Brune, S.N. 1991. "Solubility Products of the Trivalent Rare-Earth Phosphates." *Journal of Chemical and Engineering Data, 36,* 93-95. Washington, D.C.: American Chemical Society. TIC: 240863.	Entire	N/A	3	N/A: Discussion of GdPO4 solubility; not used for numeric input.	N/A	N/A	N/A	N/A

OFFICE OF CIVILIAN RADIOACTIVE WASTE MANAGEMENT
DOCUMENT INPUT REFERENCE SHEET

1. Document Identifier No./Rev.:	Change:	Title:
CAL-EDC-MD-000003 REV00		EQ6 Calculation for Chemical Degradation of Pu-Ceramic Waste Packages: Effects of Updated Materials Composition and Rates

Input Document							8. TBV Due To		
	2. Technical Product Input Source Title and Identifier(s) with Version	3. Section	4. Input Status	5. Section Used In	6. Input Description	7. TBV/TBD Priority	Unqual.	From Uncontrolled Source	Un-confirmed
10	CRWMS M&O 1999. *Electronic Data for EQ6 Calculation for Chemical Degradation of Pu-Ceramic Waste Packages: Effects of Updated Materials Composition and Rates.* CAL-EDC-MD-000003 REV 00. Las Vegas, Nevada: CRWMS M&O. ACC: MOL.19990923.0238.	Entire	N/A	3, 4, 5, 6	N/A: EQ6 database files, geometry calculations for fuel & WP (Pu-ceram.xls), EQ3/6 3i, 6i and output files. Excel (xls) files cite other references as indicated in these DIRs.	N/A	N/A	N/A	N/A
11	CRWMS M&O 1998. *Total System Performance Assessment - Viability Assessment (TSPA-VA) Analyses Technical Basis Document Chapter 4, Near-Field Geochemical Environment.* B00000000-01717-4301-00004 REV 01. Las Vegas, Nevada: CRWMS M&O. ACC: MOL.19981008.0004.	Figure 4-27	TBV-3412	3, 5	N/A: Long-term CO2 pressure (log(fO2)= -3). Used only for consistency check; fCO2 varied up 1 order magnitude from well-established ambient (Ref. 34).	3	X	N/A	N/A
12	CRWMS M&O 1996. *Second Waste Package Probabilistic Criticality Analysis: Generation and Evaluation of Internal Criticality Configurations.* BBA000000-01717-2200-00005 REV 00. Las Vegas, Nevada: CRWMS M&O. ACC: MOL.19960924.0193.	Att. VI	N/A	3	Basis for assumption of convective circulation and mixing of water inside waste package.	N/A	N/A	N/A	N/A
13	Latimer, W.M. 1952. *The Oxidation States of the Elements and their Potentials in Aqueous Solutions.* pp. 8-9, 30, 215, 272-274. New York, New York: Prentice-Hall, Inc. TIC: 238748.	p. 272	N/A	3	N/A: Similarity of Hf and Zr. This is widely used handbook. No numeric input; used only for general indication of chemical similarity.	N/A	N/A	N/A	N/A
14	Wolery, T.J. 1992. *EQ3/6, A Software Package for Geochemical Modeling of Aqueous Systems: Package Overview and Installation Guide (Version 7.0).* UCRL-MA-110662 PT I. Livermore, California: LLNL. TIC: 205087.	Entire	N/A	4	N/A: General discussion of EQ3/6 software. Not used for numeric input.	N/A	N/A	N/A	N/A
15	Daveler, S.A. and Wolery, T.J. 1992. *EQPT, A Data File Preprocessor for the EQ3/6 Software Package: User's Guide and Related Documentation (Version 7.0).* UCRL-MA-110662 PT II. Livermore, California: LLNL. TIC: 205240.	Entire	N/A	4	N/A: General discussion of EQ3/6 software. Not used for numeric input.	N/A	N/A	N/A	N/A

OFFICE OF CIVILIAN RADIOACTIVE WASTE MANAGEMENT
DOCUMENT INPUT REFERENCE SHEET

1. Document Identifier No./Rev.:	Change:	Title:
CAL-EDC-MD-000003 REV00		EQ6 Calculation for Chemical Degradation of Pu-Ceramic Waste Packages: Effects of Updated Materials Composition and Rates

Input Document							8. TBV Due To		
	2. Technical Product Input Source Title and Identifier(s) with Version	3. Section	4. Input Status	5. Section Used In	6. Input Description	7. TBV/TBD Priority	Unqual.	From Uncontrolled Source	Un-confirmed
16	Wolery, T.J. 1992. *EQ3NR, A Computer Program for Geochemical Aqueous Speciation-Solubility Calculations: Theoretical Manual, User's Guide, and Related Documentation (Version 7.0).* UCRL-MA-110662 PT III. Livermore, California: LLNL. TIC: 205154.	Entire	N/A	4	N/A: General discussion of EQ3/6 software. Not used for numeric input.	N/A	N/A	N/A	N/A
17	Wolery, T.J. and Daveler, S.A. 1992. *EQ6, A Computer Program for Reaction Path Modeling of Aqueous Geochemical Systems: Theoretical Manual, User's Guide, and Related Documentation (Version 7.0).* UCRL-MA-110662 PT IV. Livermore, California: LLNL. TIC: 205002.	Entire	N/A	4	N/A: General discussion of EQ3/6 software. Not used for numeric input.	N/A	N/A	N/A	N/A
18	CRWMS M&O 1999. *Software Change Request (SCR) LSCR198; Addendum To EQ6 Computer Program for Theoretical Manual, User's Guide, and Related Documentation.* UCRL-MA-110662 PT IV. Las Vegas, Nevada: CRWMS M&O. ACC: MOL.19990305.0112.	Entire	N/A	4	N/A: Signed SCR for EQ6 SCFT Addendum. Shows qualification completed for EQ6 Addendum. Not used for numeric input.	N/A	N/A	N/A	N/A
19	CRWMS M&O 1998. *EQ3/6 Software Installation and Testing Report for Pentium Based Personal Computers (PCs).* CSCI: LLYMP9602100. Las Vegas, Nevada: CRWMS M&O. ACC: MOL.19980813.0191.	Entire	N/A	4	N/A: Documentation of installation and test report for EQ3/6 software. Not used for numeric input.	N/A	N/A	N/A	N/A
20	Jones, R.H. 1998. "Weight of Can-in-Canister Assembly." Interoffice Memorandum from R.H. Jones (WSRC) to E.P. Maddux (WSRC), December 3, 1998, NMP-PLS-980153. TIC: 243808.	Entire	N/A	5; Electronic Media	N/A: Used as check on masses for spreadsheet Pu-ceram.xls in sheet 'Magazines, Can, Rack, Disk'. Not used for numeric input.	N/A	N/A	N/A	N/A

OFFICE OF CIVILIAN RADIOACTIVE WASTE MANAGEMENT
DOCUMENT INPUT REFERENCE SHEET

1. Document Identifier No./Rev.:	Change:	Title:
CAL-EDC-MD-000003 REV00		EQ6 Calculation for Chemical Degradation of Pu-Ceramic Waste Packages: Effects of Updated Materials Composition and Rates

Input Document							8. TBV Due To		
	2. Technical Product Input Source Title and Identifier(s) with Version	3. Section	4. Input Status	5. Section Used In	6. Input Description	7. TBV/TBD Priority	Unqual.	From Uncontrolled Source	Un-confirmed
21	Shaw, H.; Strachan, D.; Chamberlain, D.; and Bibler, N. 1999. *4.0 Performance Testing and Qualification for Repository: Immobilization Project Review, February 24-25, 1999.* Livermore, California: LLNL. TIC: 243840. *INITIAL ISSUE*	Slide 32	N/A	6; Electronic Media	Pu-ceramic degradation rates (slide 32, "SPFT tests: accomplishments"). Used in spreadsheet Pu-ceram.xls, sheet 'Rates', for Table 6-3 or 3.12 calculation. Used only to suggest broad range; rate varied 3 orders of magnitude in calculations.	N/A	N/A	N/A	N/A
22	Hamilton, L.; Haynes, H.; Hovis, G.; Jones, R.; Krilidku, E.; Ward, C.; and Stokes, M. 1998. *Plutonium Immobilization Canister Rack & Magazine Preliminary Design.* WSRC-TR-98-00333. Aiken, South Carolina: Westinghouse Savannah River Company. TIC: 245168. Includes the drawings: drawing *Prototype Magazine (slotted pipe end loader version) Assembly and Details.* EES-22624-R1-011 REVA drawing *Rack Weldment. Details - Scalloped Plates (U).* EES-22624-R4-019 REVA drawing *Rack Weldment. Base Plate Details (U).* EES-22624-R4-020 REVA. *INITIAL ISSUE*	Entire	TBV-3440 AMOPE Approval	Electronic Media	Used for volume and surface area calculations in spreadsheet Pu-ceram.xls, sheet 'Magazines, Can, Rack, Disk'. Drawings are preliminary by nature, because design of the canisters is not fixed. The drawings are used only to calculate approximate area and masses of metal. TBV can be lifted by obtaining final drawings and showing that areas and masses are little changed.	3	N/A	X	N/A
23	Westinghouse Savannah River Company 1998. *Drawing: Rack Weldment (Cold Pour Alternate 1C) Weldment.* EES-22624-R3-028 REV A. Aiken, South Carolina: Westinghouse Savannah River Company. TIC: 245356. *INITIAL ISSUE*	Entire	TBV-3441 AMOPE Approval	Electronic media	Used for volume and surface area calculations in spreadsheet Pu-ceram.xls, sheet 'Magazines, Can, Rack, Disk'. See 22 for TBV conditions.	3	N/A	X	N/A
24	CRWMS M&O 1999. *Waste Package Materials Properties.* BBA000000-01717-0210-00017 REV 00. Las Vegas, Nevada: CRWMS M&O. ACC: MOL.19990407.0172.	Sections 5.2 (p. 10) and 5.4 (p. 17).	TBV-3149	5; Electronic Media	Compositions and densities of 304L and A516 steels. These data are accepted but require concurrence from DOE AMOPE.	N/A	N/A	N/A	N/A

OFFICE OF CIVILIAN RADIOACTIVE WASTE MANAGEMENT
DOCUMENT INPUT REFERENCE SHEET

1. Document Identifier No./Rev.:	Change:	Title:
CAL-EDC-MD-000003 REV00		EQ6 Calculation for Chemical Degradation of Pu-Ceramic Waste Packages: Effects of Updated Materials Composition and Rates

Input Document							8. TBV Due To		
	2. Technical Product Input Source Title and Identifier(s) with Version	3. Section	4. Input Status	5. Section Used in	6. Input Description	7. TBV/TBD Priority	Unqual.	From Uncontrolled Source	Un-confirmed
25	CRWMS M&O 1997. *Criticality Evaluation of Degraded Internal Configurations for the PWR AUCF WP Designs.* BBA000000-01717-0200-00056 REV 00. Las Vegas, Nevada: CRWMS M&O. ACC: MOL.19971231.0251. *INITIAL ISSUE*	p. 11-13	TBV-3442	5; Electronic Media	Corrosion rates of 304L and 316L. Used in sheet 'Rates' of Pu-ceram.xls. To lift TBV, AMOPE must approve approximate rang of rates, or must approve rates within order magnitude variation used in this study.	3	X	N/A	N/A
26	CRWMS M&O 1995. *Total System Performance Assessment - 1995: An Evaluation of the Potential Yucca Mountain Repository.* B00000000-01717-2200-00136 REV 01. Las Vegas, Nevada: CRWMS M&O. ACC: MOL.19960724.0188. *INITIAL ISSUE*	p. 6-5, Fig. 6.2-5 (glass) p. 5-44 to p. 5-55, Fig. 5.4-3, 5.4-4, 5.4-5 (steel)	TBV-3443	5; Electronic Media	Glass degradation rates; carbon steel degradation rates. Used in sheet 'Rates' of Pu-ceram.xls. To lift TBV, AMOPE must approve approximate rang of rates, or must approve rates within the 3 order magnitude variation used in this study.	3	X	N/A	N/A
27	CRWMS M&O 1999. *DOE SRS HLW Glass Chemical Composition.* BBA000000-01717- 0210-00038 REV 00. Las Vegas, Nevada: CRWMS M&O. ACC: MOL.19990215.0397.	Att I, p. I-7	TBV-3022	5; Electronic Media	Composition of the glass. Used in sheet 'Compositions' of Pu-ceram.xls. Wide range tested for study; effects of variation were trivial, so TBV can be lifted if approved composition is within tested range.	3	X	N/A	N/A
28	DOE 1992. *Characteristics of Potential Repository Wastes.* DOE/RW-0184-R1, Volume 1. Oak Ridge, Tennessee: Oak Ridge National Laboratory. ACC: HQO.19920827.0001.	3.3-15, Table 3.3.8	N/A	5	N/A: Glass composition for comparison; not used for numeric input.	N/A	N/A	N/A	N/A
29	CRWMS M&O 1996. *Material Compositions and Number Densities for Neutronics Calculations.* BBA000000-01717-0200-00002 REV 00. Las Vegas, Nevada: CRWMS M&O. ACC: MOL.19960624.0023.	p. 29-31.	TBV-3384	5	Isotopic weights of 241Pu and 99Tc. Reference cited uses values from handbooks. The weights are established fact and considered accepted. Used in Pu-ceram.xls, sheet 'AtomWts'.	N/A	N/A	N/A	N/A

OFFICE OF CIVILIAN RADIOACTIVE WASTE MANAGEMENT
DOCUMENT INPUT REFERENCE SHEET

1. Document Identifier No./Rev.:	Change:	Title:
CAL-EDC-MD-000003 REV00		EQ6 Calculation for Chemical Degradation of Pu-Ceramic Waste Packages: Effects of Updated Materials Composition and Rates

Input Document							8. TBV Due To		
	2. Technical Product Input Source Title and Identifier(s) with Version	3. Section	4. Input Status	5. Section Used in	6. Input Description	7. TBV/TBD Priority	Unqual.	From Uncontrolled Source	Un-confirmed
30	Walker, F.W.; Parrington, J.R.; and Feiner, F. 1989. *Nuclides and Isotopes, Fourteenth Edition, Chart of the Nuclides.* San Jose, California: General Electric Co. TIC: 201637.	List of Elements, p. 50; Gas constant, p. 57.	Accepted	5; Electronic Media.	Atomic weights (primary source); gas constant (from Handbook). Used in Pu-ceram.xls sheet 'AtomWts'.	N/A	N/A	N/A	N/A
31	Spahiu, K. and Bruno, J. 1995. *A Selected Thermodynamic Database for REE to be Used in HLNW Performance Assessment Exercises.* SKB Technical Report 95-35. Stockholm, Sweden: Swedish Nuclear Fuel and Waste Management Co. TIC: 225493. *INITIAL ISSUE*	Entire	TBV-3428	5	SKB thermodynamic data supplied with EQ3/6 code package; basis for rare earth data in data0. TBV can be lifted if AMOPE approves LLNL Gembochs SKB data as "accepted".	3	N/A	N/A	N/A
32	Weger, H.T.; Rai, D.; Hess, N.J.; and McGrail, B.P. 1998. *Solubility and Aqueous-Phase Reactions of Gadolinium in the K^+-Na^+-CO_3^{2-}-OH^--H_2O System.* PNNL-11884. Richland, Washington: Pacific Northwest National Laboratory. TIC: 242377.	Tables 2, 4, A-3.	N/A	5	N/A: Used for comparison against SKB database; not used as input to calculations of WP degradation in section 6.	3	X	N/A	N/A
33	CRWMS M&O 1998. *EQ6 Calculations for Chemical Degradation of PWR and MOX Spent Fuel Waste Packages.* BBA000000-01717-0210-00009 REV 00. Las Vegas, Nevada: CRWMS M&O. ACC: MOL.19980701.0483.	Assump. 3.8.	N/A	5	N/A: Discussion of prior process for converting incoming water composition into EQ6 input; not used for numeric input.	N/A	N/A	N/A	N/A
34	Weast, R.C., ed. 1977. *CRC Handbook of Chemistry and Physics, 58th Edition.* Cleveland, Ohio: CRC Press, Inc. TIC: 242376.	p. F-210.	Accepted	5	Ambient CO_2 pressure. Handbook data.	N/A	N/A	N/A	N/A
35	DOE 1996. *Waste Acceptance Product Specifications for Vitrified High-Level Waste Forms.* EM-WAPS Rev. 02. Washington, D.C.: DOE. TIC: 234751.	p. 7.	N/A	5	N/A: Discusses process for obtaining projected glass compositions.	N/A	N/A	N/A	N/A

OFFICE OF CIVILIAN RADIOACTIVE WASTE MANAGEMENT
DOCUMENT INPUT REFERENCE SHEET

1. Document Identifier No./Rev.:	Change:	Title:
CAL-EDC-MD-000003 REV00		EQ6 Calculation for Chemical Degradation of Pu-Ceramic Waste Packages: Effects of Updated Materials Composition and Rates

Input Document							8. TBV Due To		
	2. Technical Product Input Source Title and Identifier(s) with Version	3. Section	4. Input Status	5. Section Used in	6. Input Description	7. TBV/TBD Priority	Unqual.	From Uncontrolled Source	Un-confirmed
36	Fowler, J.R.; Edwards, R.E.; Marra, S.L.; and Plodinec, M.J. 1995. *Chemical Composition Projections for the DWPF Product.* WSRC-IM-91-116-1, Revision 1. Aiken, South Carolina: Westinghouse Savannah River Company. TIC: 232731.	pp. 4 to 6, Tables 1 to 3.	TBV-3424	5	N/A: Projected DOE glass compositions used for comparison.	N/A	N/A	N/A	N/A
37	Bibler, N.E.; Ray, J.W.; Fellinger, T.L.; Hodoh, O.B.; Beck, R.S.; and Lien, O.G. 1998. *Characterization of Radioactive Glass Currently Being Produced by the Defense Waste Processing Facility at Savannah River Site.* WSRC-MS-97-00617. Aiken, South Carolina: Westinghouse Savannah River Company. TIC: 240859.	Table 1.	N/A	5	N/A: Measured SRL glass composition used for comparison.	N/A	N/A	N/A	N/A
38	Stockman, H.W. 1998. "Long-Term Modeling of Plutonium Solubility at a Desert Disposal Site, Including CO_2 Diffusion, Cellulose Decay, and Chelation." *Journal of Soil Contamination, 7(5),* 615-647. Boca Raton, Florida: Lewis Publishers. TIC: 240836.	pp. 632-634.	N/A	6.2	N/A: Discussion of desert soil fO_2, for broad comparison. Not used for numeric input.	N/A	N/A	N/A	N/A
39	Roberts, W.L.; Rapp, G.R., Jr.; and Weber, J. 1974. *Encyclopedia of Minerals.* New York, New York: van Nostrand Reinhold Company. TIC: 241917. *INITIAL ISSUE*	pp. 46-47, 500, 515-516, 530, 624-625, 690.	TBV-3444	Electronic Media	Density of minerals used for molar volumes of several phases in data0.nuc.R8d; widely used handbook. Given the sources and nature of the data, the densities are established fact should be considered accepted, pending DOE AMOPE approval.	N/A	N/A	N/A	N/A

Attachment II. Listing of Files on Electronic Media

This attachment contains the MS-DOS directory for files placed on the electronic media (Ref. 10). The files are of nine types:

1) Excel files (extension = xls), called out in the text and tables. The file Pu-ceram.xls is the principal source of the *.6i input files used for sections 5.4.2 and 6.
2) EQ3/6 input files (extensions = 3i or 6i), as discussed in Sections 5.3 and 5.4.2. The 6i input files described in Section 5.4 and 6 are formatted for the SCFT mode, and have 8-character names p???sgfw.6i, where the s is a steel rate index (1 or 2), the g is a HLW glass rate index (0, 1 or 2; 0 used when no undegraded HLW glass is present), the f is the fissile (ceramic) degradation rate index (0, 1, 2, or 3), and w is the incoming water drip rate index (1, 2, 3, 4). The ??? indicate run-specific nomenclature described in section 5.4.2.
3) EQ6 output files (text, extension = 6o).
4) Tab-delimited text files (extension = txt), with names p???????.elem????.txt. as discussed in Section 5.4.2; these contain total aqueous moles (*.elem_aqu.txt), total moles in minerals and aqueous phase (*.elem_m_a.txt), total moles in minerals, aqueous phase, and remain special reactants (*.elem_tot.txt), and the total moles in minerals alone (*.elem_min.txt). The *.elem_tot.txt and *.elem_min.txt also have the volume in cm^3 of the minerals and total solids (including special reactants) in the system.
5) FORTRAN source files (extension = for) for the version of EQ6 used in the calculations.
6) MS-DOS/Win95/Win98 executables (extension = exe) for the version of EQ6 and runeq6 used in the calculations, and the autoexec.bat file that sets up the environment.
7) EQ6 data files used for the calculations, with the text file data0.nuc.R8d, and the binary version data1.nuc.
8) Selected binary files (bin extension) used for plots in this document; the format of these files is specified in the EQ6 addendum source (Ref. 18). The binary files are not necessary to use the output of the calculation, but are provided as a convenience for plotting.
9) A copy of this calculation document, Pu-ceramic_312hws*.doc, as of 09-12-1999.

Below are listed the contents of the DOS directories within the electronic attachment. The file sizes are given in bytes.

```
~\Pu-ceram_CD
EXE_F7~1        <DIR>          09-12-99  4:49p Exe_f77_src_data0_data1
PU_BIN~1        <DIR>          09-12-99  5:25p Pu_bin_for_PP_plots
PU_DOC~1        <DIR>          09-12-99  5:51p Pu_doc_xls
PU_TXT~1        <DIR>          09-12-99  5:44p Pu_txt_6i_6o
SENS_G~1        <DIR>          09-12-99  2:06p sens_Gd_thermo
SENS_G~2        <DIR>          09-12-99  2:17p sens_Glass
sens_J13        <DIR>          09-12-99  2:07p sens_J13

~\Pu-ceram_CD\Exe_f77_src_data0_data1
AUTOEXEC BAT              624  09-12-99  1:20p AUTOEXEC.BAT
CONFIG   SYS              463  06-17-98  2:04p CONFIG.SYS
DATA0N~1 R8A        2,299,784  11-25-98  4:15p data0.nuc.R8a
DATA0N~1 R8D        2,300,150  12-15-98  5:26p data0.nuc.R8d
DATA0N~1 R8W        2,301,840  01-19-99 11:33a data0.nuc.R8w
data1    nuc          791,620  04-22-99  4:22p data1.nuc
```

```
data1     R8a          791,200  08-18-99   8:20a data1.R8a
data1     weg          792,936  01-19-99  11:34a data1.weg
Eq3nr     exe        2,169,333  08-18-95   5:47p Eq3nr.exe
eq6       exe        1,056,485  12-11-98   1:27p eq6.exe
eq6new    for        1,322,545  12-11-98  10:50a eq6new.for
eqlibnew  for          492,613  07-01-98   6:34p eqlibnew.for
EQPT      EXE        2,337,701  08-18-95   5:47p EQPT.EXE
EXTERNAL  FNT            9,900  06-29-95   8:27p EXTERNAL.FNT
HELP_PP                 50,724  03-31-98   6:04p HELP_PP
PP        EXE          308,609  10-10-98   4:15p PP.EXE
PREFER    PP                62  01-20-99  10:25a PREFER.PP
Readme    txt              505  09-12-99   1:51p Readme.txt
Runeq3    exe          388,005  08-18-95   5:46p Runeq3.exe
RUNEQ6    EXE          392,181  08-18-95   5:46p RUNEQ6.EXE
RUNEQPT   EXE          334,517  08-18-95   5:46p RUNEQPT.EXE

~\Pu-ceram_CD\Pu_bin_for_PP_plots
P!0_2131 BIN     20,534,072  09-12-99   3:20p P!0_2131.BIN
p00_1131 bin     25,334,888  09-12-99   3:16p p00_1131.bin
p00_1231 bin     28,125,624  09-12-99   3:18p p00_1231.bin
P00_2131 BIN      7,956,864  09-12-99   3:19p P00_2131.BIN
p00_2133 bin     98,284,944  09-12-99   3:26p p00_2133.bin
p00_2231 bin     28,453,992  09-12-99   3:29p p00_2231.bin
p02g2022 bin     97,847,912  09-07-99   2:44p p02g2022.bin
P02G2031 BIN     22,732,728  09-07-99  12:10p P02G2031.BIN
ps0_1131 bin     25,391,016  09-01-99  10:48p ps0_1131.bin

~\Pu-ceram_CD\Pu_doc_xls
DENSIT~1 XLS        206,336  09-12-99   5:51p density_Puceramicsue.xls
FFTF_S~1 XLS      3,696,640  09-12-99   5:41p fftf_short.xls
GD_PEA~1 DOC        910,848  08-30-99  11:26a Gd_peaks_Pu-ceram_083099.doc
pu-ceram xls        922,624  09-12-99   4:36p pu-ceram.xls
PU-CER~1 DOC      3,642,880  09-12-99   6:22p PU-ceramic_312hws_0911_4PM.DOC

~\Pu-ceram_CD\Pu_txt_6i_6o
p!0_2131 6i          37,292  09-12-99   2:33p p!0_2131.6i
p!0_2131 6o       2,337,650  09-12-99   2:35p p!0_2131.6o
P!0_21~3 TXT         21,511  09-12-99   2:45p p!0_2131.elem_aqu.txt
P!0_21~1 TXT         20,366  09-12-99   2:46p p!0_2131.elem_min.txt
P!0_21~2 TXT         20,379  09-12-99   2:46p p!0_2131.elem_tot.txt
P00_1111 6I          41,414  09-12-99   2:34p P00_1111.6I
p00_1111 6o       4,352,245  09-12-99   2:35p p00_1111.6o
P04D9D~1 TXT         42,771  09-12-99   2:46p p00_1111.elem_aqu.txt
P0399D~1 TXT         40,474  09-12-99   2:46p p00_1111.elem_min.txt
P03FB1~1 TXT         40,487  09-12-99   2:46p p00_1111.elem_tot.txt
P00_1113 6I          41,414  09-12-99   2:34p P00_1113.6I
p00_1113 6o       7,658,672  09-12-99   2:36p p00_1113.6o
P04D5D~1 TXT         69,411  09-12-99   2:46p p00_1113.elem_aqu.txt
P0395D~1 TXT         65,674  09-12-99   2:46p p00_1113.elem_min.txt
P03F71~1 TXT         65,687  09-12-99   2:46p p00_1113.elem_tot.txt
P00_1122 6I          41,414  09-12-99   2:34p P00_1122.6I
p00_1122 6o       8,529,473  09-12-99   2:36p p00_1122.6o
P06D3D~1 TXT         74,739  09-12-99   2:46p p00_1122.elem_aqu.txt
P0593D~1 TXT         70,714  09-12-99   2:46p p00_1122.elem_min.txt
P05F51~1 TXT         70,727  09-12-99   2:46p p00_1122.elem_tot.txt
P00_1131 6I          41,414  09-12-99   2:34p P00_1131.6I
```

```
p00_1131 6o      3,589,489  09-12-99  2:36p p00_1131.6o
P08D9D~1 TXT        34,779  09-12-99  2:46p p00_1131.elem_aqu.txt
P0799D~1 TXT        32,914  09-12-99  2:46p p00_1131.elem_min.txt
P00_11~3 TXT        32,927  09-12-99  2:46p p00_1131.elem_tot.txt
P00_1133 6I         41,414  09-12-99  2:34p P00_1133.6I
p00_1133 6o      7,539,485  09-12-99  2:37p p00_1133.6o
P00_11~4 TXT        66,747  09-12-99  2:46p p00_1133.elem_aqu.txt
P00_11~2 TXT        63,154  09-12-99  2:46p p00_1133.elem_min.txt
P00_11~1 TXT        63,167  09-12-99  2:46p p00_1133.elem_tot.txt
P00_1211 6I         41,414  09-12-99  2:34p P00_1211.6I
p00_1211 6o      3,941,015  09-12-99  2:39p p00_1211.6o
P04D8D~1 TXT        37,443  09-12-99  2:46p p00_1211.elem_aqu.txt
P0398D~1 TXT        35,434  09-12-99  2:46p p00_1211.elem_min.txt
P03FA1~1 TXT        35,447  09-12-99  2:46p p00_1211.elem_tot.txt
P00_1213 6I         41,414  09-12-99  2:34p P00_1213.6I
p00_1213 6o      8,043,246  09-12-99  2:40p p00_1213.6o
P04D4D~1 TXT        69,411  09-12-99  2:46p p00_1213.elem_aqu.txt
P0394D~1 TXT        65,674  09-12-99  2:46p p00_1213.elem_min.txt
P03F61~1 TXT        65,687  09-12-99  2:46p p00_1213.elem_tot.txt
P00_1222 6I         41,414  09-12-99  2:34p P00_1222.6I
p00_1222 6o      8,644,631  09-12-99  2:40p p00_1222.6o
P06D2D~1 TXT        75,627  09-12-99  2:46p p00_1222.elem_aqu.txt
P0592D~1 TXT        71,554  09-12-99  2:46p p00_1222.elem_min.txt
P05F41~1 TXT        71,567  09-12-99  2:46p p00_1222.elem_tot.txt
P00_1231 6I         41,414  09-12-99  2:34p P00_1231.6I
p00_1231 6o      3,846,989  09-12-99  2:41p p00_1231.6o
P08D8D~1 TXT        36,999  09-12-99  2:46p p00_1231.elem_aqu.txt
P00_12~4 TXT        35,014  09-12-99  2:46p p00_1231.elem_min.txt
P07FA1~1 TXT        35,027  09-12-99  2:46p p00_1231.elem_tot.txt
P00_1233 6I         41,414  09-12-99  2:34p P00_1233.6I
p00_1233 6o      8,171,722  09-12-99  2:41p p00_1233.6o
P00_12~2 TXT        70,743  09-12-99  2:46p p00_1233.elem_aqu.txt
P00_12~3 TXT        66,934  09-12-99  2:46p p00_1233.elem_min.txt
P00_12~1 TXT        66,947  09-12-99  2:46p p00_1233.elem_tot.txt
p00_2111 6i         41,414  09-12-99  2:33p p00_2111.6i
p00_2111 6o      4,622,145  09-12-99  2:41p p00_2111.6o
P05D9D~1 TXT        46,767  09-12-99  2:46p p00_2111.elem_aqu.txt
P0499D~1 TXT        44,254  09-12-99  2:46p p00_2111.elem_min.txt
P04FB1~1 TXT        44,267  09-12-99  2:46p p00_2111.elem_tot.txt
P00_2113 6I         41,414  09-12-99  2:34p P00_2113.6I
p00_2113 6o      8,086,978  09-12-99  2:42p p00_2113.6o
P05D5D~1 TXT        73,851  09-12-99  2:46p p00_2113.elem_aqu.txt
P0495D~1 TXT        69,874  09-12-99  2:46p p00_2113.elem_min.txt
P04F71~1 TXT        69,887  09-12-99  2:46p p00_2113.elem_tot.txt
P00_2122 6I         41,414  09-12-99  2:34p P00_2122.6I
p00_2122 6o      8,683,481  09-12-99  2:42p p00_2122.6o
P07D3D~1 TXT        76,959  09-12-99  2:46p p00_2122.elem_aqu.txt
P00_21~4 TXT        72,814  09-12-99  2:46p p00_2122.elem_min.txt
P06F51~1 TXT        72,827  09-12-99  2:46p p00_2122.elem_tot.txt
p00_2131 6i         41,479  09-12-99  2:33p p00_2131.6i
p00_2131 6o      1,820,752  09-12-99  2:42p p00_2131.6o
P09D9D~1 TXT        19,731  09-12-99  2:46p p00_2131.elem_aqu.txt
P0899D~1 TXT        18,682  09-12-99  2:46p p00_2131.elem_min.txt
P08FB1~1 TXT        18,695  09-12-99  2:46p p00_2131.elem_tot.txt
P00_2133 6I         41,414  09-12-99  2:34p P00_2133.6I
p00_2133 6o      7,892,956  09-12-99  2:43p p00_2133.6o
P00_21~1 TXT        70,299  09-12-99  2:46p p00_2133.elem_aqu.txt
```

```
P00_21~2 TXT        66,514  09-12-99  2:46p p00_2133.elem_min.txt
P00_21~3 TXT        66,527  09-12-99  2:46p p00_2133.elem_tot.txt
P00_2211 6I         41,414  09-12-99  2:34p P00_2211.6I
p00_2211 6o      4,267,590  09-12-99  2:43p p00_2211.6o
P05D8D~1 TXT        40,551  09-12-99  2:46p p00_2211.elem_aqu.txt
P0498D~1 TXT        38,374  09-12-99  2:46p p00_2211.elem_min.txt
P04FA1~1 TXT        38,387  09-12-99  2:46p p00_2211.elem_tot.txt
P00_2213 6I         41,414  09-12-99  2:34p P00_2213.6I
p00_2213 6o      8,635,980  09-12-99  2:44p p00_2213.6o
P05D4D~1 TXT        75,627  09-12-99  2:46p p00_2213.elem_aqu.txt
P0494D~1 TXT        71,554  09-12-99  2:46p p00_2213.elem_min.txt
P04F61~1 TXT        71,567  09-12-99  2:46p p00_2213.elem_tot.txt
P00_2222 6I         41,414  09-12-99  2:34p P00_2222.6I
p00_2222 6o      1,305,088  09-12-99  2:44p p00_2222.6o
P07D2D~1 TXT        75,183  09-12-99  2:46p p00_2222.elem_aqu.txt
P0692D~1 TXT        71,134  09-12-99  2:46p p00_2222.elem_min.txt
P00_22~1 TXT        71,147  09-12-99  2:46p p00_2222.elem_tot.txt
P00_2231 6I         41,414  09-12-99  2:34p P00_2231.6I
p00_2231 6o      3,971,911  09-12-99  2:44p p00_2231.6o
P09D8D~1 TXT        37,887  09-12-99  2:46p p00_2231.elem_aqu.txt
P0898D~1 TXT        35,854  09-12-99  2:46p p00_2231.elem_min.txt
P00_22~4 TXT        35,867  09-12-99  2:46p p00_2231.elem_tot.txt
P00_2233 6I         41,414  09-12-99  2:34p P00_2233.6I
p00_2233 6o      8,372,643  09-12-99  2:45p p00_2233.6o
P00_22~2 TXT        72,963  09-12-99  2:46p p00_2233.elem_aqu.txt
P00_22~3 TXT        69,034  09-12-99  2:46p p00_2233.elem_min.txt
P08F61~1 TXT        69,047  09-12-99  2:47p p00_2233.elem_tot.txt
p01g1203 6i         38,573  09-12-99  3:30p p01g1203.6i
p01g1203 6o      5,199,386  09-12-99  3:56p p01g1203.6o
P01G12~1 TXT        46,767  09-12-99  3:55p p01g1203.elem_aqu.txt
P01G12~2 TXT        44,254  09-12-99  3:55p p01g1203.elem_min.txt
P01G12~3 TXT        44,267  09-12-99  3:55p p01g1203.elem_tot.txt
p01g2203 6i         38,648  08-28-99 10:38a p01g2203.6i
p01g2203 6o      2,060,364  09-07-99  2:57p p01g2203.6o
P01G22~1 TXT        21,066  09-07-99  2:57p p01g2203.elem_aqu.txt
P01G22~2 TXT        19,945  09-07-99  2:57p p01g2203.elem_min.txt
P01G22~3 TXT        19,958  09-07-99  2:57p p01g2203.elem_tot.txt
p01g2204 6i         38,942  08-28-99 12:27p p01g2204.6i
p01g2204 6o      3,019,216  09-07-99  1:25p p01g2204.6o
P01G22~4 TXT        28,186  09-07-99  1:25p p01g2204.Elem_aqu.txt
P029AC~1 TXT        26,681  09-07-99  1:25p p01g2204.Elem_min.txt
P02FC0~1 TXT        26,694  09-07-99  1:25p p01g2204.Elem_tot.txt
p01h2204 6i         38,573  09-12-99  3:30p p01h2204.6i
p01h2204 6o      4,853,424  09-12-99  3:57p p01h2204.6o
P01H22~1 TXT        44,103  09-12-99  3:55p p01h2204.elem_aqu.txt
P01H22~2 TXT        41,734  09-12-99  3:55p p01h2204.elem_min.txt
P01H22~3 TXT        41,747  09-12-99  3:55p p01h2204.elem_tot.txt
p02g1021 6i         37,868  08-27-99  5:07p p02g1021.6i
p02g1021 6o      1,906,955  09-07-99  1:36p p02g1021.6o
P02G10~1 TXT        18,396  09-07-99  1:36p p02g1021.elem_aqu.txt
P02G10~2 TXT        17,419  09-07-99  1:36p p02g1021.elem_min.txt
P02G10~3 TXT        17,432  09-07-99  1:36p p02g1021.elem_tot.txt
p02g2021 6i         38,020  08-27-99  7:16p p02g2021.6i
p02g2021 6o      2,418,369  09-07-99  1:50p p02g2021.6o
P08D2D~1 TXT        21,956  09-07-99  1:50p p02g2021.elem_aqu.txt
P0792D~1 TXT        20,787  09-07-99  1:50p p02g2021.elem_min.txt
P07F41~1 TXT        20,800  09-07-99  1:50p p02g2021.elem_tot.txt
```

```
p02g2022 6i          36,421  08-27-99  5:08p p02g2022.6i
p02g2022 6o       7,702,259  09-07-99  2:44p p02g2022.6o
P02G20~1 TXT         66,901  09-07-99  2:44p p02g2022.Elem_aqu.txt
P02G20~2 TXT         63,308  09-07-99  2:44p p02g2022.Elem_min.txt
P02G20~3 TXT         63,321  09-07-99  2:44p p02g2022.Elem_tot.txt
p02g2031 6i          38,168  08-28-99  7:23p p02g2031.6i
p02g2031 6o       2,190,551  09-07-99 12:10p p02g2031.6o
P02G20~4 TXT         19,731  09-07-99 12:10p p02g2031.Elem_aqu.txt
P08925~1 TXT         18,682  09-07-99 12:10p p02g2031.Elem_min.txt
P09F49~1 TXT         18,695  09-07-99 12:10p p02g2031.Elem_tot.txt
p02h2022 6i          36,425  08-27-99  5:08p p02h2022.6i
p02h2022 6o       7,684,344  09-07-99  1:05p p02h2022.6o
P02H20~1 TXT         66,456  09-07-99  1:05p p02h2022.elem_aqu.txt
P02H20~2 TXT         62,887  09-07-99  1:05p p02h2022.elem_min.txt
P02H20~3 TXT         62,900  09-07-99  1:05p p02h2022.elem_tot.txt
pb1g2203 6i          34,951  06-10-99 11:08a pb1g2203.6i
pb1g2203 6o       1,049,566  06-10-99 11:16a pb1g2203.6o
pr0_2131 6i          41,923  08-22-99  2:19p pr0_2131.6i
pr0_2131 6o       4,202,810  09-12-99  5:36p pr0_2131.6o
PR0_21~1 TXT         41,981  09-12-99  5:35p pr0_2131.Elem_aqu.txt
PR0_21~2 TXT         39,732  09-12-99  5:35p pr0_2131.Elem_min.txt
PR0_21~3 TXT         39,745  09-12-99  5:35p pr0_2131.Elem_tot.txt
ps0_1122 6i          41,784  09-01-99  9:18p ps0_1122.6i
ps0_1122 6o       8,226,243  09-01-99 10:25p ps0_1122.6o
PS0_11~1 TXT         70,906  09-01-99 10:25p ps0_1122.elem_aqu.txt
PS0_11~2 TXT         67,097  09-01-99 10:25p ps0_1122.elem_min.txt
PS0_11~3 TXT         67,110  09-01-99 10:25p ps0_1122.elem_tot.txt
ps0_1131 6i          41,710  09-01-99  9:19p ps0_1131.6i
ps0_1131 6o       3,670,161  09-01-99 10:48p ps0_1131.6o
PS0_11~4 TXT         35,751  09-01-99 10:48p ps0_1131.elem_aqu.txt
PS799D~1 TXT         33,838  09-01-99 10:48p ps0_1131.elem_min.txt
PS7FB1~1 TXT         33,851  09-01-99 10:48p ps0_1131.elem_tot.txt
ps0_1222 6i          41,710  09-01-99  9:22p ps0_1222.6i
ps0_1222 6o       8,547,371  09-01-99 11:49p ps0_1222.6o
PS0_12~1 TXT         74,466  09-01-99 11:49p ps0_1222.elem_aqu.txt
PS0_12~2 TXT         70,465  09-01-99 11:49p ps0_1222.elem_min.txt
PS0_12~3 TXT         70,478  09-01-99 11:49p ps0_1222.elem_tot.txt
ps0_2131 6i          41,775  09-01-99  9:23p ps0_2131.6i
ps0_2131 6o       3,921,236  09-02-99 12:15a ps0_2131.6o
PS0_21~1 TXT         38,421  09-02-99 12:15a ps0_2131.elem_aqu.txt
PS0_21~2 TXT         36,364  09-02-99 12:15a ps0_2131.elem_min.txt
PS0_21~3 TXT         36,377  09-02-99 12:15a ps0_2131.elem_tot.txt
ps0_2133 6i          41,710  09-01-99  9:24p ps0_2133.6i
ps0_2133 6o       7,873,703  09-02-99  1:12a ps0_2133.6o
PS0_21~4 TXT         70,461  09-02-99  1:12a ps0_2133.elem_aqu.txt
PS895D~1 TXT         66,676  09-02-99  1:12a ps0_2133.elem_min.txt
PS8F71~1 TXT         66,689  09-02-99  1:12a ps0_2133.elem_tot.txt
ps2_1122 6i          41,784  09-01-99  9:26p ps2_1122.6i
ps2_1122 6o       8,376,770  09-02-99  2:12a ps2_1122.6o
PS2_11~1 TXT         72,241  09-02-99  2:12a ps2_1122.elem_aqu.txt
PS2_11~2 TXT         68,360  09-02-99  2:12a ps2_1122.elem_min.txt
PS2_11~3 TXT         68,373  09-02-99  2:12a ps2_1122.elem_tot.txt
ps2_1131 6i          41,209  09-01-99  9:26p ps2_1131.6i
ps2_1131 6o       2,387,705  09-02-99  2:29a ps2_1131.6o
PS2_11~4 TXT         21,956  09-02-99  2:29a ps2_1131.elem_aqu.txt
PS899D~1 TXT         20,787  09-02-99  2:29a ps2_1131.elem_min.txt
PS8FB1~1 TXT         20,800  09-02-99  2:29a ps2_1131.elem_tot.txt
```

```
ps2_1222 6i          41,710  09-01-99  9:26p ps2_1222.6i
ps2_1222 6o       8,584,162  09-02-99  3:34a ps2_1222.6o
PS2_12~1 TXT         74,911  09-02-99  3:34a ps2_1222.elem_aqu.txt
PS2_12~2 TXT         70,886  09-02-99  3:34a ps2_1222.elem_min.txt
PS2_12~3 TXT         70,899  09-02-99  3:34a ps2_1222.elem_tot.txt
ps2_2131 6i          41,923  09-01-99  9:25p ps2_2131.6i
ps2_2131 6o       3,886,192  09-02-99  3:58a ps2_2131.6o
PS2_21~2 TXT         38,421  09-02-99  3:58a ps2_2131.elem_aqu.txt
PS2_21~3 TXT         36,364  09-02-99  3:58a ps2_2131.elem_min.txt
PS2_21~4 TXT         36,377  09-02-99  3:58a ps2_2131.elem_tot.txt
ps2_2133 6i          41,858  09-01-99  9:24p ps2_2133.6i
ps2_2133 6o       8,115,419  09-02-99  4:56a ps2_2133.6o
PSAD5D~1 TXT         72,686  09-02-99  4:56a ps2_2133.elem_aqu.txt
PS995D~1 TXT         68,781  09-02-99  4:56a ps2_2133.elem_min.txt
PS2_21~1 TXT         68,794  09-02-99  4:56a ps2_2133.elem_tot.txt
s00_2131 6i          41,479  09-12-99  2:33p s00_2131.6i

~\Pu-ceram_CD\sens_Gd_thermo
CERD2W~1 6I          46,723  12-02-98  2:21p cerd2W0_0015I_eq6new.6i
CERD3W~1 6I          43,826  12-10-98  5:16p Cerd3W0_0015I_CO2_LO_new.6i
DATA0N~1 R8W      2,301,840  01-18-99  7:51p data0.nuc.R8w
GDCO3_~1 XLS         19,968  01-21-99  5:41p GdCO3_Weger_Rai_2_EQ6.xls
weger    3I           1,551  01-19-99  1:55p weger.3I
weger1   6i           4,126  01-19-99  2:17p weger1.6i
weger2   6i           4,130  01-19-99  4:08p weger2.6i
weger2s  6i           4,900  01-20-99  8:55a weger2s.6i
weger3   6i           4,428  01-19-99  4:28p weger3.6i
weger3s  6i           4,701  01-20-99  8:57a weger3s.6i
weger3sx 6i           4,756  01-20-99 10:11a weger3sx.6i
weger_d  3i           8,439  01-19-99  2:06p weger_d.3i
WEGER_~1 DOC        471,040  01-27-99 11:02a Weger_Rai_vs_SKB.doc
Weg_fig3 xls         27,648  01-21-99  5:41p Weg_fig3.xls

~\Pu-ceram_CD\sens_Glass
CE40C5~1 6I          43,010  01-31-99  4:53p Cerd2W0_0015I_base.6i
CERD2W~2 TXT         23,536  01-31-99  6:16a Cerd2w0_0015I_base.elem_aqu.txt
CERD2W~3 TXT         22,247  01-31-99  6:16a Cerd2w0_0015I_base.elem_min.txt
CERD2W~4 TXT         22,260  01-31-99  6:16a Cerd2w0_0015I_base.elem_tot.txt
CERD2W~1 6I          43,222  01-31-99  4:53p Cerd2W0_0015I_batch1.6i
CERD2W~2 6I          43,222  01-31-99  5:59p Cerd2W0_0015I_batch1a.6i
CEFB4F~1 TXT         16,171  01-31-99  6:25a Cerd2w0_0015I_batch1a.elem_aqu.txt
CEFB2B~1 TXT         15,314  01-31-99  6:25a Cerd2w0_0015I_batch1a.elem_min.txt
CE144D~1 TXT         15,327  01-31-99  6:25a Cerd2w0_0015I_batch1a.elem_tot.txt
CERD2W~3 6I          40,522  01-31-99  6:16p cerd2w0_0015I_batch1b.6i
CE3C4F~1 TXT          8,606  01-31-99  6:31a Cerd2w0_0015I_batch1b.elem_aqu.txt
CE3C2B~1 TXT          8,157  01-31-99  6:31a Cerd2w0_0015I_batch1b.elem_min.txt
CE544D~1 TXT          8,170  01-31-99  6:31a Cerd2w0_0015I_batch1b.elem_tot.txt
CERD2W~4 6I          43,632  01-31-99  4:53p Cerd2W0_0015I_batch3.6i
CE96C8~1 TXT         24,181  01-31-99  7:01a Cerd2w0_0015I_batch3.elem_aqu.txt
CE82C8~1 TXT         22,892  01-31-99  7:01a Cerd2w0_0015I_batch3.elem_min.txt
CE98EC~1 TXT         22,905  01-31-99  7:01a Cerd2w0_0015I_batch3.elem_tot.txt
CEDE02~1 6I          43,632  01-31-99  4:55p Cerd2W0_0015I_blend.6i
CEDCF0~1 TXT         26,851  01-31-99  6:46a Cerd2w0_0015I_blend.elem_aqu.txt
CEDCD8~1 TXT         25,418  01-31-99  6:46a Cerd2w0_0015I_blend.elem_min.txt
CEF4F6~1 TXT         25,431  01-31-99  6:46a Cerd2w0_0015I_blend.elem_tot.txt
CEFFF5~1 6I          46,723  12-02-98  2:21p cerd2W0_0015I_eq6new.6i
CEFBF7~1 6I          43,550  01-31-99  4:54p Cerd2W0_0015I_hm.6i
CE5A47~1 TXT         22,846  01-31-99  8:40p Cerd2w0_0015I_hm.elem_aqu.txt
CE4647~1 TXT         21,629  01-31-99  8:40p Cerd2w0_0015I_hm.elem_min.txt
```

```
CE5C6B~1 TXT        21,642  01-31-99  8:40p Cerd2w0_0015I_hm.elem_tot.txt
CECEF6~1 6I         43,222  01-31-99  4:54p Cerd2W0_0015I_purex.6i
CE5481~1 TXT        21,511  01-31-99  7:16a Cerd2w0_0015I_purex.elem_aqu.txt
CE546D~1 TXT        20,366  01-31-99  7:16a Cerd2w0_0015I_purex.elem_min.txt
CERD2W~1 TXT        20,379  01-31-99  7:16a Cerd2w0_0015I_purex.elem_tot.txt
GLASS2~1 DOC        50,688  02-08-99  2:24p glass2sensitivity.doc
GLASS2~1 XLS       113,664  02-01-99 10:29a glass2sensitivity.xls
README~1 TXT           380  09-12-99  2:20p Readme_dates.txt
```

~\Pu-ceram_CD\sens_J13

```
j13cal25 3i         12,547  02-12-99  4:43p j13cal25.3i
j13cal25 3p         10,396  02-12-99  6:05p j13cal25.3p
j13cal30 3i         12,993  02-12-99  4:41p j13cal30.3i
j13cal30 3p         10,840  02-12-99  6:05p j13cal30.3p
j13cal35 3i         12,991  02-12-99  4:40p j13cal35.3i
j13cal35 3p         10,840  02-12-99  6:05p j13cal35.3p
j13noc25 3i         12,846  02-12-99  4:43p j13noc25.3i
j13noc25 3p         10,692  02-12-99  6:05p j13noc25.3p
j13noc30 3i         12,920  02-12-99  4:42p j13noc30.3i
j13noc30 3o        127,230  04-21-99  7:53a j13noc30.3o
j13noc30 3p         10,766  04-21-99  7:53a j13noc30.3p
j13noc35 3i         12,920  02-12-99  4:50p j13noc35.3i
j13noc35 3p         10,766  02-12-99  6:05p j13noc35.3p
J13SEN~1 DOC        39,936  02-15-99  1:46p j13sensitivity.doc
r4base   6i         40,547  01-31-99 12:59p r4base.6i
R4BASE~1 TXT        22,260  02-14-99  7:44p r4base_.elem_tot.txt
R4BASE~1 XLS        47,616  02-14-99  7:47p r4base_.elem_tot.xls
r4cal25  6i         40,855  02-14-99  3:39a r4cal25.6i
r4cal25_ 6i         42,996  02-14-99 10:13a r4cal25_.6i
R4CAL2~1 TXT        20,800  02-14-99 11:43a r4cal25_.elem_tot.txt
R4CAL2~1 XLS        44,032  02-14-99  7:13p r4cal25_.elem_tot.xls
r4cal30  6i         41,299  02-14-99  3:38a r4cal30.6i
r4cal30_ 6i         43,406  02-14-99 10:14a r4cal30_.6i
R4CAL3~1 TXT        24,589  02-14-99 11:54a r4cal30_.elem_tot.txt
R4CAL3~1 XLS        41,472  02-14-99  7:10p r4cal30_.elem_tot.xls
r4cal35  6i         41,299  02-14-99  3:39a r4cal35.6i
r4cal35_ 6i         43,570  02-14-99 10:15a r4cal35_.6i
R4CAL3~2 TXT        27,115  02-14-99 12:06p r4cal35_.elem_tot.txt
R4CAL3~2 XLS        53,248  02-14-99  7:15p r4cal35_.elem_tot.xls
r4noc25  6i         40,872  02-13-99  7:52p r4noc25.6i
r4noc25_ 6i         42,996  02-14-99 10:16a r4noc25_.6i
R4NOC2~1 TXT        23,326  02-14-99 11:05a r4noc25_.elem_tot.txt
R4NOC2~1 XLS        47,616  02-14-99  7:18p r4noc25_.elem_tot.xls
r4noc30  6i         41,225  03-05-99 10:35a r4noc30.6i
r4noc30_ 6i         43,406  02-14-99 10:16a r4noc30_.6i
R4NOC3~1 TXT        25,431  02-14-99 11:17a r4noc30_.elem_tot.txt
R4NOC3~1 XLS        51,200  02-14-99  7:21p r4noc30_.elem_tot.xls
r4noc35  6i         41,225  02-14-99 10:07a r4noc35.6i
r4noc35_ 6i         43,570  02-14-99 10:25a r4noc35_.6i
R4NOC3~2 TXT        25,852  02-14-99 11:29a r4noc35_.elem_tot.txt
R4NOC3~2 XLS        51,712  02-14-99  7:24p r4noc35_.elem_tot.
```